MOLECULAR CONSEQUENCES OF ELASTIN GENE MUTATIONS IN AUTOSOMAL DOMINANT CUTIS LAXA AND SUPRAVALVULAR AORTIC STENOSIS

by

Sevinc Akcay

BS, Ankara University, Turkey, 2008

MS, University of Pittsburgh, 2012

Submitted to the Graduate Faculty of

Graduate School of Public Health in partial fulfillment

of the requirements for the degree of

Doctor of Philosophy

University of Pittsburgh

2016

UNIVERSITY OF PITTSBURGH

GRADUATE SCHOOL OF PUBLIC HEALTH

This dissertation was presented

by

Sevinc Akcay

It was defended on

June 1, 2016

and approved by

Dissertation Advisor:
Zsolt Urban, PhD
Associate Professor, Department of Human Genetics
Graduate School of Public Health, University of Pittsburgh

Committee Member:
Beth Roman, PhD
Visiting Associate Professor, Department of Human Genetics
Graduate School of Public Health, University of Pittsburgh

Committee Member:
Ryan Minster, PhD, MSIS
Assistant Professor, Department of Human Genetics
Graduate School of Public Health, University of Pittsburgh

Committee Member:
Youhua Liu, PhD
Professor, Department of Pathology
School of Medicine, University of Pittsburgh

Zsolt Urban, PhD

MOLECULAR CONSEQUENCES OF ELASTIN GENE MUTATIONS IN AUTOSOMAL DOMINANT CUTIS LAXA AND SUPRAVALVULAR AORTIC STENOSIS

Sevinc Akcay, PhD

University of Pittsburgh, 2016

ABSTRACT

Elastic fibers are components of the extracellular matrix (ECM) that contribute resilience to tissues and bind and regulate transforming growth factor beta (TGFβ). Elastin gene (*ELN*) mutations cause several phenotypes including Williams-Beuren Syndrome (WBS), supravalvular aortic stenosis (SVAS) and autosomal dominant cutis laxa (ADCL). This work focused on the molecular consequences of the *ELN* gene mutations in ADCL and SVAS.

ADCL is characterized by loose and inelastic skin, pulmonary emphysema, aortic root dilation, and peripheral pulmonary aortic stenosis. Our goal was to evaluate the impact of *ELN* mutations on TGFβ signaling and molecular pathology of ADCL. Dermal fibroblasts from four patients with *ELN* mutations in exon 34 or exon 30 and controls were used. Increased intracellular TGFβ signaling was found in patients with exon 30 mutations, despite unchanged extracellular TGFβ activity. TGFBR1 levels were increased at the protein and the RNA level. Patients with exon 34 mutations had normal TGFβ signaling. Our results indicate mutation-specific TGFβ signaling changes in *ELN*-related cutis laxa patients, which may influence to disease severity. Elastin assay showed decreased elastin deposition in ADCL cells and long-term TGFβ treatment improved elastin deposition. Semi-quantitative RT-PCR experiments showed increased expression of the mutant compared to the wild-type allele in ADCL cells under baseline conditions. Long-term TGFβ treatment normalized this allelic imbalance in expression. Therefore, we conclude that increased TGFβ signaling is a protective mechanism in ADCL at the molecular level.

SVAS is characterized by narrowing of the ascending aorta. An SVAS family with a duplication in the *ELN* gene was analyzed genetically and functionally. Gene-dosage analysis showed that a tetranucleotide repeat in intron 1 was within the duplicated region. RT-PCR of pre-mRNA showed that a SNP in intron 23 of the mutant allele was not expressed. Decreased elastin deposition was found in affected individuals, supporting that this partial duplication yielded a null allele.

Uncovering the nature of connections between elastin and TGFβ may help developing treatments for cutis laxa. Our findings are relevant to complex diseases characterized by elastin degradation and TGFβ dysregulation, including aneurysms and chronic obstructive pulmonary disease that have major public health impact.

TABLE OF CONTENTS

LIST OF TABLES

LIST OF FIGURES

ACKNOWLEDGEMENTS

This dissertation would not have been possible and completed without the support and dedication of special people.

First and foremost, I would like to thank and express my deepest appreciation and gratitude to my dissertation committee chair, my mentor and my advisor, Dr. Zsolt Urban, who helped me overcome so a lot of difficulties. I would have never completed my degree without his encouragement, countless guidance, mentorship, and strong support as I wrote my dissertation. His dedication, leadership, and beliefs in my ability throughout this process were very appreciated. His support throughout this project has helped shape my scientific career.

Besides my advisor, I would like to thank outstanding committee members, Dr. Beth Roman, Dr. Ryan Minster and Dr. Youhua Liu, for their academic support and encouraging advice.

I would like to express my sincerest gratitude to my fellow labmates, Elizabeth Lawrence, Sandeep Khatri, Dr. Chi-Ting Su and Michelle Zorrilla for their technical and moral support and encouragement during my scientific career. Words cannot express the unwavering, unending, phenomenal support that they gave me. I cannot thank you enough for their friendships. I would also like to thank the Human Genetics Department faculty and graduate students who have supported, encouraged, and helped guide me throughout my time here, especially Dr. Candace Kammerer and Dr. M. Micheal Barmada.

I would like to express my gratitude to my loving family for their unconditional support, love, help and guidance from the beginning of my career path. They have been always with me with their love and encouragement.

I would like to thank Turkish Ministry of Education for providing scholarship throughout my graduation study.

Last but not least, I would like to thank my beloved husband, Dr. Ahmet Oguz Akcay, for his emotional support and encouragement. I could not be successful without his unconditional support, love, patience, and extraordinary courage to finish this extensive work. I love you, Ahmet.

Thank you all for your support in the completion of my goal in getting my PhD!

ABBREVIATIONS

ABAM	antibiotic-antimycotic
ADAMTS	a disintegrin and metalloprotease with thrombospondin type-I motif
ADCL	autosomal dominant cutis laxa
BAC	bacterial artificial chromosome
BMP	bone morphogenetic protein
BCP	1-bromo-3-chloropropane
cDNA	complementary DNA
Co-SMAD	co-operating SMAD
CTGF	connective tissue growth factor
DEPC	diethyl-pyrocarbonate
DMEM	Dulbecco's modified Eagle's medium
DNA	deoxyribonucleic acid
ECM	extracellular matrix
EDTA	ethylenediaminetetraacetic acid
ELN	elastin
ERK	extracellular-signal regulated kinase
FAM	6-carboxyfluorescein amidite
FBN	fibrillin
FBLN	fibulin
FBS	fetal bovine serum
FN	fibronectin
GAG	glycosaminoglycan
HS	heparan sulfate

iPSC	induced pluripotent stem cells
I-SMAD	inhibitory SMAD
JNK	c-Jun N-terminal
LAP	latency-associated peptide
LDS	Loeys-Dietz syndrome
LLC	large latent complex
LOX	lysyl oxidase
LTBP	latent TGFβ binding protein
MAGP	microfibril-associated glycoprotein
MFS	Marfan syndrome
MLEC	mink lung epithelial cell
PAI1	plasminogen activator inhibitor-1
PBS	phosphate-buffered saline
PCR	polymerase chain reaction
pERK	phosphorylated ERK
PI3KK	phosphoinositide 3-kinase
pSMAD2	phosphorylated SMAD2
pTGBFR1	phosphorylated transforming growth factor β receptor 1
R-SMAD	receptor-associated SMAD
RNA	ribonucleic acid
RT	reverse transcriptase
SDS-PAGE	sodium dodecyl sulfate polyacrylamide gel electrophoresis
SLC	small latent complex
SMC	smooth muscle cell
SNP	single-nucleotide polymorphism
SVAS	supravalvular aortic stenosis
TAK1	TGFβ associated kinase 1
TGFBR1	transforming growth factor β receptor 1
TGFBR2	transforming growth factor β receptor 2

TGFBR3	transforming growth factor β receptor 3
TGFβ	transforming growth factor β
UNG	uracil-N-glycosylase
UPR	unfolded protein response
WBS	Williams-Beuren Syndrome

1.0 INTRODUCTION

1.1 EXTRACELLULAR MATRIX

The extracellular matrix (ECM) acts as a scaffold that supports cells in all tissues and organs. The ECM is comprised of a fibrous material, including collagen fibers, microfibrils and elastic fibers and ground substance surrounding the fibers, including proteoglycans and glycoproteins. The ECM has roles in cell-cell communication, cell proliferation, migration, cell differentiation, development, and survival. The ECM is also crucial for the storage of growth factors, cytokines and ECM-remodeling enzymes (Naba et al., 2012).

Collagen fibers are a major component of ECM, which provide tensile strength and have roles in cell adhesion, chemotaxis and migration and tissue morphogenesis (Kadler et al., 2007). Elastic fibers complement collagen fibers to provide resilience to the tissues, whereas glycoproteins contribute to tissue cohesiveness. Proteoglycans are bulky polysaccharides (glycosaminoglycans, GAGs) covalently attached to relatively smaller core proteins, which counteract compressive forces (Gandhi and Mancera, 2008) and are important in cell signaling and wound healing (Gandhi and Mancera , 2008).

1.1.1 ELASTIC FIBERS

Elastic fibers are major insoluble components of ECM that are vital for connective tissues including large arteries, skin, lung, ligaments, and auricular cartilage (Figure 1.3). Elastic fibers show tissue-specific and morphologically distinct networks based on the elasticity requirements of tissues (Baldwin, Simpson et al. 2013). The thick elastic fiber networks in the reticular dermis and thin fibers in the papillary dermis provide skin elasticity. Highly branched networks of elastic fibers that provide respiratory expansion and recoil are main providers of pulmonary elasticity. Arterial elastic fibers form lamellar layers for vascular elasticity (Kielty 2006). Elastic fibers also have a crucial role in vascular smooth muscle cell differentiation during arterial development (Karnik et al., 2003). In addition, elastic fibers also regulate the bioavailability of TGFβ family (Nistala et al., 2010).

1.1.1.1 Composition of elastic fibers

Elastic fibers are composed of two primary components: an inner core of cross-linked elastin and microfibrils (Baldwin et al. 2013). In addition, several 'accessory' molecules interact with microfibrils and elastin as well as its precursor, tropoelastin (Baldwin et al. 2013).

1.1.1.2 Elastin

Elastin is the key insoluble protein in the elastic fibers (90%) (Kielty, 2006) and it is the primary provider of elasticity and resilience. At first, elastin is synthesized as tropoelastin, a precursor protein of 60-70 kDa secreted from elastogenic cells such as fibroblasts, smooth muscle cells (SMCs) and auricular chondrocytes (Baldwin et al. 2013). Its primary structure includes valine-, proline-, and glycine-rich hydrophobic domains and hydrophilic cross-linking domains, which are rich in lysine and alanine (Figure 1.1). Hydrophobic domains are important during the self-aggregation of tropoelastin by coacervation (Vrhovski et al., 1997). Coacervation brings tropoelastin monomers together, and their association is stabilized by cross-links, known as desmosines or isodesmosines (Viglio et al., 2007). The asymmetric structure of elastin includes an N-terminal part that provides spring-like properties and a C-terminal part that has a role in cell adhesion by αvβ3 integrin and cell surface proteoglycans (Bax et al. 2009). The human elastin gene is localized to chromosome 7q11.2 and has 34 exons spanning 45 kb of the genome (Fazio et al., 1998). Human elastin primary transcript undergoes alternative splicing leading to many different mRNA isoforms.

Elastin is a crucial protein in the aorta and great arteries. $ELN^{-/-}$ mice die immediately after birth due to the vascular obstruction, caused by an enhanced proliferation of smooth muscle cells (Li et al., 1998). In contrast, $ELN^{+/-}$ mice survive until adulthood and show systemic

hypertension, enhanced a number of elastic lamellae, the elastin layers associated with SMCs (Li et al., 1998; Faury et al., 2003) and a thinner wall of blood vessels (Wagensil et al., 2005).

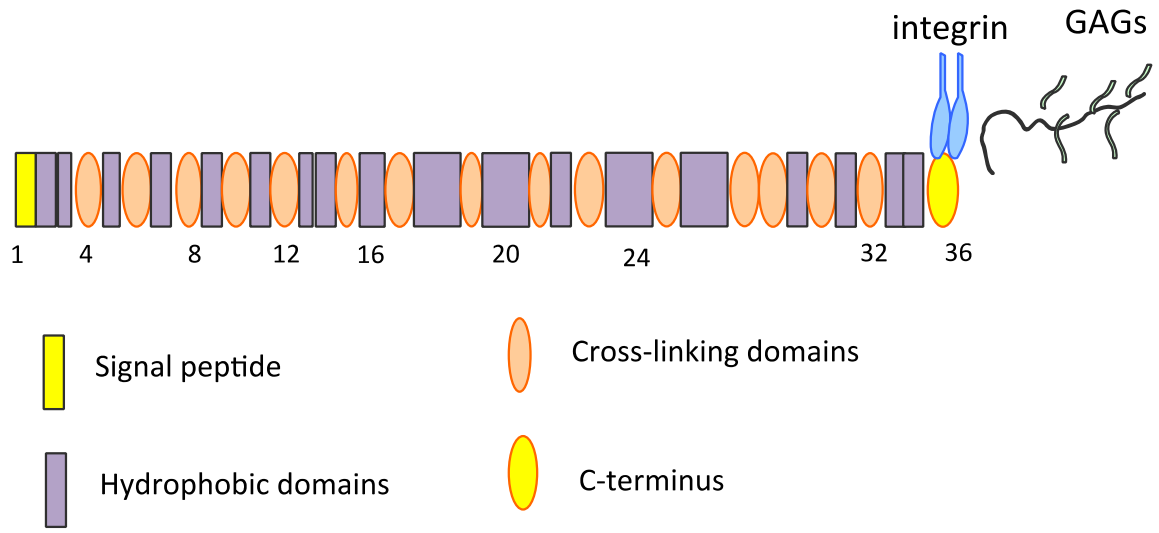

Figure 1.1 Schematic representation of human tropoelastin
The domain organization of tropoelastin is shown with the keys for domain types. GAGs: glycosaminoglycan

1.1.1.3 Fibrillin

Fibrillins are the main components of the microfibril scaffold, which provide a template for elastin deposition. Fibrillins are large (350 kDa) extracellular cysteine-rich glycoproteins, and the fibrillin family has three fibrillin genes in humans, fibrillin-1, fibrillin-2 and fibrillin-3 (Piha-Gossack, 2012). Each fibrillin gene has 43 calcium-binding epidermal growth factor-like (cbEGF) domains, five EGF-like domains, seven eight-cysteine-containing (TB) motifs and two hybrid domains with similarities to TB and cbEGF-like domains (Figure 1.2) (Baldwin et al. 2013).

The most predominant fibrillin is fibrillin-1, and its gene is localized on chromosome 15q21.1. Fibrillin-1 is expressed all the time, responsible for microfibril homeostasis; however, fibrillin-2 and fibrillin-3 are mostly expressed during development (Charbonneau et al., 2003; Zhang et al., 1994; Corson et al., 2004; Sabatier et al., 2011). The interior parts of microfibrils with fibrillin-1 might be made from fibrillin-2 (Charbonneau et al., 2010). Fibrillin-1 is indicated to have crucial roles in vascular development in mouse models. FBN-$1^{-/-}$ mice die from an aortic aneurysm, but FBN-$2^{-/-}$ mice have normal vascular development (Carta et al., 2006).

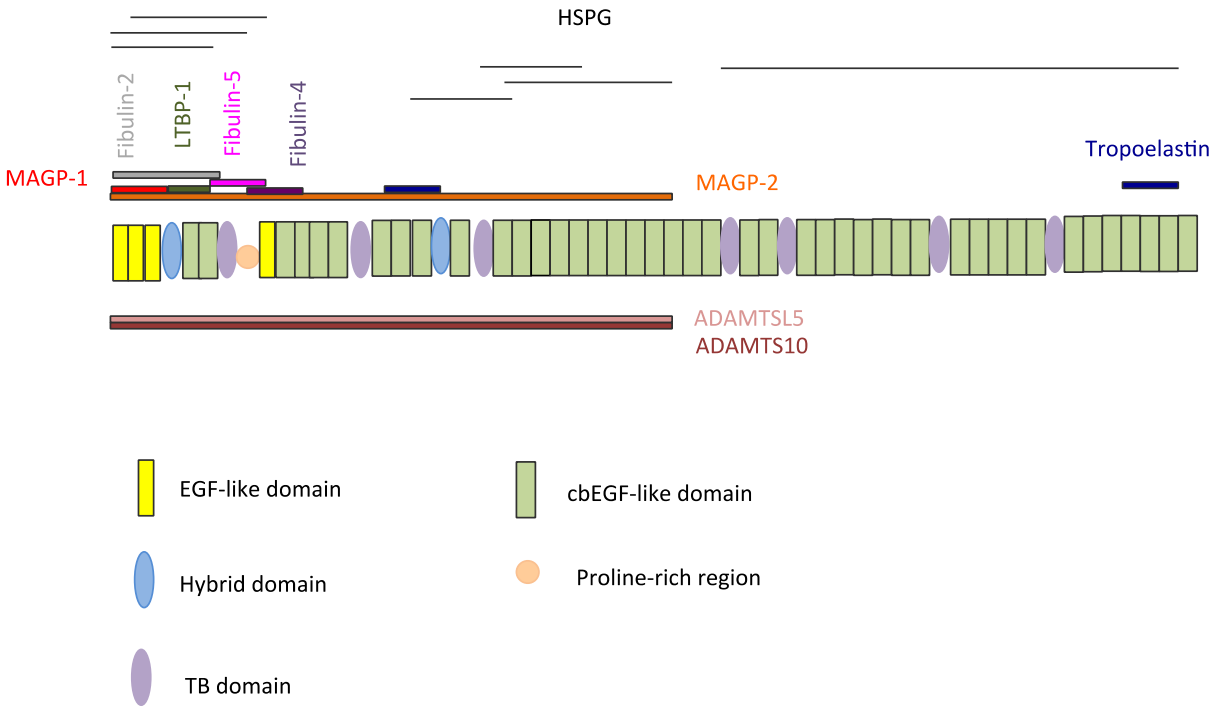

Figure 1.2 Schematic representation of fibrillin-1
The localization of binding sites for key proteins is shown above and below fibrillin-1 as color-coded horizontal lines. HSPG: heparan sulfate proteoglycan.

1.1.1.4 Accessory molecules associated with microfibrils and elastic fibers

Several microfibril and elastic fiber associated accessory molecules have been identified based on functional biochemical and morphological analyses. The microfibril-associated molecules include latent TGFβ binding proteins (LTBPs), a disintegrin and metalloprotease with thrombospondin type-I motif (ADAMTS) and ADAMTS-like proteins, and microfibril-associated glycoproteins (MAGPs) and elastic-fiber associated molecules include fibulin 3-5 and lysyl oxidase (LOX) and lysyl oxidase-like 1 (LOXL1) proteins (Baldwin et al. 2013).

The ADAMTS superfamily consists 19 zinc metalloproteases and 7 ADAMTS-like (ADAMTSL) proteins, which have roles in ECM deposition, microfibril biology and morphogenesis (Apte et al., 2009). ADAMTSL members only have multiple thrombospondin type 1 repeats (TSRs), whereas ADAMTS family members have disintegrin-like and a cysteine-rich modules in addition to a single TSR (Baldwin et al., 2003). ADAMTS-10 and ADAMTSL 2-6 are important in microfibril biology (Hubnacher et al., 2011). The binding of fibrillin-1 and fibrillin-2 to ADAMTSL-5 help colocalization with microfibrils (Bader et al., 2012).

MAGP-1 can associate with elastin and possibly help elastin deposition on microfibrils (Jensen et al., 2001; Rock et al., 2004) and can also regulate of TGFβ signaling by binding TGFβ and BMP-7 (Weinbaum et al., 2008). MAGP-1 might also affect fibronectin-mediated microfibril deposition by interacting with fibronectin (Werneck et al., 2008). MAGP-2 was found to colocalize with microfibrils in several tissues (Lemaire et al., 2007; Gibson et al., 1998; Penner et al., 2002; Hanssen et al., 2004), however, $MAGP1^{-/-}$ mice demonstrated normal microfibrils and elastin, indicating that it is not essential for elastic fiber assembly (Craft et al., 2010). Overexpression of MAGP-2 can enhance elastic fiber formation (Lemaire et al., 2007).

The LTBPs (LTBPS 1-4) are large glycoproteins, and their multi-domain structure includes cbEGF and TB domains similar to fibrillins. LTBPs 1-4 are expressed in several tissues including the heart, lung, and ovary (Piha-Gossack et al., 2012; Todorovic et al., 2005). The third TB domains of LTBPs bind the small latent complex (SLC) of TGFβ comprising the latency-associated peptide (LAP) and the tightly but non-covalently bound TGFβ growth factor (Gleizes et al., 1996; Saharinen et al., 1996) to form the large latent complex (LLC) and also regulate the bioavailability of TGFβ (Todorovic et al., 2005; Gleizes et al., 1996; Saharinen et al., 1996). The interaction between fibrillin-1 and the fourth TB domain of LTBPs ensures the sequestration of the LLC to fibrillin microfibrils, which therefore themselves regulate TGFβ activity too (Saharinen et al., 1996). Fibronectin is needed for LTBP-1 and LTBP-4 deposition into the ECM (Zilbergberg et al., 2012; Reber-Muller et al., 1995; Kantola et al., 2008).

Fibulins are extracellular glycoproteins including fibulin 1-5 (Yanagisawa et al., 2010). Fibulin-4 and fibulin-5 can interact with LOX and LOX-like (LOXL) enzymes and fibrillin-1, and these interactions were implicated in elastin crosslinking and deposition onto microfibrils (Baldwin et al., 2013). Fibulin-3, -4 and -5 have important roles in the assembly of elastic fibers (Yanagisawa et al, 2010; Kobaya et al., 2007). In addition, one likely role of fibulin-4 is to help sequestration of LTBPs (Ono et al., 2009). Fibulin-5 is a regulator of the deposition of elastin onto microfibrils (Zheng et al., 2007).

LOX family has five members including LOX and LOXL1-4 (Molnar et al., 2003). They oxidatively deaminate the peptidyl lysine residues in elastin to form allysine, a reactive aldehyde. Three allysine and one lysine side chains spontaneously condense to form tetrafunctional desmosine and isodesmosine crosslinks to form insoluble elastin (Molnar et al., 2003). The N-

terminal regions of LOX family members provide specificity to the extracellular LOX enzymes (Baldwin et al., 2013).

1.1.1.5 Assembly of elastic fibers

Fibronectin acts as a platform for microfibril deposition (Kinsey et al., 2008; Sabatier et al., 2009), but microfibril formation occurs in several lower organisms without fibronectin and in fibronectin-null cultures (Reber-Muller et al., 1995; Dallas et al., 2005), suggesting fibronectin acts as a facilitator rather than an essential precursor of microfibril assembly.

Fibrillin monomers adopt a head-to-tail arrangement and form a beads-on-a-string appearance of microfibrils (Marson et al., 2005). However, the precise arrangement of the fibrillin monomers with microfibrils is a subject of intense research and debate with several, equally plausible working models (Baldwin et al., 2013).

In addition to a self-assembly, a cellular involvement might also contribute to the microfibril formation (Kinsey et al., 2008). It has been shown that microfibril assembly requires fibronectin Arg-Gly-Asp (RGD)-dependent α5β1 integrins (Kinsey et al., 2008). The interaction of fibrillin-1 with cells can occur through integrins α5β1, αvβ3 and αvβ6 in epithelial cells (Jovanovic et al., 2007; Bax et al., 2007). It remains unresolved whether the microfibril assembly requires direct interaction between fibrillin-1 and cells or indirect interaction through fibrillin-binding proteins (Baldwin et al. 2013).

The glycosaminoglycan heparan sulfate (HS), a component of syndecan and glypican receptors and a perlecan, is essential for fibrillin microfibril assembly as indicated by the inhibition of microfibril assembly by heparin supplementation (Tiedemann et al., 2001; Ritty et al., 2003). So far, six high affinity-binding sites between heparin and fibrillin-1 have been found (Tiedemann et al., 2001; Ritty et al., 2003; Cain et al., 2005). Further insights are needed to

determine how HS contributes to microfibril deposition. The competition between HS and MAGP-1 and tropoelastin to bind fibrillin-1 may regulate elastin deposition onto microfibrils (Cain et al., 2008).

The first step of elastic fiber formation is the self-association of tropoelastin monomers, a process known as coacervation that requires thermodynamic interactions (Yeo et al., 2011). It has been shown that the coacervation rate depends upon the pH and temperature, salt and tropoelastin concentration and the presence of microfibril-associated molecules (Cirulis et al., 2010). Fibulin-4 and fibulin-5 delay the maturation of the tropoelastin (Choi et al., 2009). C-terminal region of tropoelastin interact with αvβ3 (Bax et al., 2007) integrin and HS (Broekelmann et al., 2005). Until transfer to the microfibril platform, tropoelastin coacervate interacts with integrins (Bax et al., 2009) and HS (Akhtar et al., 2011; Broekelmann et al., 2005). This process is called microassembly. LOX or LOXL1, fibulin-4, and fibulin-5 facilitate the stabilization of globules by forming cross-links and help to form the insoluble elastin core, known as macroassembly (Yeo et al., 2011; Cirulis et al., 2010) (Figure 1.3).

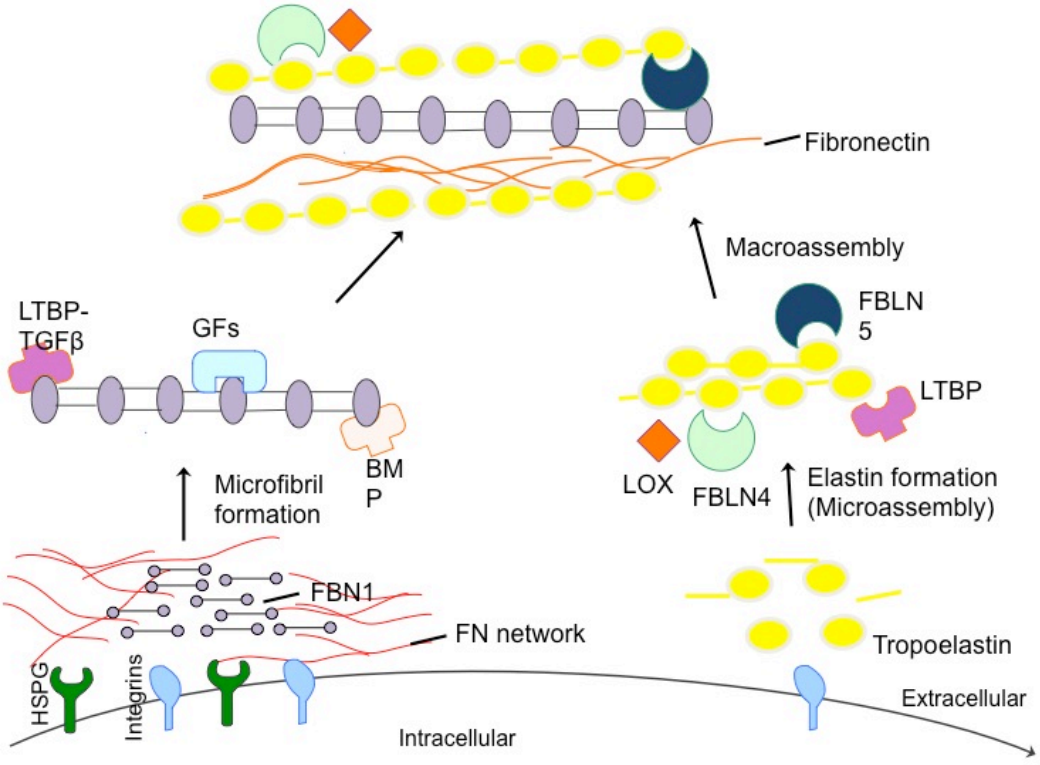

Figure 1.3 Schematic representation of microfibril and elastic fiber assembly
FN: fibronectin; FBN1: fibrillin-1; BMP: bone morphogenetic factor; GF:growth factor; FBLN4:fibulin-4; FBLN5: fibulin-5; LOX: lysyl oxidase.
Microfibrils are formed pericellularly with the interaction of fibronectin, integrins and HSPG. The head-to-tail alignment of FBN monomers forms 'beads-on-a-string' appearance of microfibrils. Microassembly, coacervation of tropoelastin, is the first step of elastin assembly and involves the interaction of C-terminal region of tropoelastin with integrin and HSPG. After the deposition into the microfibril scaffold, the elastin globules are stabilized by LOX and LOXL1. Fibulin-4 or fibulin-5 facilitate the localization of LOX to microfibrils. This macroassembly forms the insoluble elastin core.

1.2 TGFβ SIGNALING

1.2.1 TGFβ signaling and TGFβ receptor system

TGFβs are a family of soluble cytokines, and they serve as multifunctional regulators in myriad cellular processes including cell differentiation, proliferation, recognition, apoptosis, adhesion, embryonic development and migration (Santibanez et al., 2011). TGFβ also modulates ECM structure and composition. TGFβ has three isoforms: TGFβ1, TGFβ2, and TGFβ3, each synthesized as homodimeric proteins with a mass of 75 kDa (Annes et al., 2003), and cleaved by a furin protease to the mature TGFβ and its propeptide, also known as the latency-associated peptide (LAP). The LAP and TGFβ form a small latent complex (SLC) by non-covalent bonds. TGFβ remains inactive in this form. The LAPs form large latent complexes (LLCs) with one of the LTBPs (LTBP1, -3 or -4) by disulfide bonds. Most cells secrete TGFβs in LLC form. Consistently, LTBPs are known to facilitate the correct folding and secretion of TGFβ (Saharinen et al., 1999). LTBPs promote the incorporation of different TGFβs into the ECM. TGFβ signaling pathway alterations are found in several diseases such as cardiovascular, fibrotic, reproductive, wound healing disorders and cancer (Santibanez et al., 2011).

1.2.2 Canonical TGFβ signaling pathway

TGFβ can be activated by release from the LAP by several mechanisms, such as direct proteolysis, non-proteolytic dissociation by thrombospondin-1, integrins, reactive oxygen species or low pH (Annes et al., 2003). After activation, TGFβ binds to a TGFβ receptor in the first step of the signaling pathway (Wrana et al., 1994). There are three types of TGFβ receptors. Type 1

(TGFBR1) and type 2 (TGFBR2) receptor are the primary receptors of the canonical pathway and have serine/threonine kinase activity. Type 3 receptor (TGFBR3) serves as an accessory receptor by binding TGFβ and bringing it to the TGFBR1 and TGFBR2 (Wrana et al., 1992).

Binding of TGFβ to dimeric TGFBR2 that induces autophosphorylation triggers the signaling (Figure 1.4). This autophosphorylation recruits a homodimer of TGBFR1 and then forms a ligand-receptor complex. Then, TGFBR1 is activated by TGFBR2 by transphosphorylation (Wrana et al., 1994). The kinase domain of the activated TGFBR1 triggers the downstream signaling by phosphorylation of receptor-associated SMAD proteins (R-SMADs; SMAD 2 and 3), then undergo formation of heteromeric complexes with the co-operating SMAD (Co-SMAD), SMAD4. After activation, SMAD complexes are translocated into the nucleus and serve as regulators of the transcription of target genes (Moustakas et al., 2001). The inhibitory (I-SMAD) SMAD6 and SMAD7 compete with the R-SMADs for receptor or Co-SMAD binding, and thus negatively regulate TGFβ signaling (Shi and Massague, 2003). SMAD6 inhibits TGFβ signaling by binding to TGFBR1 and repressing the phosphorylation of R-SMAD proteins (Imamura et al., 1997). Another mechanism is to reduce the nuclear translocation (Hata et al., 1998). SMAD7 conducts the inhibition of TGFβ signaling by the ubiquitination and degradation of TGFBR1 and TGFBR2 as a result of the release of SMURF proteins (Wicks et al., 2006; Ebisawa et al., 2001).

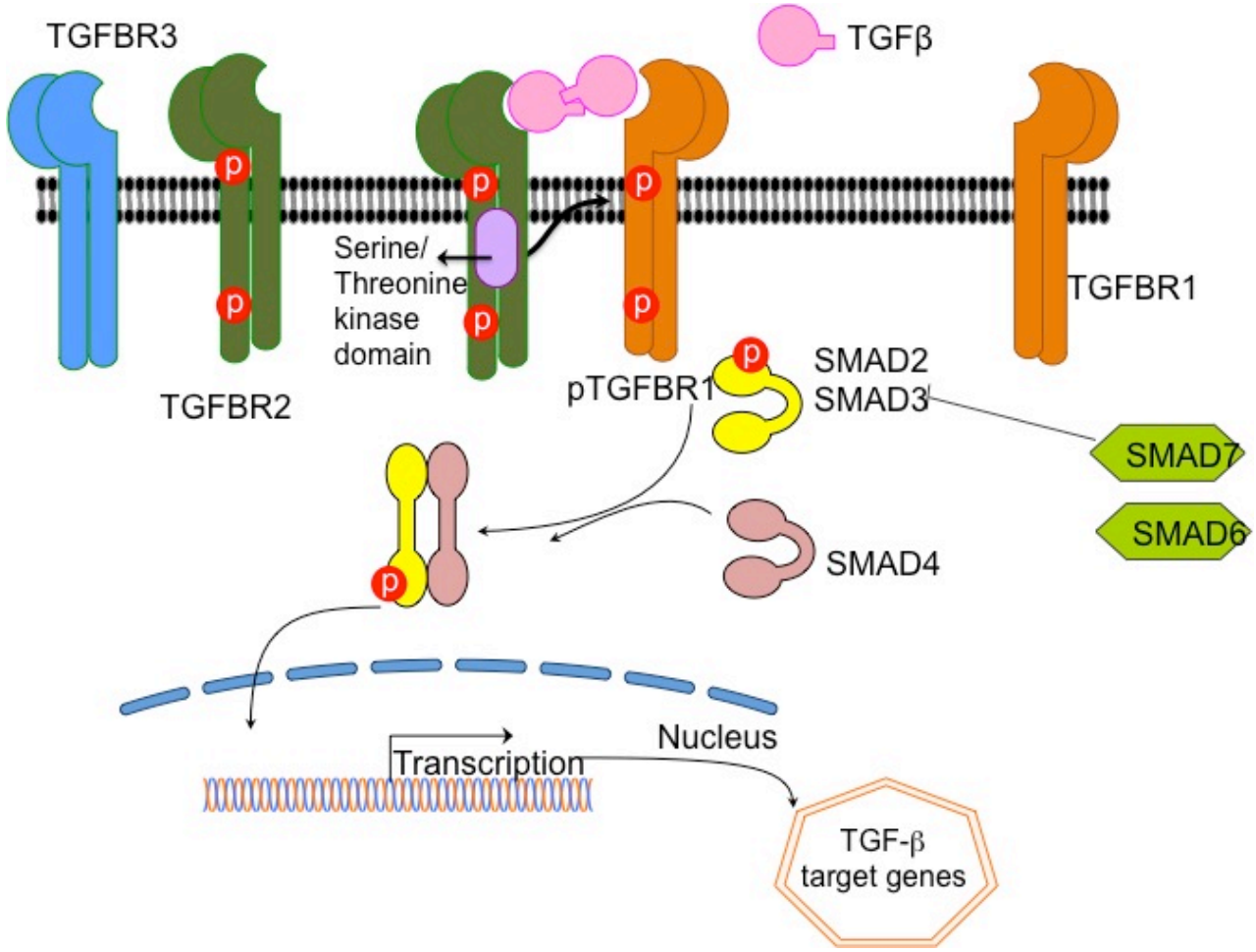

Figure 1.4 A schematic diagram of canonical TGFβ signaling pathway
TGFβ binds to a TGFBR2, which recruits and phosphorylates a TGFBR1. TGFBR1 recruits and phosphorylates a R-SMAD (SMAD2 or SMAD3). The R-SMAD binds to a SMAD4 and forms a heterodimeric complex. This complex enters the nucleus and interacts with other transcription factors to activate and suppress target genes.

1.2.3 Non-canonical TGFβ signaling pathway

Tumor necrosis factor receptor-associated factor 6 (TRAF6) associates with the TGFBR1 in a TGFβ dependent manner (Sorrentino et al., 2008). This complex recruits and activates TGFβ associated kinase 1 (TAK1) which causes an activation of p38 MAPK by phosphorylation (Yamashita et al., 2008; Sorrentino et al., 2008) (Figure 1.5). There are other non-canonical signaling pathways activated in response to TGFβ including extracellular-signal regulated kinase 1 and 2 (ERK1/2) (Lee et al., 2007), c-Jun N-terminal kinase (JNK) (Yamashita et al., 2008; Sorrentino et al., 2008), and phosphoinositide 3-kinase-Akt (PI3KK-Akt) (Wilkes et al., 2005). Additionally, the canonical and non-canonical pathways cross-talk with each other and have different effects.

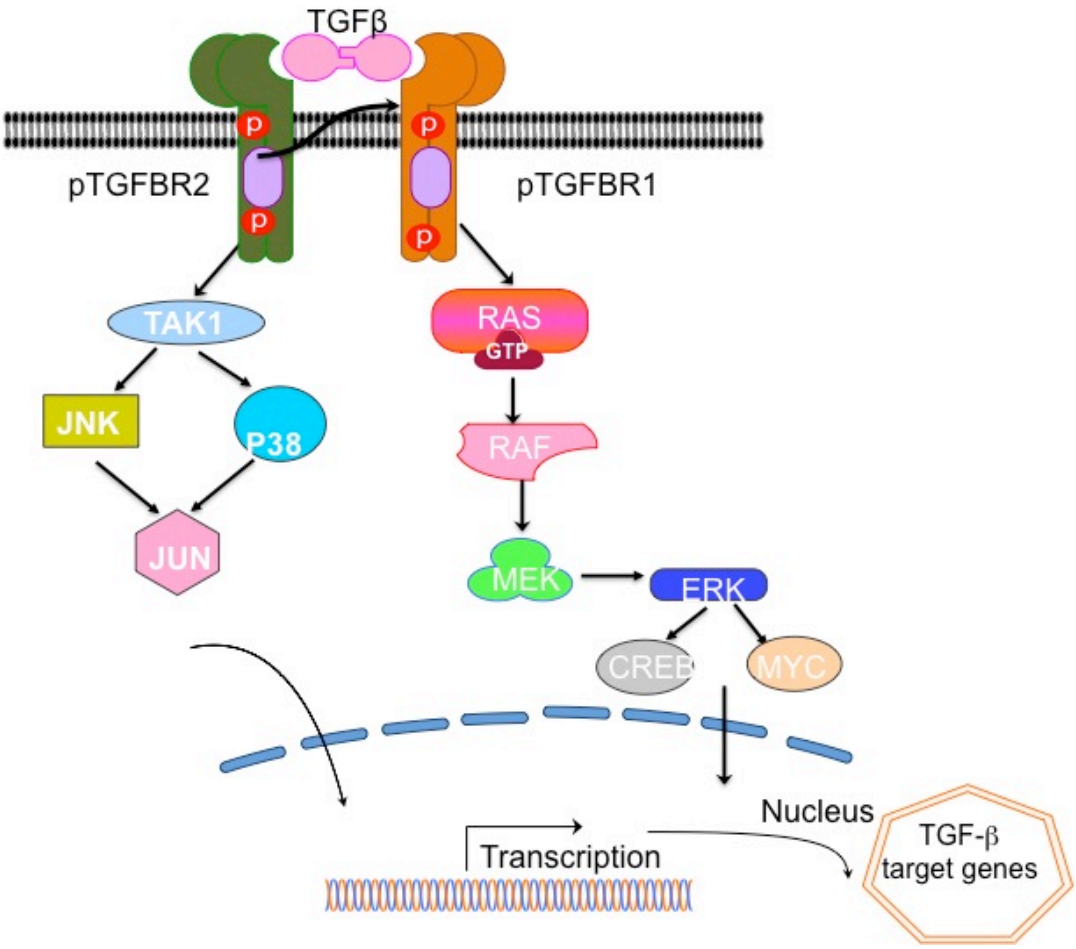

Figure 1.5 A schematic diagram of non-canonical TGFβ signaling pathway
TAK1 is activated with the interaction of TGFBRs and TRAF6 and it leads to activation of p38 and JNK. TGFβ also activates ERK MAPK by activation of RAS and leads to the recruitment of RAF and ERK through MEK1. ERK and JUN enters the nucleus and interacts with other transcription factors to activate and suppress target genes.

1.2.3.1 TGFβ signaling and human inherited disease

TGFβ upregulates several genes required for the elastic fibers, including fibronectin (Ignotz et al.,1987), *LTBP*s (Ahmed et al.,1998; Weikkolainen et al., 2003), *ELN* (Kahari et al., 192; Kucich et al., 1997), *LOXs* (Boak et al.,1994;Kim et al, 2008) and *FBLN5* (Kuang et al., 2006). This regulation could be either transcriptional as in the case of fibronectin, *LTBPs*, *LOXs*, and *FBLN5* or post-transcriptionally in the *ELN* and *FBN1* gene. One possible mechanism how *ELN* and *FBN-1* is regulated at the post-transcriptional level is through the repression of the miR29 family by TGFβ (van Rooij et al., 2008). miR29 binding sites have been identified in many mRNAs of elastic fiber genes such as *ELN*, *FBN1* and *LTBP1* (Urban et al., 2014).

Many heritable connective tissue disorders caused by mutations in ECM proteins and TGFβ signaling pathway components result in altered TGFβ signaling (Table 1.1). Marfan syndrome (MFS) is caused by the mutations in fibrillin-1, which interacts with LTBPs in the ECM. Increased TGFβ signaling was observed in the lung tissue of an MFS mouse model (Neptune et al., 2003). In these MFS mice, aortic aneurysms were also improved with an anti-TGFβ antibody, indicating enhanced TGFβ signaling was a major factor in MFS pathogenesis (Habashi et al., 2006). Increased non-canonical TGFβ signaling appears to contribute to aortic defects in MFS mice whereas canonical TGFβ signaling is thought to be protective (Holm et al., 2011).

Autosomal recessive cutis laxa type 1 (ARLC1C) patients, caused by the mutations in *LTBP4* showed increased TGFβ activity in the dermal fibroblasts (Urban et al., 2009; Dabovic et al.,2009). Loeys- Dietz syndrome (LDS) patients with TGFBR1 and TGFBR2 mutations also showed increased TGFβ signaling as well as enhanced collagen and connective tissue growth factor (CTGF) expression (Loeys et al., 2005). Arterial tortuosity syndrome patients with

SLC2A10 mutations had increased TGFβ signaling in aortic tissue samples (Coucke et al., 2006). Furthermore, increased TGFβ signaling was found in ADCL patients and ADCL mouse model with *ELN* mutations (Callewaert et al., 2011; Hu et al., 2010), a mouse model (Hanada et al., 2007) and patients with fibulin-4 mutations (Renard et al., 2010), and in patients with *ATP6V0A2* mutations (Fischer et al., 2012).

Table 1.1 Heritable disorders associated with TGFβ signaling

Disease	**Mutations**	**Clinical presentations**
Loeys-Dietz Syndrome (LDS)	TGFBR1 and TGFBR2	Severe vascular effects, ocular, skeletal and craniofacial abnormalities
Marfan Syndrome (MFS)	FBN-1	Aortic aneurysms, skeletal and ocular abnormalities
ADCL	ELN	Loose skin, aortic stenosis, pulmonary emphysema
ARLC1/URDS	LTBP4	Developmental delay, redundant, inelastic skin
Arterial tortuosity syndrome	SLC2A10	Cutis laxa with tortuous arteries

1.3 INHERITED DISEASES CAUSED BY ELASTIN MUTATIONS

Elastin gene mutations result in several skin, cardiovascular and pulmonary phenotypes. Elastinopathies, including Williams-Beuren Syndrome (WBS), supravalvular aortic stenosis (SVAS), and autosomal dominant cutis laxa (ADCL) are all caused by the mutations in the *ELN* gene (Ewart et al. 1993; Olson et al.1993; Tassabehji et al., 1998) (Table 1.2). Familial SVAS and ADCL are caused by two distinct groups of point mutations within the elastin gene. In contrast, WBS is caused by the microdeletions of the region on 7q11, which includes the *ELN* gene (Ewart, 1993) and approximately 26-28 other neighboring genes (Pober et al. 2008). The clinical characteristics include intellectual disability, connective tissue defects, metabolic defects, and cardiovascular malformations, including SVAS.

Table 1.2 Elastinopathies

Disease	Mutations	Clinical presentations	Molecular mechanisms
SVAS	Heterozygous loss-of-function mutations	Narrowing or obstruction of the aorta	Haploinsufficiency
WBS	Microdeletions of the region on chromosome 7q11.23; 25-28 genes including *ELN*	Connective tissue and metabolic defects, cardiovascular abnormalities	Haploinsufficiency
ADCL	Heterozygous frameshift mutations	Loose skin, aortic stenosis, pulmonary emphysema	Dominant-negative or toxic gain of function

1.3.1 Autosomal dominant cutis laxa

Cutis laxa (CL) is a heterogeneous group of connective tissue disorders caused by the elastic fiber abnormalities (Berk et al., 2012). Acquired and inherited forms of cutis laxa patients show loose, inelastic, redundant and sagging skin. There are autosomal dominant, autosomal recessive and X-linked recessive inherited forms of CL and each has different clinical manifestations (Berk et al., 2012). Human genetic studies have identified several genes in different forms of cutis laxa comprising A*LDH18A1, ATP6V0A2, ATP7A, EFEMPS/FBLN4, ELN*, *FBLN5, LTBP4, PYCR1* and *RIN2.*

1.3.1.1 Clinical presentation

The ADCL is mostly diagnosed during early childhood, however, it might appear in late childhood or early adulthood. An aged-appearance as a result of redundant and inelastic skin, prominent ears, long philtrum, high forehead, hoarse voice and beaked nose are the most important facial characteristics of ADCL patients (Berk, 2012). Clinical characteristics of ADCL can be mild to benign (Berk et al., 2012). However, severe systemic manifestations can be present including pulmonary emphysema (Rodriguez-Revenga, 2004, Urban et al., 2005), aortic root dilation (ARD) (Szabo et al., 2006), hernia (Szabo et al., 2006) and peripheral pulmonary aortic stenosis (Tassebehji et al., 1998). The pulmonary and aortic lesions can result in significant morbidity and mortality and to date only symptomatic treatments are available. For example, severe pulmonary emphysema was addressed in at least one patient with ADCL using lung transplantation with satisfactory results (Urban et al., 2005). Aortic root dilatation can be delayed by administration of beta-adrenergic blockers and rupture of aneurysms can be prevented by timely aortic root replacement (Szabo et al., 2006).

1.3.1.2 Mutational spectrum

ADCL is mostly caused by frameshift mutations within the last five exons of the *ELN* gene which result in C-terminally elongated and secreted tropoelastin (Rodriguez-Revenga, 2004, Szabo et al., 2006, Tassabehji, 1998, Zhang, 1999, Hadj-Rabia, 2013; Callewaert et al., 2011). Unusual mutations include a heterozygous mutation in exon 25 of the elastin gene (Graul-Neumann, 2008) and tandem duplication in the elastin gene (Urban et al., 2005). A recent *de novo* intronic mutation has been found in intron 31 of a young ADCL patient (Vodo et al., 2015). Approximately 30% of the ADCL patients have *de novo* dominant *ELN* mutations. Recessively inherited missense mutations in *ELN* have been described in one family with cutis laxa to date, suggesting heterogeneity in terms of inheritance patterns in *ELN*-related cutis laxa (Megarbane et al., 2009). Furthermore, identification of a heterozygous tandem duplication in the fibulin-5 gene of a cutis laxa patient raised the possibility of locus heterogeneity in ADCL (Markova et al., 2003).

1.3.1.3 Molecular mechanisms

he mutations in ADCL have several cellular and biochemical effects. Alternative splicing of exon 32 of the *ELN* gene and mutation-induced exon skipping often result in several mutant mRNA isoforms, and this makes harder to analyze the molecular consequences of the ADCL mutations in exons 30-32 (Hu et al., 2010). ADCL mutations produce stable mutant mRNAs, and their protein products are secreted into the extracellular space (Tassabehji et al. 1998; Zhang et al. 1999; Rodriguez-Revenga et al. 2004; Urban et al. 2005; Szabo et al. 2006), albeit with reduced efficiency in some cases (Tassabehji et al., 1998; Urban et al., 2005). The histological abnormalities in ADCL include a disorganized and reduced amount of elastic fibers that result in loss of elasticity in the connective tissue (Szabo et al., 2006). The weak fibrillin-binding capacity

of mutant tropoelastins leads to increased compliance and reduced stiffness of lung tissue (Hu et al., 2010).

A transgenic mouse model expressing human ADCL mutant elastin was generated using a human elastin cDNA with a c.2114_2138del mutation in exon 30 of *ELN* (Hu et al., 2010). ADCL transgenic mouse had healthy skin and blood vessels. However, lung disease including airspace enlargement and severe emphysema was observed. Also, ADCL mice had enhanced endoplasmic reticulum stress, activation of the unfolded protein response (UPR), enhanced apoptosis and increased TGFβ signaling (Hu et al., 2010). Similar findings were found in ADCL patient dermal fibroblasts with exon 30 mutations with longest missense peptide sequence (Callewaert, 2011). Lower amounts of insoluble elastin were found as a result of increased coacervation and elastin globule formation (Callewaert et al., 2011). The partially secreted mutant tropoelastin hinders the binding of tropoelastin to fibulin-5 and fibrillin-1 and results in changes in elastic fiber assembly such as abnormalities in elastin accumulation on microfibrils in ADCL cells (Sato et al., 2006).

A human ADCL mutation (c.2012delG) in exon 30 was introduced into the human elastin bacterial artificial chromosome (BAC), then the mutant BAC was expressed as a transgene in mice with the wild-type human gene (Sugitani et al., 2012). The mutant protein was incorporated into elastic fibers in the skin and lung resulting in some abnormalities, however, relatively low levels of the mutant protein was found in the aorta suggesting tissue-specific effects on elastin assembly (Sugitani et al., 2012). These findings suggest different mechanisms of elastin assembly in aorta and lung and skin (Sugitani et al., 2012).

Enhanced TGFβ signaling has been found in patient fibroblasts (Callewaert, 2011) and in a transgenic mouse model (Hu et al., 2010), however, the precise mechanisms of TGFβ signaling

alterations remain unclear, as does the possible contribution of these changes to the development of ADCL. The exact molecular mechanisms of how *ELN* mutations cause ADCL are still unknown, but dominant negative and toxic gain-of-function mechanisms have been proposed as molecular mechanisms for ADCL (Hu et al. 2010, Callewaert et al. 2011).

1.3.2 Supravalvular aortic stenosis

1.3.2.1 Clinical presentation

SVAS occurs approximately 1 in 5,000 individuals. SVAS can occur as an isolated vascular disease (Eisenberg et al., 1964) or as part of the WBS with identical clinical and structural characteristics (Urban et al., 2001; Micale, 2010). SVAS is characterized by narrowing or obstruction of the ascending aorta (Eisenberg et al., 1964). Segmental narrowing of major arteries such as pulmonary, carotid, cerebral, renal and coronary arteries may also be part of SVAS (Rein et al., 1993; Kaplan et al., 1995). In children, SVAS might result in more severe conditions, such as myocardial infarcts and sudden death (Conway et al., 1990). Systemic hypertension, cerebrovascular accident, myocardial infarction and obstructive cardiomyopathy are the most severe and life-threatening clinical characteristics. Severe forms of SVAS may result in dyspnea, angina, systemic murmur and left ventricular hypertrophy. The primary treatment of SVAS is vascular surgery, which has an increased risk of morbidity and mortality.

1.3.2.2 Mutational spectrum

SVAS can be a part of WBS, a complex developmental genomic disorder, caused by microdeletions of the region on chromosome 7q11.23 encompassing 26-28 genes surrounding *ELN* (Ewart et al., 1993; Pober et al., 2008) or might be isolated. Several mutations consisting

translocations (Curran et al., 1993; von Dadelszen et al., 2000), gene deletions (Ewart et al., 1994; Olson et al., 1995; Fryssira et al., 1997) and point mutations in the *ELN* (Li et al., 1997; Boeckel et al., 1999; Urban et al., 1999, 2000; Metcalfe et al. 2000) lead to the isolated form of SVAS. SVAS is inherited in an autosomal dominant manner. Most of the mutations produce premature termination codons and result in haploinsufficiency through nonsense-mediated decay (NMD) (Urban et al., 2000). If left untreated, SVAS might result in progressive heart failure and death.

1.3.2.3 Molecular mechanisms

Different types of heterozygous loss-of-function mutations in the *ELN* gene lead to SVAS (Urban et al., 2001). As a result of point mutations, translocations and partial deletions in the *ELN* gene, premature stop codons, and unstable mRNA has been observed (Metcalfe et al., 2000; Urban et al., 2000). Decreased levels of elastin mRNA (Urban et al., 2000, 2001) and protein levels as well as the reduced elastin deposition indicate that SVAS is caused by null mutations in *ELN* (Urban et al., 2002) through haploinsufficiency.

Decreased levels of elastin in SVAS arteries leads to enhanced proliferation of vascular smooth muscle cells (Brooke et al., 2003). Hyperproliferation of smooth muscle cells in turn yields thicker, narrower arteries that lack flexibility (Baldwin et al., 2013). Similar to SVAS patients, heterozygous elastin knockout mice (Eln+/-) showed hypertension, enhanced lamellar units in all elastic arteries, enhanced number of SMC layers and decreased elastin amount similar to SVAS patients (Li et al., 1998). Ge et al. generated a human induced pluripotent stem cell (iPSC) model of SVAS to study the mechanism of the disease (Ge et al., 2012). Their model showed that SVAS SMCs had less organized networks of smooth muscle alpha-actin and increased proliferation rate than control iPSC-SMCs. Adding recombinant ELN or decreasing

ERK1/2 activity have been reported as promising therapy, causing inhibition of SMC overproliferation (Ge et al., 2012). Another potential SVAS therapy is rapamycin, an inhibitor of mTOR signaling, which rescues increased SMC proliferation and aortic obstruction (Li et al., 2013). Human iPSCs model of SVAS, SVAS patients, and elastin mutant mice showed enhanced integrin β3 expression and activation (Misra et al., 2016). In addition, the inhibition of integrin β3 rescued aortic hyperproliferation and aortic stenosis, uncovering a potential therapeutic strategy for SVAS patients (Misra et al., 2016).

1.3.3 Comparison of ADCL and SVAS

SVAS and ADCL are two phenotypically different autosomal dominant inherited diseases caused by the mutations in the *ELN* gene. The clinical phenotype of ADCL includes predominantly abnormalities in skin and lung including aged appearance, pulmonary aortic stenosis, emphysema and aortic root dilatation and aneurysms. However SVAS patients have mostly stenoses the aorta and other elastic vessels, such as the pulmonary and coronary arteries. Thus, generally, ADCL predisposes to aneurysms whereas SVAS is associated with stenoses, an opposite vascular phenotype. However a shared vascular manifestation of both disorders is pulmonary artery stenosis (Milewicz et al., 2000).

Loss-of-function mutations including premature stop mutations, large intragenic deletions in SVAS lead to degradation of mRNA through NMD as a result of haploinsufficiency, whereas ADCL-causing mutations yield stable mRNAs and their protein products are secreted into the extracellular space, where the mutant protein interferes with elastic fiber assembly in a dominant-negative manner (Tassabehji et al. 1998; Zhang et al. 1999; Rodriguez-Revenga et al. 2004; Urban et al. 2005; Szabo et al. 2006). In addition, mutant ADCL tropoelastin also activates

the unfolded protein response and apoptosis considered to be a toxic gain of function effects (Hu et al. 2010; Callewaert et al. 2011). ADCL is mostly caused by the mutations within the 3’ end of the *ELN* gene while SVAS mutations are broadly distributed in the *ELN* gene (Figure 1.6).

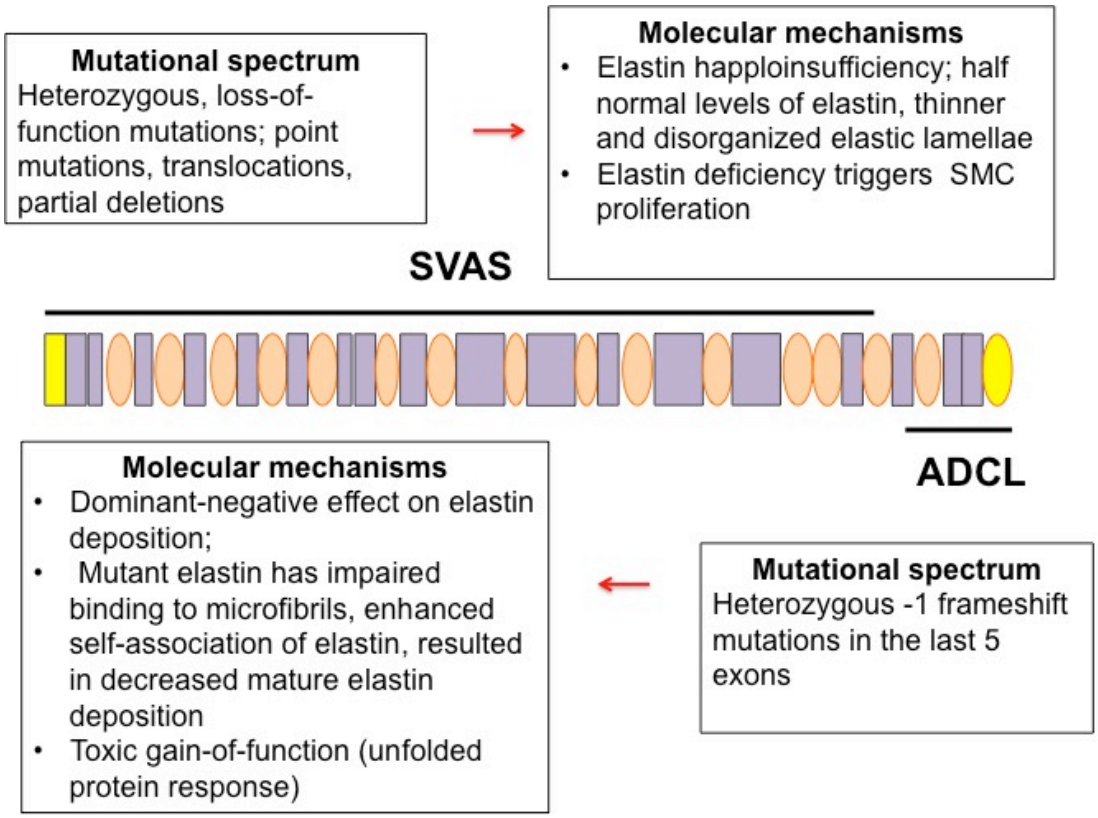

Figure 1.6 Comparison of ADCL and SVAS mutations and molecular mechanisms
ADCL is caused by the mutations within the last 5 exons, whereas SVAS is caused by the mutations broadly distributed throughout the *ELN* gene. The disease mechanism of ADCL is dominant-negative and toxic gain-of-function, whereas the disease mechanism of SVAS is haploinsufficiency.

1.4 SUMMARY

ECM and associated molecules have a myriad of roles comprising cell-cell communication, cell proliferation, and survival. Elastic fibers are integral parts of ECM of the connective tissues such as skin and large arteries. Their function is to provide elastic stretch and recoil to the connective tissues. The elastic fibers are assembled from fibrillin microfibrils and elastin and many accessory molecules facilitate the assembly process such as fibulins, LTBPs and lysyl oxidases. The TGFβ family of growth factors, in addition to its roles in cell differentiation, proliferation, apoptosis and embryonic development, has reciprocal interactions with elastic fibers. On one hand, through LTBPs, elastic fibers sequester and store TGFβ and permit developmentally and physiologically appropriate levels of growth factor activity. However, in disease states, where this sequestration is impaired, excess TGFβ is released and can contribute to the disease process as observed in Marfan syndrome. On the other hand, TGFβ serves as a major signal to enchance the deposition of elastic fibers, as it up-regulates the expression of all major elastic fiber components. Thus, TGFβ sequestration by elastic fibers serves as a negative feedback to limit growth factor signaling once the quality and quantity of elastic fibers is sufficient for tissue function.

Structural abnormalities in elastin lead to a decrease in the integrity of elastic tissues including skin, lungs and large blood vessels. Therefore, elastin gene mutations lead to several skin, cardiovascular and pulmonary phenotypes. Microdeletions of the chromosome 7q11 including the *ELN* gene lead to WBS (Ewart et al., 1993) and characterized by mental retardation, dysmorphic features, and arterial stenosis. Missense and premature truncation mutations throughout the *ELN* gene lead to SVAS (Curran et al., 1993). ADCL is caused by the frameshift mutations at the 3’ end of the elastin gene. Dominant-negative and toxic gain-of-

function are the most important *ELN*-related ADCL mechanisms and haploinsufficiency is the SVAS disease mechanism. However, the exact molecular mechanisms of ADCL and SVAS are still under investigation, especially the potential connection of these disorders to altered TGFβ signaling.

1.5 SIGNIFICANCE

1.5.1 Public Health Significance

Rare diseases affect millions of people worldwide. Some extremely rare diseases only have an impact on a couple of individuals, but there are ones affect thousands or approximately 200,000 people in USA and 1 in every 2000 in Europe. 7,000 rare diseases have been identified to date (Anon, 2013). The spectrum of clinical manifestations has broad diversity and heterogeneity. Approximately 80% of the rare diseases have genetic origin including single or multiple genes and chromosomal abnormalities (Boat et al., 2012). More than 200 connective tissue disorders have been identified to date. Individuals with a rare disease confront a wide range of challenges including diagnostic odyssey, lack of understanding of the natural history of diseases (what to expect), causes of diseases (etiology), insufficient management guidelines for physicians and lack of treatment. Understanding the disease etiology and molecular and physiological mechanisms can improve diagnosis and the development of molecularly targeted treatments, such as enzyme replacement therapy for lysosomal storage diseases, channel potentiators for cystic fibrosis and and exon skipping therapy for Duchenne muscular dystrophy.

The genetic profile of ADCL and SVAS are known, but the genotype and phenotype spectrum is incomplete, and the genotype-phenotype correlations are unclear. Some molecular mechanisms are emerging, however the full impact of these mechanisms on disease development is not understood. My study will improve the understanding of the molecular mechanisms of ADCL and SVAS.

1.5.2 Basic scientific significance

ECM and associated proteins have many mechanical, chemical and biological functions such as cell-cell communication, cell proliferation, migration, cell differentiation, development, and survival. ECM molecules bind and regulate several growth factors such as TGFβ. TGFβ families have roles in cell proliferation, cell growth, inflammation, apoptosis and extracellular matrix production (Santibanez et al., 2011). Defects in TGFβ lead to many pathological conditions such as fibrosis, autoimmune disease and tumor cell growth (Santibanez et al., 2011). Previous studies showed that there is an increased TGFβ signaling in ADCL patients (Callewaert et al., 2011; Hu et al., 2010), but the exact molecular mechanism of the disease still unknown. In this study, we will look for the possible mechanisms of ADCL and TGFβ signaling leading to pathogenesis of the disease and the effects of *ELN* mutations in elastic fibers. Our findings will establish new connections between elastin biosynthesis and growth factor signaling and shed light to the contribution of allelic imbalance to the molecular disease mechanisms in ADCL. In addition, genetic and functional analysis of SVAS will contribute to the molecular mechanisms of elastinopathies.

Uncovering the nature of connections between elastin and growth factor signaling may help developing treatments for cutis laxa that restores correct growth factor regulation and

improve elastic fiber function. In addition, molecular insights into rare diseases might be relevant to common, complex diseases characterized by elastin degradation including aneurysms, chronic obstructive pulmonary disease and emphysema (Robinson et al., 2006; Shifren and Mecham, 2006).

1.6 HYPOTHESIS AND SPECIFIC AIMS

1.6.1 ADCL

ADCL is caused by the mutations in *ELN* the gene and characterized by the loose, redundant and inelastic skin, pulmonary emphysema, aortic root dilation (ARD), hernia and peripheral pulmonary aortic stenosis. My major goal was to identify the molecular and cellular mechanisms caused by which defects in *ELN* gene and its product contribute to the pathogenesis of ADCL. I hypothesized that *ELN* mutations in ADCL patients result in enhanced TGFβ signaling contributing to the pathology of ADCL.

Aim 1. Analyze the cellular consequences of *ELN* mutations and investigate the molecular mechanism of signaling by the TGFβ pathway in *ELN* mutant cells.

Human dermal fibroblasts from ADCL patients with exon 30 or exon 34 mutations in the *ELN* gene and age and sex-matched controls were used to study the alterations in intracellular TGFβ signaling and extracellular TGFβ activity. The expression and activation of TGFβ receptors (TGFBRs) and TGFβ pathway components and target genes were also studied to identify the possible mechanisms of altered TGFβ signaling. Allelic expression of wild-type and mutant alleles and elastin deposition were also analyzed.

Aim 2. Manipulate TGFβ signaling and evaluate the assembly of elastic fibers by wild-type and mutant cells.

TGFβ signaling was manipulated to understand the output of the TGFβ signaling pathway in *ELN*-mutant and control cells. TGFβ was administered to ADCL patient and control cells for ten days, and allelic expression, and elastin assay experiments were performed. This aim helped me determine if TGFβ signaling contributes to the disease, ameliorates it or simply a marker of the disease.

1.6.2 SVAS

SVAS is also caused by the mutations in the *ELN* gene and characterized by narrowing or obstruction of the ascending aorta. I studied an SVAS family segregating an 80 kb duplication which includes 5'-flanking sequences, exon 1 and intron 1 of the *ELN* gene. My primary goal is to solve the exact nature of this duplication and how it may lead to the gene dysfunction. In addition, my studies might shed light into the mutational spectrum of SVAS.

Aim 1. Genetic and functional analysis of SVAS family with a duplication of the *ELN* gene

Dermal fibroblasts from an SVAS family with an 80 kb duplication were used to solve the exact nature of the duplication. Expression analysis of the duplication was performed, and elastin levels were measured in SVAS cells.

2.0 MATERIALS AND METHODS

2.1.1 Cell culture conditions

Dermal fibroblast cells were cultured from control individuals and ADCL and SVAS patients and were maintained in Dulbecco's modified Eagle's medium (DMEM) supplemented with 10% fetal bovine serum (FBS), 1% antibiotic-antimycotic (ABAM), 20 mM 4-(2-hydroxyethyl)-1-piperazineethanesulfonic acid (HEPES) and 45 mM sodium bicarbonate ($NaHCO_3$). All dermal fibroblast cells were incubated at 37 °C, 5% CO_2 in a humid atmosphere, and used at passages 3-6 for ADCL patient and control fibroblasts and 4-6 for SVAS patient and control fibroblasts. The media was exchanged every 48 hours, and the cells were subcultured using 0.05%-0.25% trypsin/ethylenediaminetetraacetic acid (EDTA) solution. As a part of regular quality control procedure, cells were tested for mycoplasma by PCR (Table S1).

2.1.2 DNA isolation

Genomic DNA was extracted from dermal fibroblast cultures using the Gentra PurGene Cell Kit (Qiagen, USA). Briefly, the cells were trypsinized and resuspended in 3 mL Cell Lysis Solution. 15µL RNase A Solution was added, and the sample was incubated at 37°C for 5 min followed by 3 min incubation on ice.

One mL Protein Precipitation Solution was added, and the mixture was centrifuged at 2000xg for 10 min. After adding 3mL Isopropanol, the solution was centrifuged at 2000xg for 3 min. The DNA pellet was washed with 3 mL 70% ethanol, centrifuged at 2000xg for 1 min and air-dried for 10 min. The cell pellet was dissolved in 400 µL DNA Hydration Solution. DNA concentration was measured by UV spectrophotometry, and the concentration was set to 200 ng/µL in all samples. The DNA was stored at -20°C.

Identity test was performed with genomic DNA of all SVAS samples using AmpFlSTR Identifier PCR Amplification Kit using GS500LIZ standard (Applied Biosystems) (Table S2).

2.1.3 RNA purification

Total RNA was extracted from fibroblast cultures using TRIzol reagent (Invitrogen) according to the manufacturer's protocol for large-scale extraction. For homogenization, 1 mL TRIzol reagent was added per 10 cm^2 cell culture dish surface area after washing with PBS and for complete lysis, cells were pipetted up and down many times. 0.1 mL BCP per 1 mL TRIzol reagent was added and after 2-3 min incubation at room temperature, the sample was centrifuged at 12,000xg for 15 min at 4°C. This step separates the sample into a clear top layer with RNA, an interface and a red bottom organic layer with DNA and proteins. The top clear phase was placed into a new tube, and 0.5 mL of 100% isopropanol per 1mL TRIzol reagent was added for RNA precipitation. After 10 min incubation at room temperature, the sample was centrifuged at 12,000xg for 10 min and a gel-like RNA pellet was formed. The RNA pellet was washed with 1 mL 75% ethanol and the sample was centrifuged at 7500xg for 5 min. The pellet was air-dried 5-10 min and was resuspended in 100 µL diethyl-pyrocarbonate (DEPC)-treated water.

RNase-free DNase (Qiagen) treatment was performed to remove DNA from RNA samples before RT-PCR. Briefly, 2.5 μL DNase I stock solution, RNA, and Buffer RDD were mixed and incubated at room temperature (20-25 °C) and the RNA was purified using RNeasy mini kit (Qiagen). RNA concentration was measured by UV spectrophotometry, and the concentration was set to 200 ng/μL.

For small-scale RNA extraction from 6-well plates, RNeasy Mini Kit (Qiagen) was used. 350μL Buffer RLT was added to lyse the cells. Homogenization was performed by pipetting up and down the solution several times and by vortexing for 1 min. To remove the DNA, on-column DNase digestion was performed during RNA purification. After several buffer washes and centrifugation steps, the RNA was eluted in 50μl RNase-free water. RNA concentration was measured by UV spectrophotometry and the concentration was set to 200 ng/μL.

2.1.4 Reverse transcription polymerase chain reaction

cDNA was synthesized from 1 μg total RNA using Superscript III Reverse Transcriptase kit (Invitrogen). First, 1 μL of random hexamers (50ng/μL), 1 μL of dNTPs and the template RNA and DEPC-treated water (up to 10μL) were mixed and the mixture was incubated at 65ºC for 5 min and then placed on ice at least 1 min. cDNA Synthesis Mix was prepared including 2μL 10XRT Buffer, 4μL 25 mM $MgCl_2$, 2μL 0.1 M DTT, 1μL RNaseOUT^{TM} (40 U/μl) and 1μL SuperScript III RT (200 U/μL) and added to each RNA/primer mixture and incubated at 25ºC for 10 min, 50ºC for 50 min and 85ºC for 5 min. After chilling the reaction tubes on ice, 1μL RNase H was added to each tube and incubated at 37ºC for 20 min. The final cDNA was either stored at -20ºC or used for further studies immediately. No template and no RT controls were included as quality controls for SVAS RT reactions used for the analysis of pre-mRNA (Figure 4.4).

2.1.5 Polymerase chain reaction (PCR)

Genotyping was performed to look for heterozygous individuals for allele-specific gene expression studies (SVAS family). 9 SNPs were tested (rs884843, rs868005, rs2071307, rs28763986, rs17855988, rs41500150, rs20062910, rs4556939 and rs4717865) (Table S1). PCR was performed using the Qiagen Multiplex PCR Kit with primers specific to each SNP (Supplementary Table S3). The PCR products were visualized using agarose gel electrophoresis in gels containing 0.35 μg/mL ethidium bromide (Fisher).

2.1.6 DNA fragment analysis

The first-strand cDNA was amplified using fluorescently labeled primers in ADCL patients. The primers used in PCRs are shown in Table 2.1. PCR was performed with the tailed primer (M13-hELNe29-1s) and hELNe34-1a for 10 cycles. A second PCR reaction was performed with 1 μL of previous PCR product using the M13-FAM and hELNe34-1a primers for 15 cycles. 1:10 dilutions of fragments were run with a GeneScan 500 LIZ size standard (Applied Biosystems) on an Applied Biosystems 3730 genetic analyzer (Applied Biosystems). The data were processed using Peak Scanner software (Applied Biosystems) (Table 2.1, Figure 2.1). To determine the exponential range of the PCR, different cycles ranging from 20-40 were used in pilot experiments and cycle numbers 28-30 were determined to be within the exponential range; therefore, cycle number 30 was used in subsequent experiments. Another pilot experiment was performed to see whether TGFβ treatment affects the allelic expression of wild- type and mutant alleles using 5 different time points including 1-day, 2-day, 4-day, 10-day and 15-day.

Table 2.1 Primers used in ADCL fragment analysis

Name of primers	Primer sequence (5'➔3')	Tm
M13-hELNe29-1s	/5-M13/AGCCAAAGCTGCTGCCAAAG	68.9
hELNe34-1a	CATGGGATGGGGTTACAAAG	58.5
M13-FAM	/56-FAM/GCTCACGACGTTGTTAAACGAC	56.6
hELNe29-1s	AGCCAAAGCTGCTGCCAAAG	59.2

Genotyping for a tetranucleotide repeat in intron 1 (Urban et al., 1997) was performed on genomic DNA (gDNA) and cDNA from fibroblasts of each indicated individual using fluorescently labeled primers shown in Table 2.2. First PCR reaction was performed with hELNi1.11s and hELNi1.11a primers for 20 cycles. A second PCR reaction was performed with 5'-FAM-hELNi1.3s and hELNi3.1a for 30 cycles.

Table 2.2 Primers used in SVAS fragment analysis

Name of primers	Primers sequence (5'➔3')	Tm
hELNi1.11s	GAGAAAAGTAAATGGGGCCA	52.8
hELNi1.11a	AATCACCACCTCCAAATGCT	54.6
5'-FAM-hELNi1.3s	/56-FAM/GCCCACATGGGCAGATTGCT	61
hELNi3.1a	CCCTCATCCACAGACAGGTC	57.2

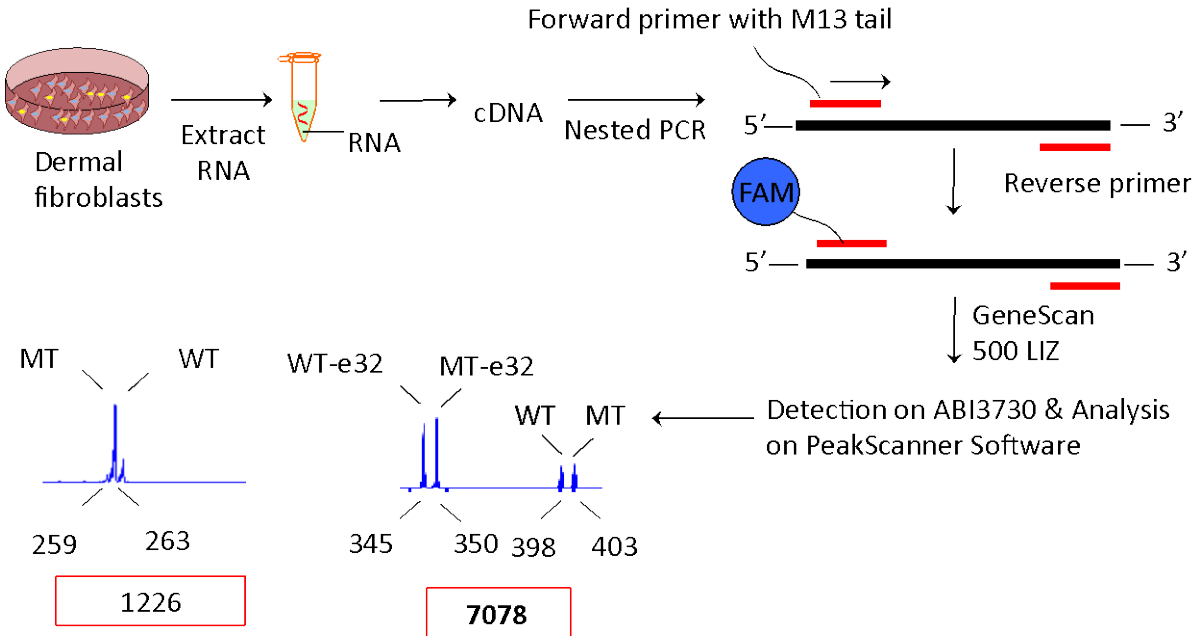

Figure 2.1 DNA fragment analysis experiment
RNA was extracted from dermal fibroblasts and cDNA was synthesized. PCR was performed using tailed and fluorescently-labeled primers, fragments were run with a GeneScan 500 LIZ standard on ABI3730 genetic analyzer.

2.1.7 Quantitative PCR

Q-PCR was performed to determine the expression of *ELN, TGFBR1, TGFBR2, CTGF, PAI1, TGFB1, SMAD6* and *SMAD7* in ADCL patients and control individuals. Real-time PCR was performed using the QuantStudio 12K Flex Real-Time PCR System (ThermoFisher Scientific). An inventoried TaqMan ® Gene Expression Assay (Applied Biosystems) was used for each gene. The reaction mix was prepared including 4.5µL cDNA, 5µL Taqman Universal Master Mix II, with UNG and 0.5µL 20x FAM dye-labeled TaqMan Gene Expression Assay. The reagents were pipetted into a 384-well plate. The plate was briefly centrifuged before running under the following conditions (Table 2.3).

Each sample was run with 3 biological and 4 technical replicates and Ct measurements for each sample were normalized to a housekeeping control gene, GAPDH. The comparative Ct method ($2^{-\Delta\Delta Ct}$) was used to determine the relative expression of the previously described genes in *ELN*-mutant and control human dermal fibroblasts.

Table 2.3 Q-PCR conditions

	UNG Incubation	**Polymerase Activation**	**Denaturation**	**Annealing/Extension**
Temperature (ºC)	50	95	95	60
Time	2 min	10 min	15 sec	1 min
Cycles	1	1	40	

2.1.8 Topo TA cloning

To identify the mutant *ELN* mRNA transcripts of patients with mutations in exon 34 (c.2236-7C>A), cDNA samples were prepared from dermal fibroblast cultures using the Superscript III Reverse Transcriptase kit (Invitrogen) as described above. PCR was performed using primers complementary to exon 29 (hELNe29-1s) and exon 34 (hELNe34-1a) (Table 2.1). PCR products were cloned into a TOPO TA vector (Invitrogen) and transformed using TOP10 competent *Escherichia coli* (*E-coli*) cells (Invitrogen) according to the manufacturer's instructions (Invitrogen). The colonies were selected and grown overnight in LB broth containing 50 μg/mL ampicillin. Plasmid DNA was isolated using the Qiaprep Spin Miniprep Kit (Qiagen).

2.1.9 DNA sequencing

Plasmid DNA (100 ng/μL) was mixed with 4 μL water and 3 μL of the primer (0.8 μM). 10 μl of PCR product was treated with 1μl exonuclease I, shrimp alkaline phosphatase (ExoSAP-IT, Thermo Fisher) and incubated 37°C for 40min to remove unincorporated primers and dNTPs, followed by 15 min at 80°C to inactivate the enzymes. The treated PCR product (4 μL) was mixed with 3.5 μL water and 3 μL primer (0.8 μM). Plasmid DNA or PCR product mixtures were sent for sequencing to Eurofins MWG Operon. The sequences were analyzed using the Sequencher v5.2.4 software.

2.1.10 Fastin elastin assay

The colorimetric Fastin Elastin Assay (Biocolor) was carried out in accordance with the manufacturer's instructions to quantify the amount of soluble elastin. Between 5 μg and 70 μg elastin could be measured with this assay. Human dermal fibroblasts were harvested 1 week after confluence from 60 mm dishes by scraping and insoluble elastin was converted to a soluble form by incubating the cell suspensions at 100 °C in 0.25M oxalic acid for 1 hour. α-elastin standards (0, 12.5, 25.0 and 50.0 μL) were prepared. The extract and the α-elastin standards were treated with Elastin Precipitating Reagent and the tubes were centrifuged at 10,000 g for 10 minutes. One mL of dye reagent was added into each tube. After a 90-minute incubation, the tubes were centrifuged at 10,000 g for 10 minutes and unbound dye was drained off. Dye Dissociation Reagent (250 μL) was added to each tube, and the samples were then transferred to a transparent 96-well plate to measure the absorbance at 513 nm, using GeNIOS plate reader (Tecan) (Figure 2.2).

A pilot Fastin elastin assay was also performed to see if TGFβ treatment affects elastin deposition in ADCL and control dermal fibroblasts. TGFβ was administered in cells cultured in 60 mm dishes in 5 different time points including 1, 2, 4, 10, and 15 days. Parallel cell cultures for each time point were used and the elastin concentration was normalized by cell numbers. The number of cells were counted by Cellometer Mini Cell Counter (Nexcelom). Based on the results of this pilot experiment, a 10-day TGFβ treatment was performed, and elastin levels were quantified.

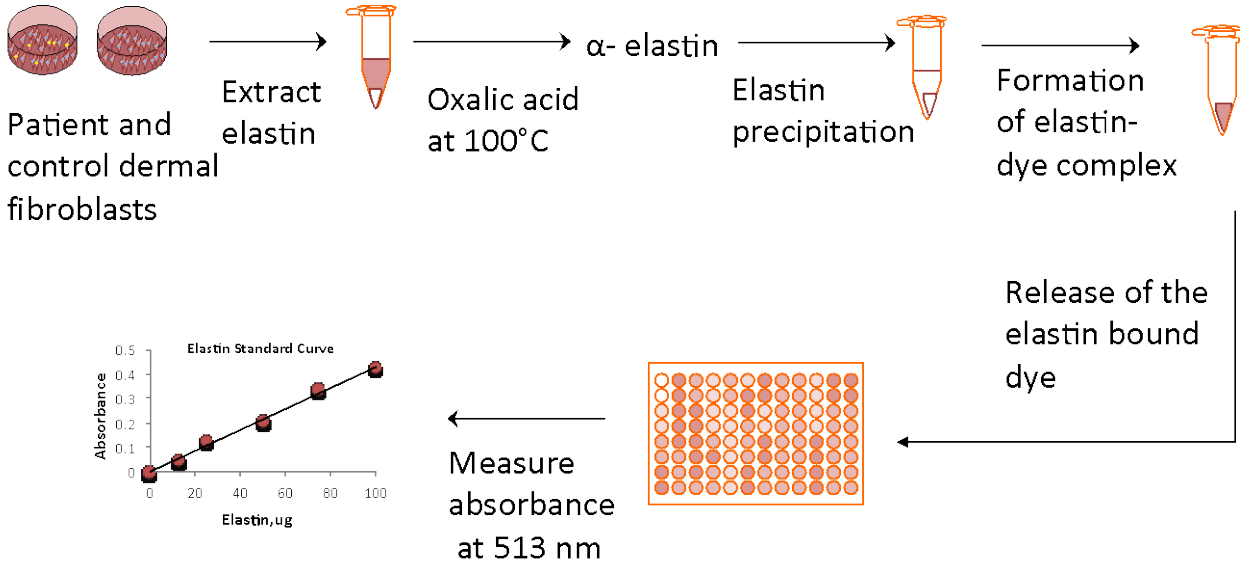

Figure 2.2 Fastin elastin assay
Elastin is extracted from dermal fibroblasts and the sample is heated at 100 C to extract the elastin as alpha elastin. Following the precipitation of elastin with the Elastin Precipitating Reagent, an elastin-dye complex was formed by adding the Dye Reagent. To release the elastin bound dye, Dye Dissociation Reagent was added and elastin concentration was measured at 513 nm.

2.1.11 Protein extraction

To study intracellular pathways, cell lysates were collected from dermal fibroblasts using lysis buffer (CelLytic™ M, Sigma) with Protease and Phosphatase Inhibitors (1:100) (Sigma). Briefly, the plates were incubated with 500 µL lysis buffer per 10 cm plate 40 min at 4°C on a shaker and were detached from the plates by scraping with chilled cell scrapers. Glass homogenizers were used to complete the cell lysis and the samples were centrifuged for 20 min, at 13200 rpm, at 4°C.

The Mem-PER™ Plus Membrane Protein Extraction Kit (Thermo Scientific) with Protease and Phosphatase Inhibitors (1:100) was used to collect membrane proteins. Adherent, dermal fibroblasts were washed with the Cell Wash Solution twice in 10 cm plates and were scraped in 3 mL Cell Wash Solution After the cell pellet was centrifuged at 300xg for 5 min, cell pellets were resuspended in 500 µL Cell Permeabilization Buffer by vortexing and incubated 10 min at 4°C with intermittent mixing. Following a 15-minute centrifugation at 16000xg, the pellets containing membrane proteins were resuspended in 250 µL Solubilization Buffer and incubated at 4°C for 30 min with intermittent mixing. The mixture was centrifuged at 16000xg for 15 min at 4°C and the supernatant containing the membrane proteins were collected.

To calculate the protein concentration, a Bradford assay (Zor T., et al. 1996) was performed. Briefly, a standard curve was prepared diluting the albumin standards (1000 µg/mL, 100 µg/mL and 10 µg/mL) and the absorbance was measured at a wavelength of 595 nm and the cell lysate or membrane protein concentrations were determined using the standard curve.

2.1.12 Immunoblotting

For the baseline conditions, cells were left in serum-free or serum-containing (10% FBS) media overnight, and cell lysates were collected. TGFβ1 (PeproTech, Rocky Hill, NJ) and TGFBR1 inhibitor (LY364947; Calbiochem) were prepared in tissue culture medium at concentrations of 5 ng/mL and 25 μM, respectively, and cells were treated for 90 minutes.

Proteins were separated by size by sodium dodecylsulfate polyacrylamide gel electrophoresis (SDS-PAGE). The samples were mixed with Laemmli Sample Buffer (2X, Bio-Rad) with 1% β-mercaptoethanol or Lithium Dodecyl Sulfate (LDS) Sample Loading Buffer (4X, Thermo Scientific Pierce). The cell lysates were denatured at 95°C for 5 min and the membrane proteins were incubated at room temperature for 30 min. The samples and protein size markers were loaded on the gel, and subjected to electrophoresis at 90V for 90 min. After electrophoresis, the proteins were transferred to a polyvinylidine fluoride (PVDF) membrane at 80V for 120 min in a Bio-Rad Mini Trans-Blot® Electrophoretic Transfer Cell. When the transfer was finished, the PVDF membranes were removed, washed in PBST (1x PBS, 0.1% Tween-20) and non-specific binding sites were blocked in blocking buffer (PBS with 0.1% Tween 20 containing 5% non-fat milk powder) at 4°C overnight or 2 hours at room temperature. To detect the proteins of interest, the membranes were incubated at 4°C overnight with the primary antibody (Table 2.4). Membranes were washed 5 times for 10 min in PBST (1xPBS-0.1% Tween 20) and incubated with secondary antibodies for 1 hour at room temperature (Table 2.4). After final washes with PBST (5X for 10 min), immunoreactive signals were detected with SuperSignalWest Pico Chemiluminescent Substrate (Thermo Scientific), SuperSignal West Femto Maximum Sensitivity Substrate (Thermo Scientific) or Luminata Forte Western HRP Substrate (Millipore).

Table 2.4 Antibodies for immunoblotting

Antibody		Species	Dilution	Manufacturer/Cat.No.
Primary	pSMAD2	Rabbit polyclonal	1:1000	Cell Signaling; 3101
	pERK	Rabbit polyclonal	1:1000	Cell Signaling; 197G2
	pSMAD3	Rabbit polyclonal	1:1000	Cell Signaling; 9520
	pJNK1	Rabbit polyclonal	1:1000	Cell Signaling; 4668
	pP38	Rabbit polyclonal	1:1000	Cell Signaling; 9211
	pTGFBR1	Rabbit polyclonal	1:500	Abcam; ab112095
	TGFBR1	Rabbit polyclonal	1:1000	Cell Signaling; 3712
	TGFBR2	Rabbit polyclonal	1:500	Sigma; SAB4502958
	TGFBR3	Rabbit polyclonal	1:1000	Cell Signaling; 2519
	Tubulin	Mouse monoclonal	1:1000	Sigma; T8203
Secondary	Anti-rabbit	Goat polyclonal	1:10,000	Thermo; PAI-20391
	Anti-mouse	Goat polyclonal	1:10,000	Jackson & Immunology

2.1.13 TGFβ activity assay

Cultured mink lung epithelial cells (MLECs) stably transfected with a plasmid construct with a TGFβ-responsive plasminogen activator inhibitor-1 promoter connected to a luciferase cDNA (Abe et al., 1994) were used as reporter cells to measure the activity of TGFβ. MLECs grown in DMEM with 2% FBS were plated in 96-well plate ($2x10^5$ cells/mL) and incubated 6 hours.

Conditioned medium was collected and used untreated to measure active TGFβ and an aliquot was heat-activated (10 min at 100°C) to measure total TGFβ levels. A standard curve was generated with decreasing concentrations of TGFβ1 (PeproTech) starting from 2000 pg/mL. The media from MLECs were removed and replaced with different concentrations of TGFβ1, conditioned media samples and heat-activated media samples and the plate was incubated overnight at 37°C. The media were aspirated, the cells layer were washed with PBS, and were lysed using the Reporter Lysis Buffer (Promega). The luciferase activity was measured in a plate reader as relative light units (RLU). RLU values were converted to TGFβ activity using the TGFβ standard curve.

2.1.14 Statistics

Means and standard errors of means (s.e.m) were calculated, and either paired or unpaired, two-tailed student's t-tests were used to compare means, as specified in the figure legends. The number of replicates for each experiment is also shown in the figure legends. GraphPad Prism 6 software was used for statistical tests. Results with p values < 0.05 were considered to be statistically significant.

3.0 MOLECULAR CONSEQUENCES OF ELASTIN GENE MUTATIONS IN AUTOSOMAL DOMINANT CUTIS LAXA

3.1 RESULTS

3.1.1 Mutations

Dermal fibroblasts from ADCL patients with ELN mutations in exon 30 and exon 34 were selected, with 4 cell lines each (Figure 3.1, Table 3.1). The predicted protein products of mutations in exon 30 and exon 34 gene are shown in Figure 3.2. A matching control fibroblast line was selected for each ADCL cell line. ADCL/control pairs were perfectly matched for passage, and 63% matched by sex. The maximum age difference between cases and controls was 9 years. The mean age difference was 1 years and the difference was not significant statistically (t-test).

The identities of the mutant mRNA products in the cells with c.2336-7C>A mutation in exon 34 were determined by cloning RT-PCR products and sequencing them. We found that there was a TCCAG insertion between exon 33 and exon 34 as a result of the activation of a cryptic splice site (c.2335_2336insTCCAG). All ADCL cell lines had frameshift mutations except one with a missense mutation in exon 34 (p.G779D). Two cell lines (7009 and 7002) were from patients published previously (Szabo et al., 2006). Mutation p.G779D has been reported previously (Hu et al., 2006 and Kelleher et al., 2005) in other patients. The mutations of in

patients 7157, 7159, 7078, 7304 and 7164 are first reported here. The mean ages for patients with mutations in exon 30 and 34 were 16 and 26.5 years, respectively, but the difference was not significant statistically (t-test). The passage numbers were also not significantly different between the 2 ADCL groups. Chi-square test was performed to see if the sex is different between patients with exon 30 mutations and patients with exon 34 mutations and found that there was not a statistically significant difference in sex between 2 ADCL groups.

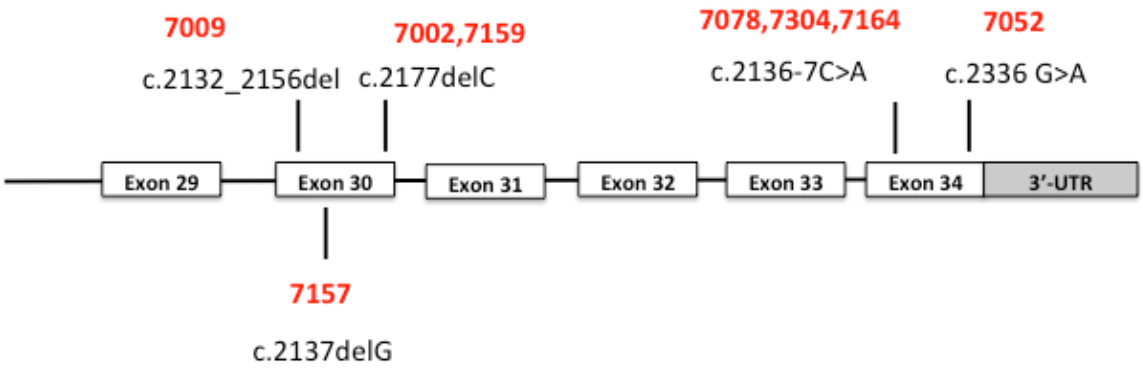

Figure 3.1 Schematic representation of the 3'-end of *ELN* with the location of the mutations identified in each patient
The patient identification numbers are shown in red and the corresponding mutations are in black.

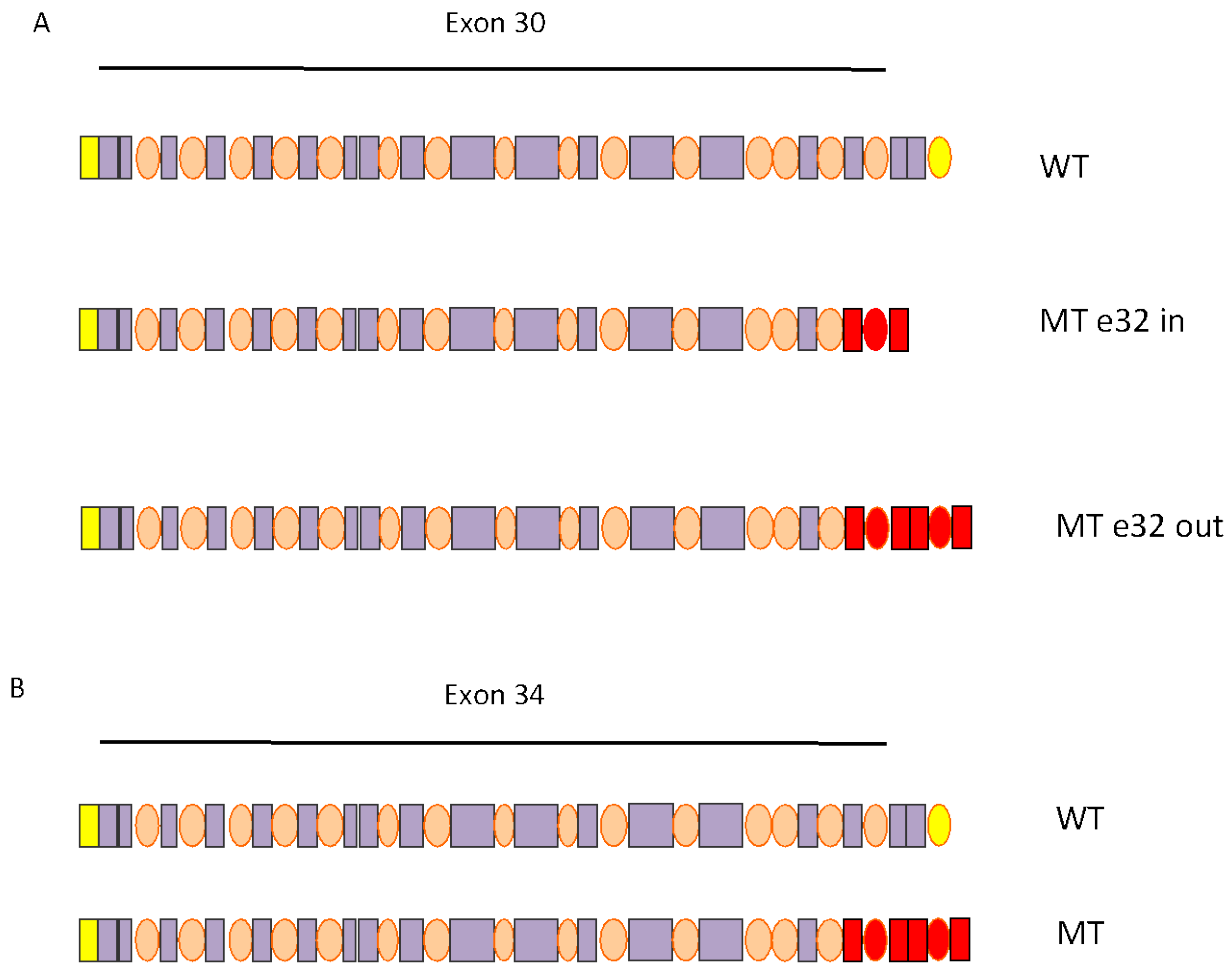

Figure 3.2 Predicted protein products of ADCL mutations located in exon 30 and exon 34 compared to wild-type (WT) tropoelastin
Purple rectangles: hydrophobic domains, orange ovals: crosslinking domains, yellow rectangle: signal peptide, yellow oval: C-terminal domain, red: domains translated in reading frame 3. A: protein products of ADCL mutations located in exon 30. Note that when exon 32 is retained, it contains a premature termination codon in this frame (MT e32 in). However, when exon 32 is skipped as a result of an alternative splicing event, which occurs in 75% of the transcripts, reading frame 3 extends past the normal termination codon found in reading frame 1 (MT e32 out). B: protein products of ADCL mutations located in exon 34.

Table 3.1 *ELN* mutations in subjects

ID	Exons	cDNA	Genomic	Protein
7009	30	c.2132_2156del	g.35443_35466del	p.G711fs*36,p.G711fs*82
7157	30	c.2137delG	g.35448delG	p.A713fs*42,p.A713fs*88
7002	30	c.2177delC	g.35488delC	p.P726fs*29, p.P726fs*75
7159	30	c.2177delC	g.35488delC	p.P726fs*29, p.P726fs*75
7078	34	c.2336-7C>A	g.40463C>A	p.G779Vfs*42
7304	34	c.2336-7C>A	g.40,463C>A	p.G779Vfs*42
7164	34	c.2336-7C>A	g.40463C>A	p.G779Vfs*42
7052	34	c.2336G>A	g.40470G>A	p.G779D

cDNA and protein numbering are based on transcript ENST00000358929. In addition, exon 30 mutation names at the protein level are also shown based on ENST00000358929 with exon 32 deleted to reflect common alternative splicing of this exon.

Table 3.2 ELN mutant and control cells used in the study

ID	Age (years)	Sex	Passage Number
7009	12	Male	P5
9215 (CRL-2211)	9	Female	P5
7157	6	Female	P5
9175	12	Female	P5
7002	2	Female	P6
9214 (CRL-1509)	0	Male	P6
7159	44	Female	P4
9173	35	Female	P4
7078	30	Male	P5
9001	31	Male	P5
7304	40	Male	P3
9001B	37	Male	P3
7164	23	Male	P4
9063	26	Female	P4
7052	13	Female	P5
9175	12	Female	P5

3.1.2 Increased expression of the mutant allele in ADCL

To evaluate the consequences of ADCL mutations, I checked first whether the mutations in exon 30 and exon 34 affect the overall *ELN* expression levels. Quantitative RT-PCR showed a decreased *ELN* mRNA expression in patients with exon 30 mutations and an increased *ELN* mRNA expression in patients with exon 34 mutations compared to controls (Figure 3.3A). However, with the two patient groups combined, no significant difference was found in the total *ELN* mRNA expression of ADCL cells compared to controls (Figure 3.3B).

Because the expression of the mutant allele relative to wild type allele could influence the severity of the disease, I sought to analyze allelic expression in the samples. Consistent with previous studies showing increased abundance of mutant mRNA in ADCL patients (Callewaert et al., 2011), I found higher levels of mutant mRNA in all patients except a patient with a c.2177delC mutation where the increase in the expression of the mutant allele did not reach statistical significance (Figure 3.4). In one patient (7052), I could not differentiate between WT and MT alleles, because she had a missense mutation in exon 34 (c.2336G>A), thus the mutant product could not be distinguished from the normal by size (data not shown). The allele sizes for each patient either with exon 30 or exon 34 mutations are shown in Table 3.3.

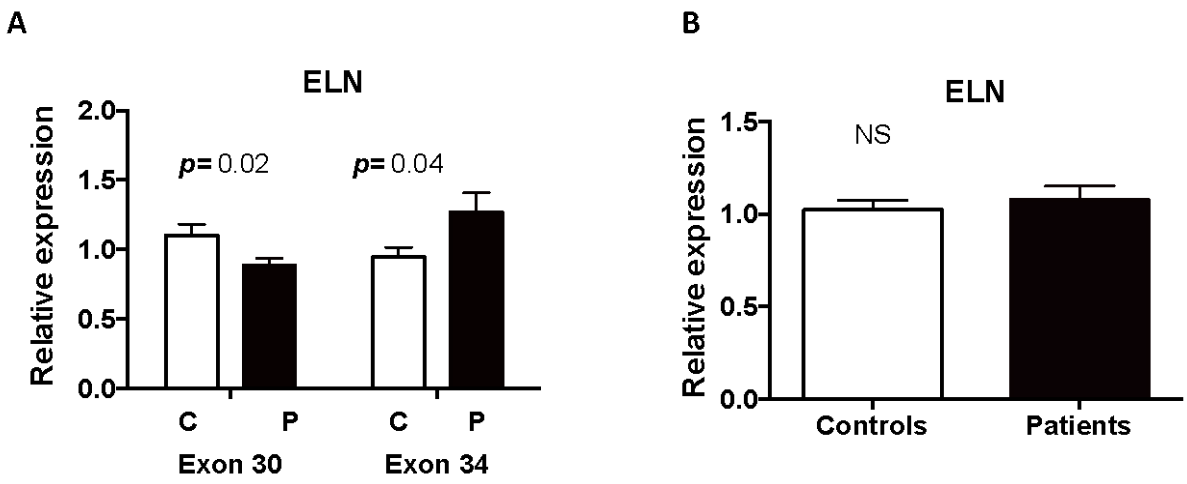

Figure 3.3 *ELN* mRNA levels among patients and controls
A: Quantitative RT-PCR shows a decreased ELN mRNA expression in exon 30 patients and increased ELN mRNA expression in exon 34 patients. B: No significant difference was found in ELN mRNA levels by combining exon 30 and exon 34 patients and controls. Data are means ± s.e.m of 3 biological replicates and 4 technical replicates were used in each individual. The reference gene was GAPDH. Unpaired t-tests were used to compare the expression levels of controls and patients with p values shown above each graph. This experiment was performed once. C: controls, P: patients.

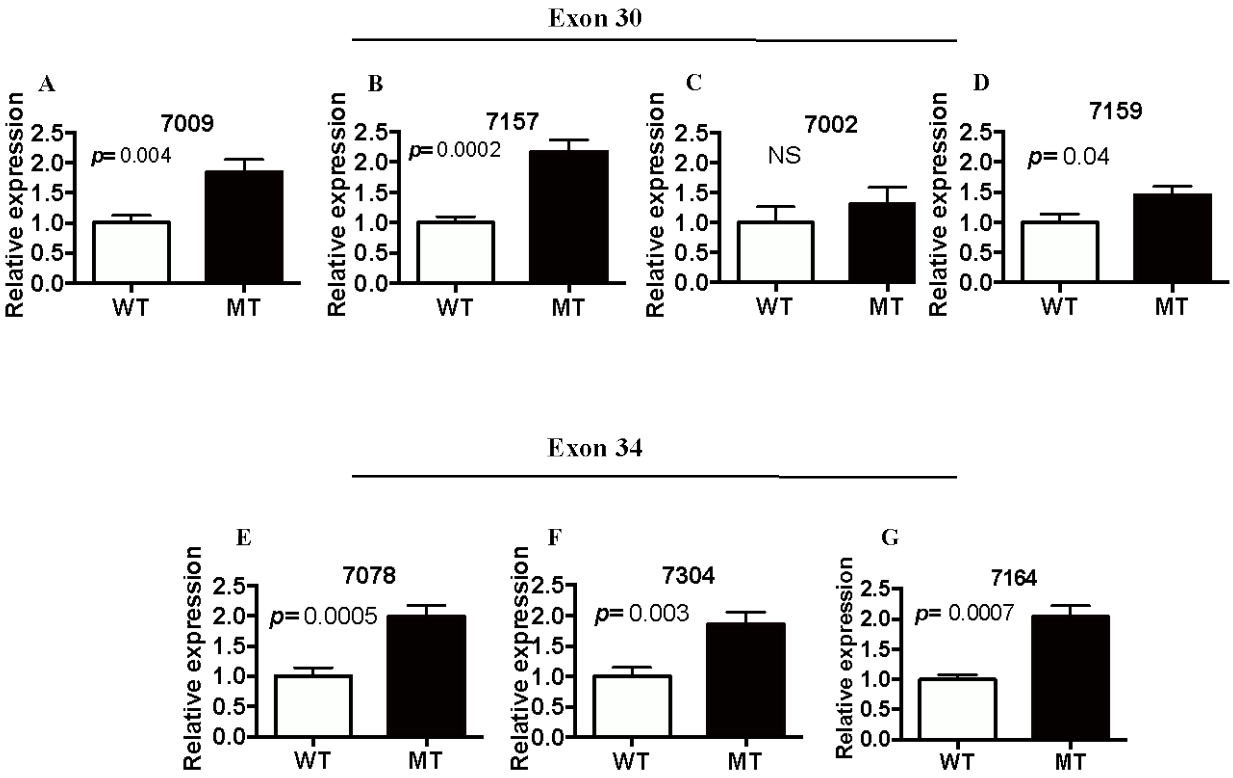

Figure 3.4 Semiquantitative fragment analysis of mRNA products of wild type and mutant alleles

A-G: Increased relative expression of mutant and wild type alleles in patients with mutations in patients with exon 30 and 34 mutations in *ELN* gene. A-D: patients with exon 30 mutations, E-G: patients with exon 34 mutations.Wild-type and mutant transcripts were studied in each indicated individual using fluorescently labeled primers. The products were sized and quantified using a genetic analyzer and the Peak Scanner software. Allele intensities were normalized to average wild type (WT) allele signals in each sample. Data are means ± s.e.m of 3 biological replicates and 3 technical replicates in each individual. WT allele intensity was compared to mutant (MT) allele intensity using unpaired 2-tailed t-tests with the p-values shown above each graph. This experiment was performed twice with similar results.

Table 3.3 Allele sizes for each ADCL sample based on fragment analysis

Sample	Full Length WT	Full length MT	WT-e32	MT-e32
7009	398 bp	374 bp	345 bp	321 bp
7157	398 bp	397 bp	345 bp	344 bp
7002	398 bp	397 bp	345 bp	344 bp
7159	398 bp	397 bp	345 bp	344 bp
7078	398 bp	403 bp	345 bp	350 bp
7304	398 bp	403 bp	345 bp	350 bp
7164	398 bp	403 bp	345 bp	350 bp

3.1.3 Reduced elastin deposition in ADCL

Previous studies showed approximately 25-35% reduction in the levels of elastin in ADCL patients compared to control cells (Callewaert et al., 2011). Fastin elastin assay detected significantly lower amounts of elastin (33% reduction in patients with exon 30 mutations and 24% reduction in patients with exon 34 mutations) in our ADCL cells compared to controls, confirming elastin deposition is impaired in our samples (Figure 3.5).

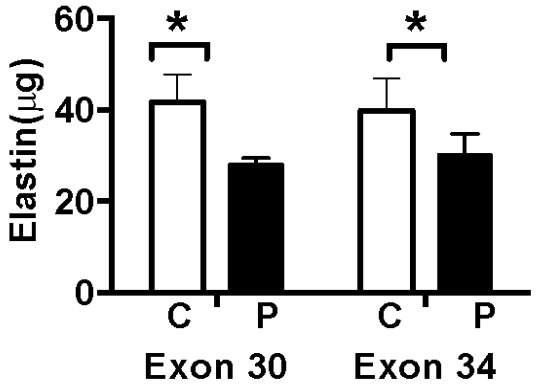

Figure 3.5 Reduced elastin deposition in patients with exon 30 and exon 34 mutations
Fastin elastin assay was performed to measure the elastin from ADCL and matched control fibroblasts. Data are means ± s.e.m of 3 biological and 3 technical replicates in each individual. * $P<0.05$ using the unpaired student's t-test. C: controls; P: patients. This experiment was performed twice with similar results.

3.1.4 Increased canonical TGFβ signaling in ADCL patients with exon 30 mutations

In previous studies, increased TGFβ signaling, as measured by increased levels of SMAD2 phosphorylation was observed in ADCL patients with *ELN* mutations (Callewaert et al., 2011). To understand the molecular mechanisms of these changes and Eln is intermittently involved in TGFβ signaling, I studied canonical (SMAD-dependent) and non-canonical (SMAD-independent) pathways in ADCL samples. Protein lysates from patients with exon 30 and exon 34 patients and age and sex matched controls were used and immunoblotting was performed using pSMAD2 and pSMAD3. In patients with exon 30 mutations, SMAD2 phosphorylation was increased under serum and serum-free baseline conditions (Figure 3.6A and B) and remained increased upon TGFβ supplementation (Figure 3.6C). TGFBR1 inhibitor treatment abolished the difference in SMAD2 phosphorylation between patients and controls (Figure 3.6D). No significant difference was found in pSMAD3 levels under the 10% serum condition (Figure 3.6A), but SMAD3 phosphorylation was increased under the serum-free condition (Figure 3.6B) and remained increased upon TGFβ supplementation (Figure 3.6C). TGFBR1 inhibitor treatment abolished the difference in SMAD3 phosphorylation between patients and controls (Figure 3.6 D).

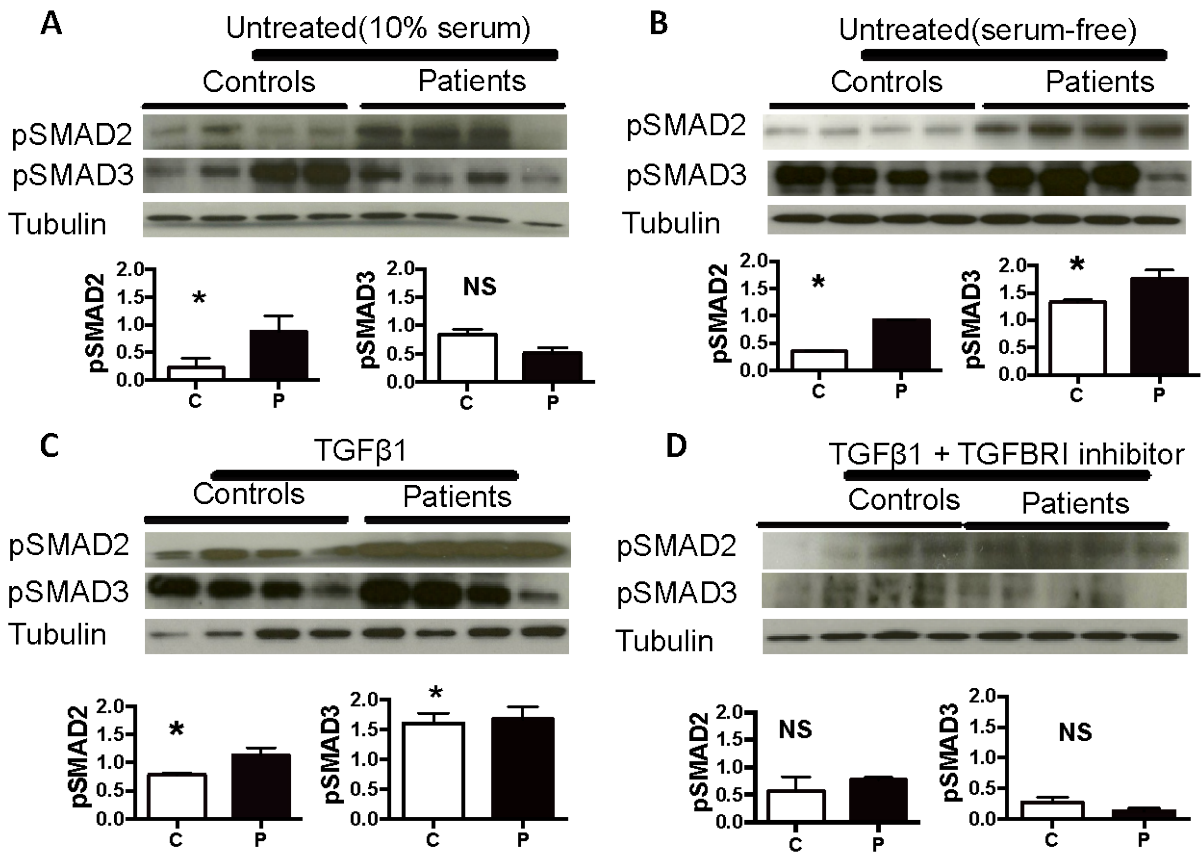

Figure 3.6 Increased canonical TGFβ signaling in patients with exon 30 mutations
Immunoblotting of protein extracts from dermal fibroblasts under the following conditions: A-B: untreated (10% serum and serum-free), C: TGFβ1 stimulation for 90 min or D: TGFβ1 and TGFBR1 inhibitor for 90 min in patients with exon 30 mutations. Immunoblots were quantified by densitometry. pSMAD2: phosphorylated SMAD2; pSMAD3: phosphorylated SMAD3, NS: non-significant. Bar graphs show the mean ± s.e.m. * $P<0.05$: obtained from t-test. C: controls (n=4); P: patients (n=4). This experiment was performed once.

To investigate whether increased TGFβ signaling is a shared mechanism in *ELN*-related cutis laxa, I analyzed the 4 patients with exon 34 mutations and 4 control dermal fibroblasts. No significant difference was observed in the levels of pSMAD2 and pERK levels between patient and controls under any treatment conditions (Figure 3.7).

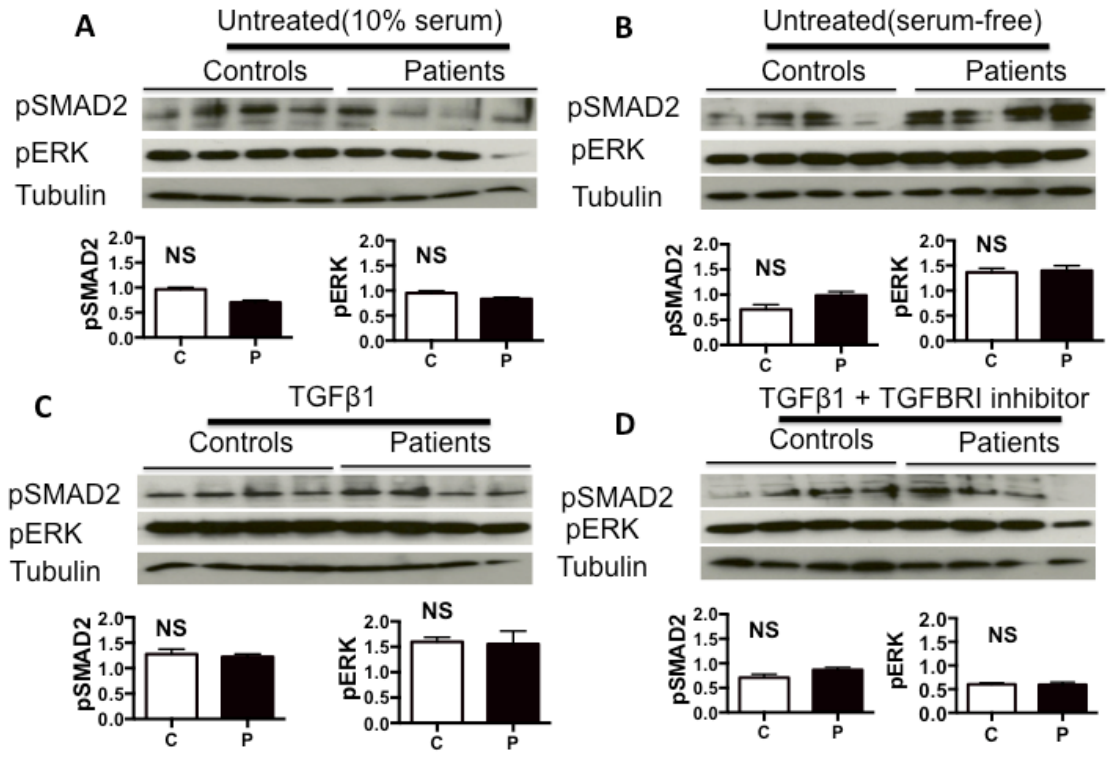

Figure 3.7 Normal TGFβ signaling in patients with exon 34 mutations

Immunoblotting of protein extracts from dermal fibroblasts under the following conditions: A-B: untreated (10% serum and serum-free), C: TGFβ1 stimulation for 90 min or D: TGFβ1 and TGFBR1 inhibitor for 90 min in patients with exon 34 mutations. Immunoblots were quantified by densitometry. pSMAD2: phosphorylated SMAD2; NS: non-significant. Bar graphs show the mean ± s.e.m. * $P<0.05$: obtained from t-test. C: controls (n=4); P: patients (n=4). This experiment was performed once.

3.1.5 TGFβ activity in exon 30 mutant cells

As we found an increased canonical TGFβ signaling in ADCL, we wanted to test if this was related to any alterations in the levels of extracellular TGFβ. Conditioned media samples were collected from 4 mutant and 4 control fibroblast cell lines to measure active and total TGFβ levels. TGFβ reporter cells (Abe et al., 1994) were used for activity measurements. To assay for total TGFβ, samples were heated (100°C, 10 min) to activate latent TGFβ prior to adding them to MLECs. Neither active nor total forms of TGFβ showed any significant difference between mutant and control cells (Figure 3.8), although there was a trend towards lower activity in patients. Therefore, increased intracellular TGFβ activity in patient cells was not explained by commensurate changes in extracellular growth factor activity.

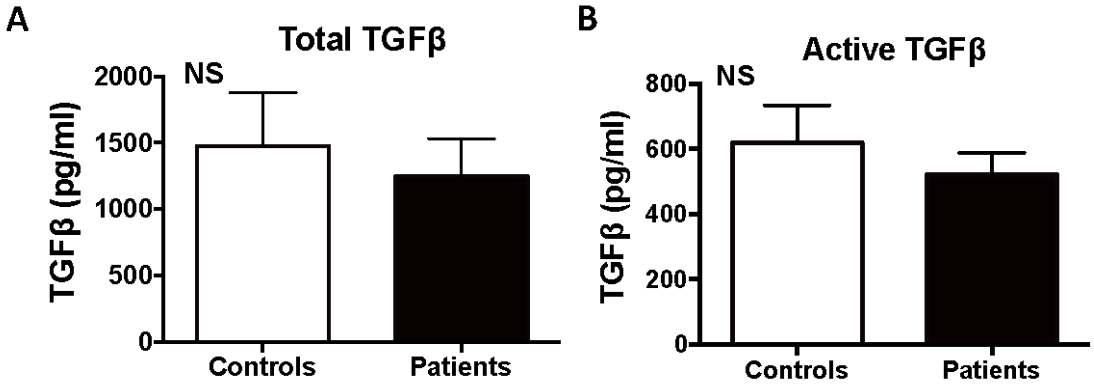

Figure 3.8 TGFβ activity in conditioned media of controls and exon 30 mutant dermal fibroblasts
A: Total TGFβ; B: Active TGFβ. The t-test was used for statistical analysis, error bars represent the standard error of the mean values (SEM). NS: non-significant. Controls (n=4); Patients (n=4). This experiment was performed once.

3.1.6 Non-canonical TGFβ signaling in exon 30 mutant cells

We also tested for other non-canonical signaling pathway components including pJNK1, pP38 and pERK to see if there were any changes in the activation of these molecules at the protein level. P38 and JNK1 phosphorylation were not changed between patient and controls under any treatment conditions (Figure 3.9). The level of pERK was slightly decreased in mutant cells under serum-free condition and upon TGFβ treatment (Figure 3.9B and Figure 3.9C), but no significant difference was observed in pERK between mutant cells and controls treated with 10% serum or a TGFBR1 inhibitor (Figure 3.9D).

Overall, our results showed elevated canonical, but unaffected non-canonical TGFβ signaling despite unaltered extracellular TGFβ activity in exon 30-mutant cells, whereas cells with *ELN* mutations in exon 34 had normal TGFβ signaling. Our results indicate mutation-specific TGFβ signaling changes in *ELN*-related cutis laxa patients.

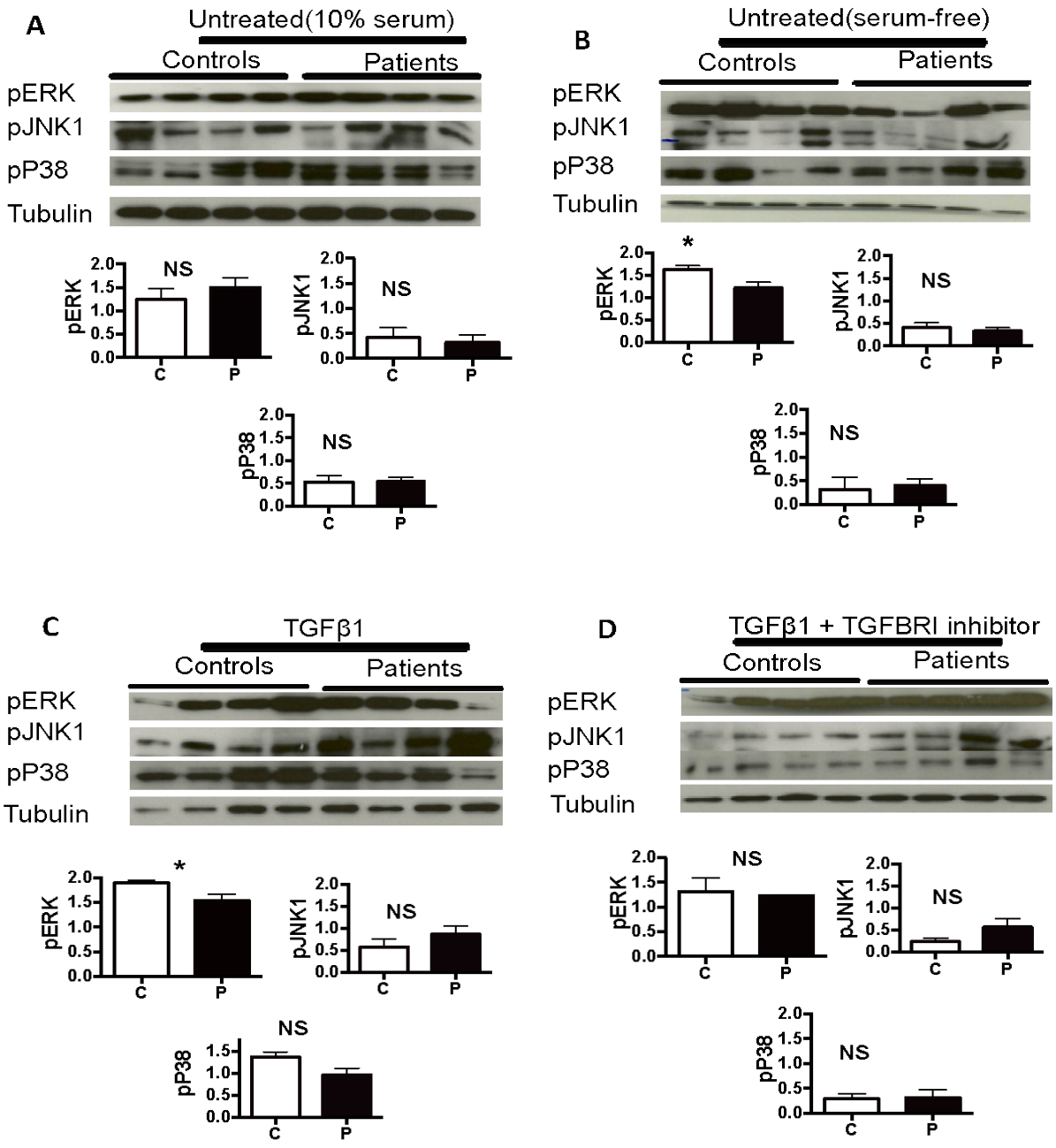

Figure 3.9 Largely normal non-canonical TGFβ signaling in patients with exon 30 mutations

Immunoblotting of protein extracts from dermal fibroblasts under the following conditions: A-B: untreated (10% serum and serum-free), C: TGFβ1 stimulation for 90 min or D: TGFβ1 and TGFBR1 inhibitor for 90 min in patients with exon 30 mutations. Quantitative data normalized by the loading control are shown below the blots. NS: non-significant. Bar graphs show the mean ± s.e.m. * P<0.05: obtained from t-test. C: controls (n=4); P: patients (n=4). This experiment was performed once.

3.1.7 The expression of TGFβ receptors at the protein and RNA levels

To investigate if changes in TGFβ receptor expression could explain the increased TGFβ activity in ADCL fibroblasts, membrane proteins from 4 patients and 4 controls were extracted, and immunoblotting was performed using pTGFBR1, TGFBR1, TGFBR2, and TGFBR3. TGBFR1 and pTGFBR1 levels were increased in *ELN*-mutant cells in both baseline conditions (Figure 3.10A and Figure 3.10B) and remained increased relative to the controls upon TGFβ supplementation (Figure 3.10C). TGFBR1 inhibitor treatment abolished the in pTGFBR1 and TGFBR1 abundance (Figure 3.10D), suggesting abnormal auto-regulation of TGFBR1 in mutant cells. These findings were consistent with the increased SMAD2 phosphorylation levels under the same conditions. There was no significant difference in TGFBR2 and TGFBR3 levels between control and patients groups under any of the treatment conditions (Figure 3.10). Thus, elevated TGFβ signaling in exon 30 mutant cells was associated with increased levels of pTGFBR1 and TGFBR1, but not TGFBR2 or TGFBR3.

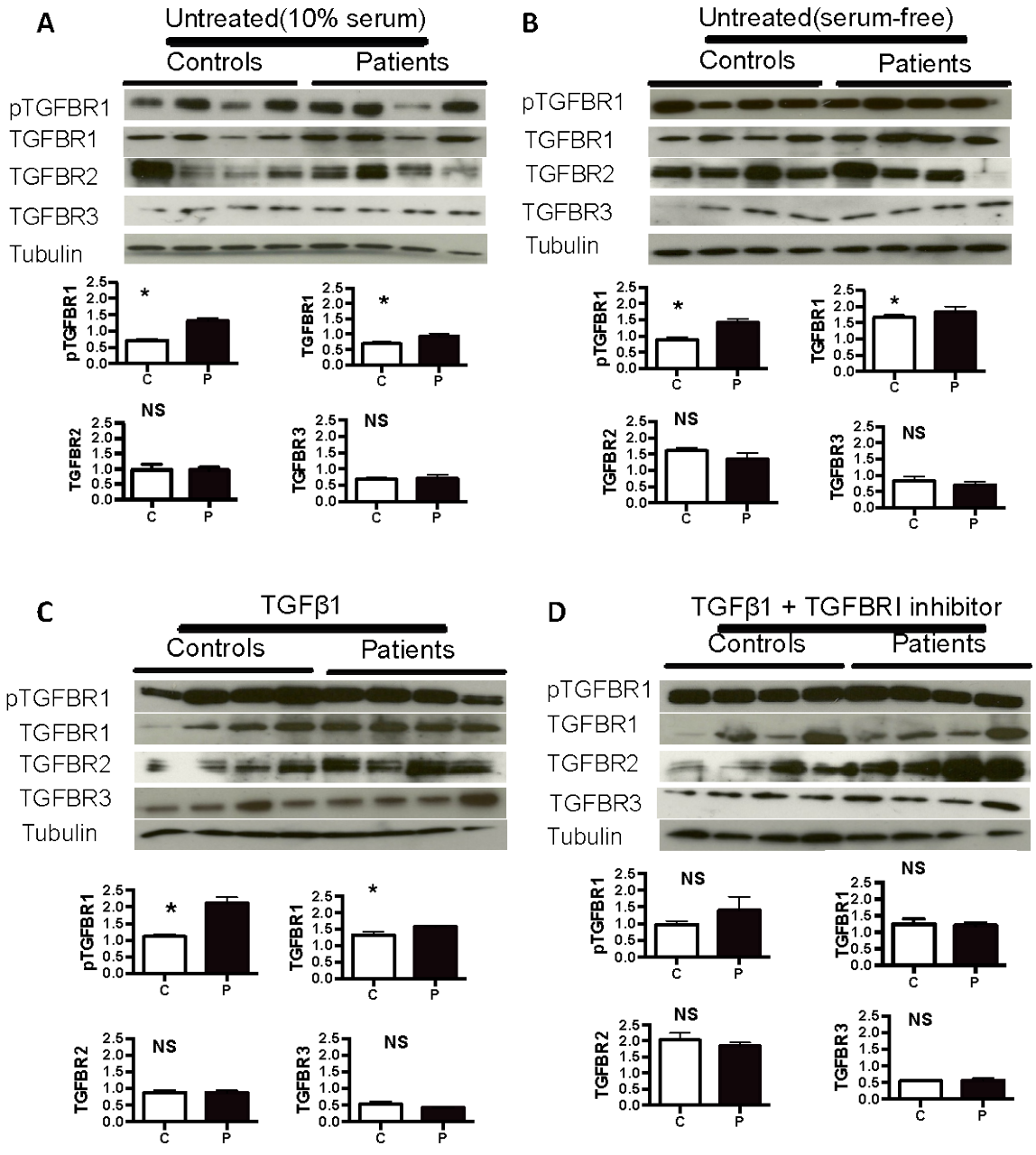

Figure 3.10 Increased pTGFBR1 and TGFBR1 abundance in patients with exon 30 mutations

A-B: Immunoblotting of membrane protein extracts from dermal fibroblasts left untreated (10% serum and serum-free), C: treated with TGFβ1 or D: with TGFβ1 and TGFBR1 inhibitor. Immunoblots were quantified by densitometry. Tubulin served as a loading control. pTGFBR1: phosphorylated TGFBR1. Quantitative data normalized by the loading control are shown below the blots. Bar graphs show the mean ± s.e.m. *: Statistically significant as demonstrated by $p < 0.05$ obtained with a *t*-test, NS: non-significant. C: controls (n=4); P: patient (n=4). This experiment was performed once.

Because we found increased TGBFR1 levels at the protein level, I wanted to test whether there is an enhanced TGBFR1 level at the mRNA level. Q-PCR was performed to measure the mRNA levels of TGFBR1 and TGBFR2 under baseline conditions. TGFBR1 mRNA levels were increased in mutant cells (Figure 3.11A) however, no significant difference was found in the expression of TGFBR2 levels in patients and controls (Figure 3.11B).

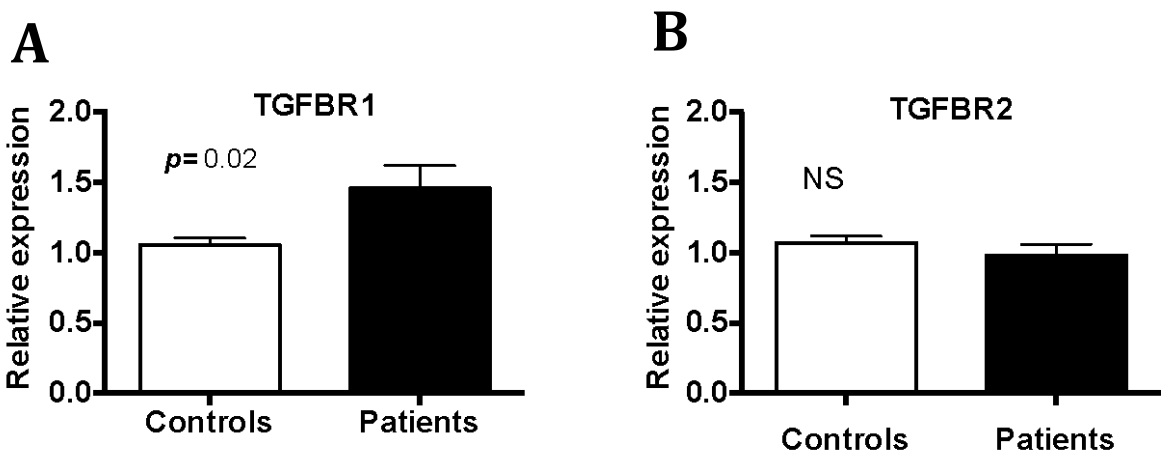

Figure 3.11 Increased *TGFBR1* mRNA levels in ADCL patients with exon 30 mutations
Quantitative RT-PCR showed A: increased *TGFBR1* mRNA expression in patients compared to controls. B: same *TGFBR2* mRNA expression in patients and controls. Bar graphs show the mean ± s.e.m 3 biological replicates and 4 technical replicates. The reference gene was *GAPDH*. RNA expression levels were compared between controls and patients using unpaired t-tests with the p values shown above each graph. NS: non-significant. This experiment was performed once.

3.1.8 Expression of TGFβ pathway components and target genes

To further probe the activity of the TGFβ signaling pathway, I tested if there were any changes in the expression of key TGFβ pathway components and target genes. *CTGF* mRNA levels were slightly increased in patients with exon 30 mutations; however, there was no significant difference in the expression of *TGFB1* and *PAI1*. *SMAD6* and *SMAD7* mRNA expression was decreased by about 50% in ADCL patients (Figure 3.12).

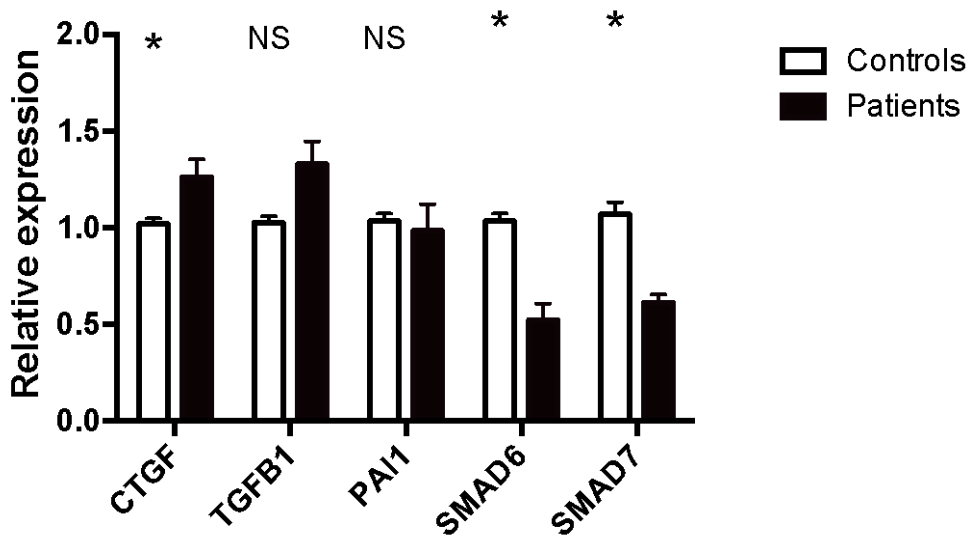

Figure 3.12 Q-PCR analysis of *CTGF, TGFB1, PAI1, SMAD6* and *SMAD7* in patients with exon 30 mutations
Data are means ± s.e.m of 3 biological replicates and 4 technical replicates. The reference gene was *GAPDH*. Unpaired t-tests were used to compare the expression levels of controls and patients. *: Statistically significant as demonstrated by $p<0.05$, NS: non-significant. This experiment was performed once.

3.1.9 Normalized allelic expression upon long-term TGFβ treatment

A pilot experiment was performed to see whether TGFβ treatment affects the relative expression of wild-type and mutant alleles. No difference was found between WT and MT alleles upon TGFβ treatment in 30 min, 90 min, 4 hr, 8 hr and 24 hr when compared to untreated levels of WT and MT alleles (data not shown). These time periods might be too short to reflect the differences in the allelic expression, so I extended the TGFβ treatment time points to 1 day, 2 days, 4 days, 10 days and 15 days. TGFβ treatment for 10 days resulted in normalized allelic expression in cell line 7159 (Figure 3.13), so I administered TGFβ to each of the the dermal patient fibroblasts for 10 days, which consistently normalized the expression of the mutant allele in each (Figure 3.14).

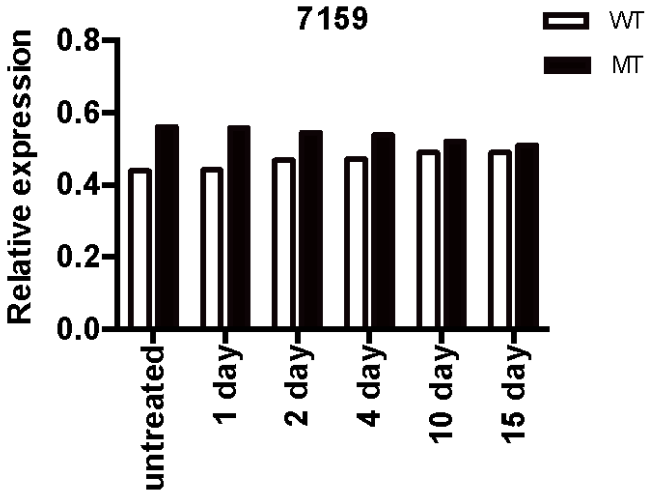

Figure 3.13 A pilot experiment with different TGFβ treatment time points
TGFβ was administered to patient cell line 7159 for 1 day, 2 days, 4 days, 10 days and 15 days and mRNA products of wild-type and mutant alleles were studied at each indicated time point using fluorescently labeled primers. The products were sized and quantified using a genetic analyzer and the Peak Scanner software.

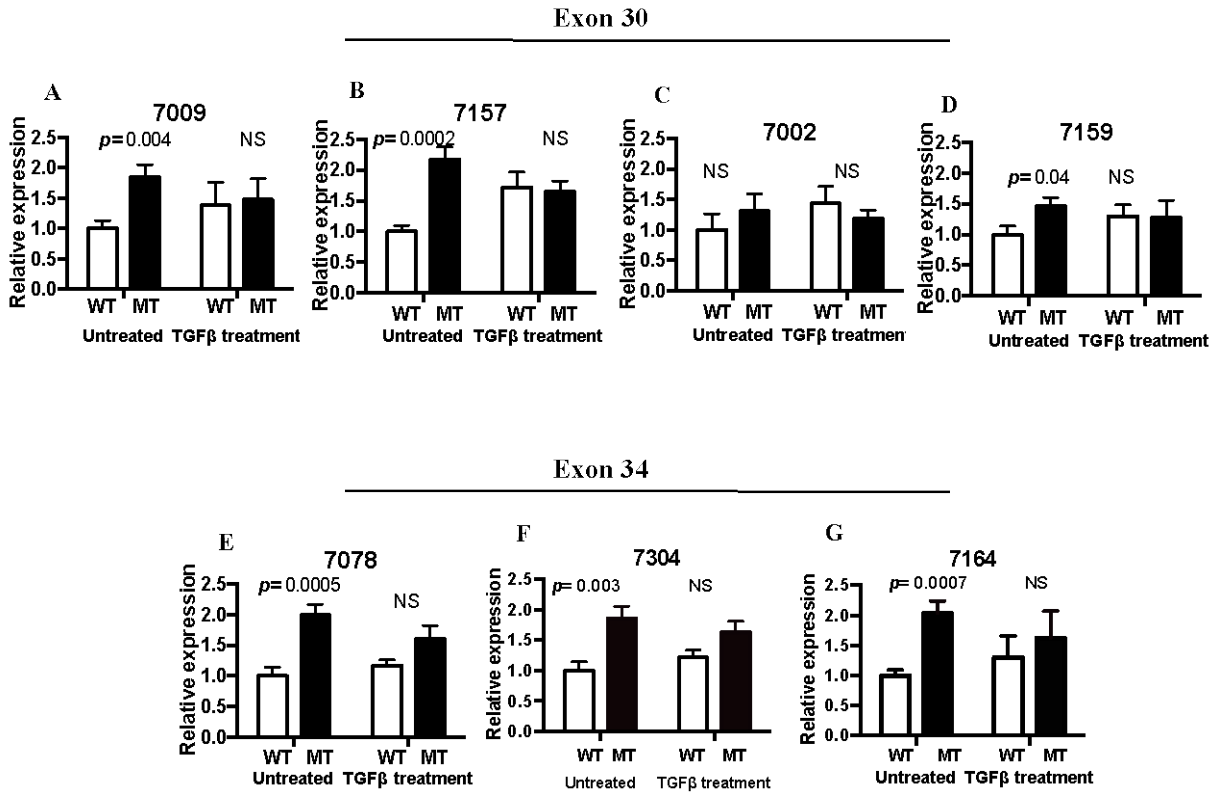

Figure 3.14 Normalized allelic expression upon long-term TGFβ treatment

A-G: Long-term TGFβ treatment normalized allelic imbalance in the expression. A-D: patients with exon 30 mutations, E-G: patients with exon 34 mutations. mRNA products of wild-type and mutant alleles were studied in each indicated individual using fluorescently labeled primers. The products were sized and quantified using a genetic analyzer and the Peak Scanner software. Allele intensities were normalized to average of the untreated wild type (WT) allele signals in each sample. Data are means ± s.e.m of 3 biological replicates and 3 technical replicates in each individual. WT allele intensity was compared to mutant (MT) allele intensity using unpaired 2-tailed t-tests with the p values shown above each graph. NS:non-significant. This experiment was repeated once with similar results.

We also identified the relative expression of mRNA products of wild-type and mutant alleles in patients with exon 30 and exon 34 mutations in the elastin gene either untreated or TGFβ treatment (All patients showed four different mRNA isoforms: a normal full length mRNA, a shortened mRNA isoform missing exon 32 due to alternative splicing, a mutant full length mRNA and a mutant shortened mRNA isoform missing exon 32. Normal dermal fibroblasts expressed two mRNA isoforms as a result of alternative splicing of exon 32 (data not shown). Upon 10-day TGFβ treatment, we found an increase in the WT mRNA isoforms and a decreased MT mRNA isoforms (Figure 3.15).

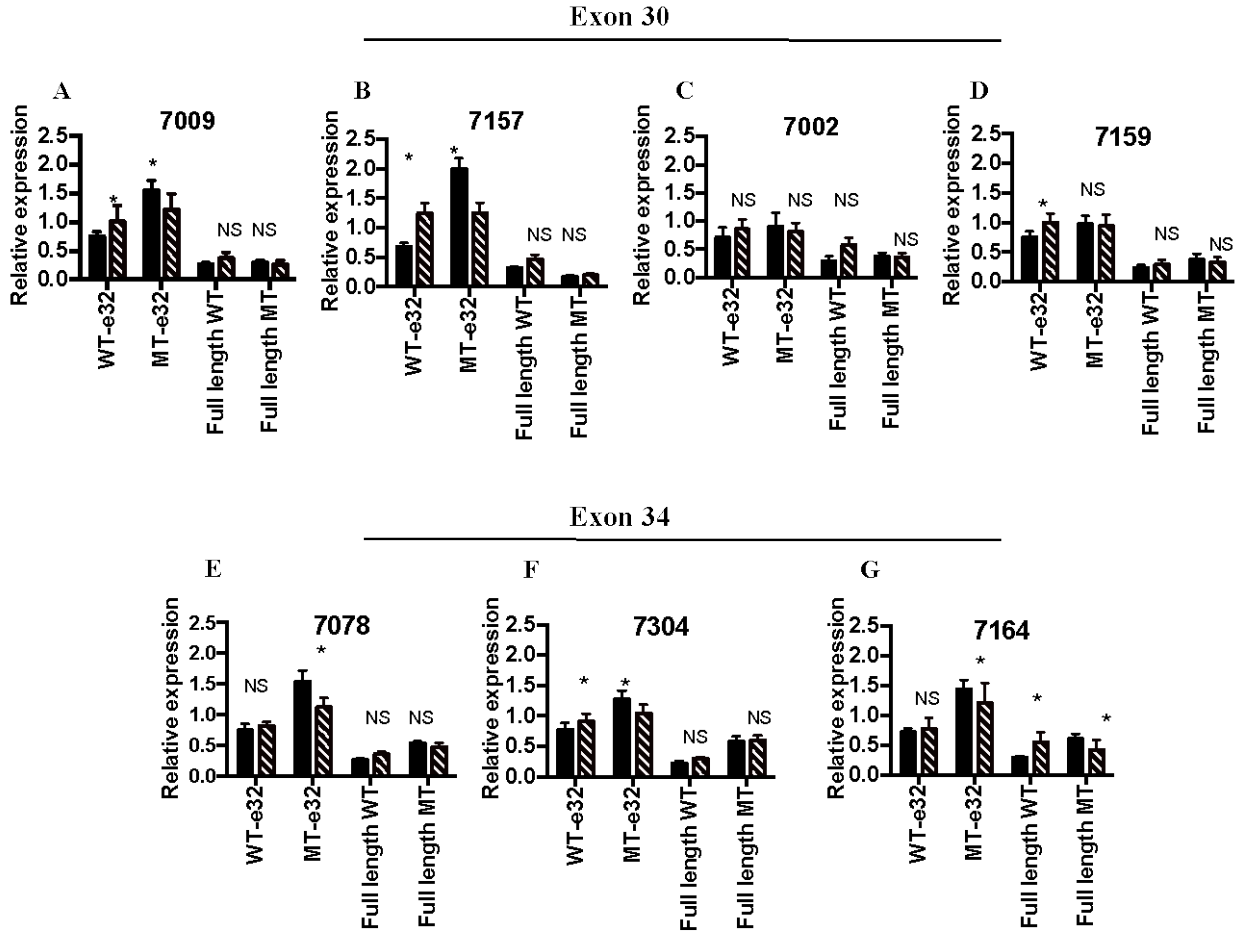

Figure 3.15 Relative expression of *ELN* transcripts

Relative expression of splicing products in patients with exon 30 and exon 34 mutations with and without TGFβ treatment. A-D: patients with exon 30 mutations, E-G: patients with exon 34 mutations. mRNA products of wild-type and mutant alleles were studied in each indicated individual using fluorescently labeled primers. The products were sized and quantified using a genetic analyzer and the Peak Scanner software. Allele intensities were normalized to average wild type (WT) allele signals in each sample. Data are means ± s.e.m of 3 biological replicates and 3 technical replicates in each individual. Unpaired t-tests were used and *: statistically significant as demonstrated $p<0.05$; NS: non-significant. MT:mutant ; e32: exon 32. This experiment was performed once with similar results.

3.1.10 Improved elastin deposition in ADCL cells upon long-term TGFβ treatment related to increased cell number

A pilot experiment was performed to see whether TGFβ affects the elastin deposition in ADCL cells. Dermal fibroblasts were subjected to TGFβ treatment for 1 day, 2 days, 4 days, 10 days and 15 days. We observed an increase in the number of patient cells upon TGFβ treatment; however, the number of control cells remained unchanged. Based on the results, 10-day TGFβ treatment was chosen, which the TGFβ treated levels of elastin in a patient fibroblast reached the untreated levels of elastin in a control dermal fibroblast (Figure 3.16).

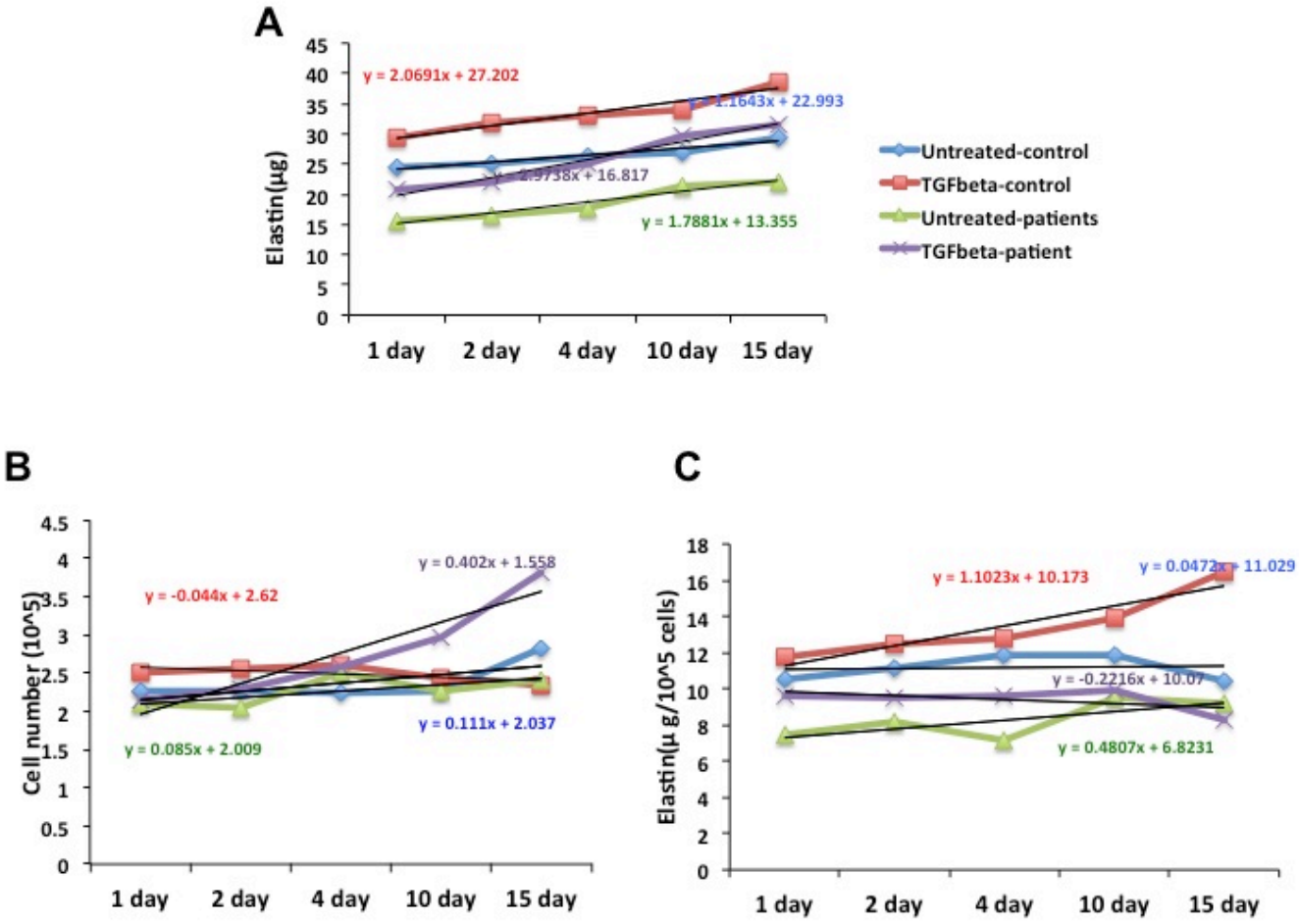

Figure 3.16 Pilot TGFβ treatment experiment with different time points in a patient with exon 30 mutation and a matched control.

TGFβ was administered to a control (9175) and a patient (7159) dermal fibroblast for 1 day, 2 days, 4 days, 10 days and 15 days. Cell numbers were counted by Cellometer Mini Cell Counter. Fastin elastin assay was performed to measure the elastin levels. Elastin concentration was normalized by cell numbers.

Ten day TGFβ supplementation enhanced elastin levels in controls and ADCL patients with exon 30 and exon 34 mutations (Figure 3.17A and Figure 3.17D). Parallel cell cultures were used to count the cells in untreated and TGFβ treated dermal fibroblasts. An increase was observed in the number of cells in ADCL patients, whereas no change was observed in cell numbers of control individuals (Figure 3.17B and Figure 3.17E). Normalization by cell numbers indicated that increased elastin deposition in ADCL cells was primarily caused by increased cell numbers, not increased elastin production per cell (Figure 3.17C and Figure 3.17F).

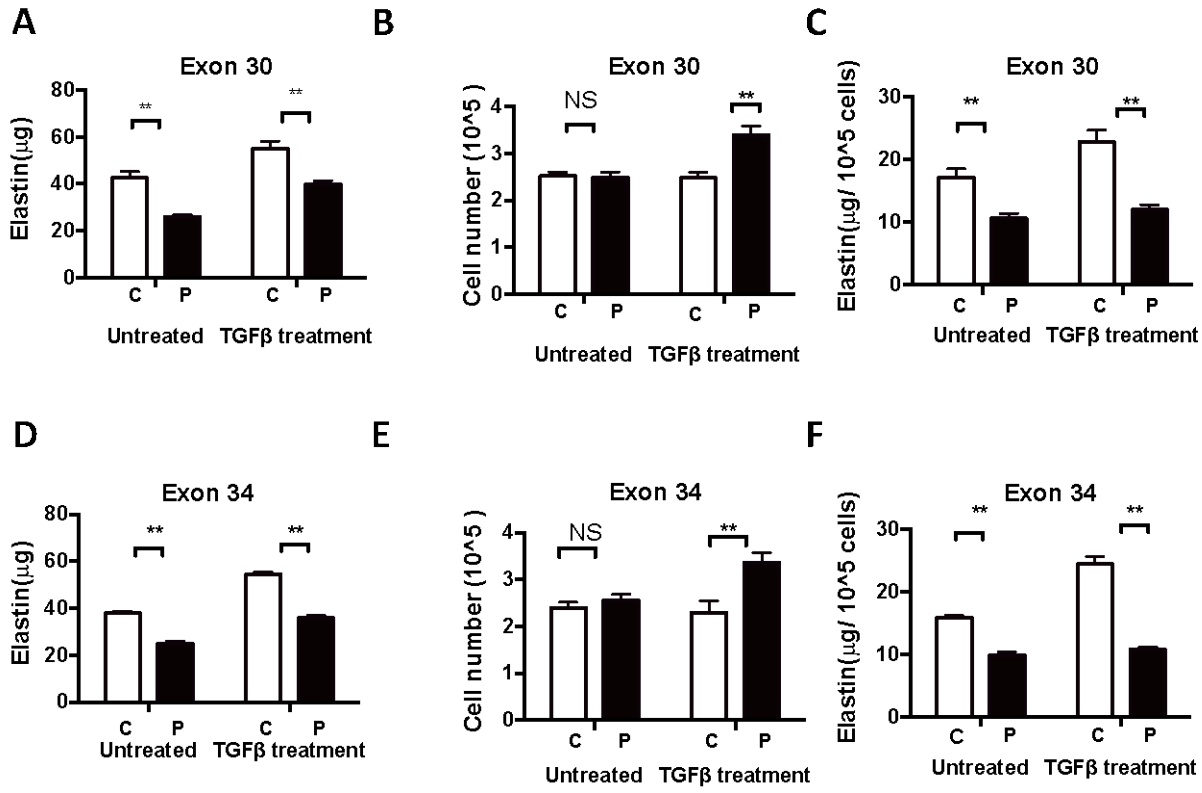

Figure 3.17 Improved elastin deposition in ADCL cells upon long-term TGFβ treatment related to increase cell number

A,D: Fastin elastin assay was performed to measure the elastin levels upon 10 day TGFβ treatment in ADCL with exon 30 and exon 34 mutations in the *ELN* and matched control fibroblasts. B,E: Cell numbers were counted using Cellometer mini cell counter in ADCL patients and controls. C,F: Elastin concentrations were normalized by cell number. Data are means ± s.e.m of 3 biological and 3 technical replicates in each individual. ** P<0.001 using the unpaired t-test, NS: non-significant. This experiment was performed once.

The long term TGFβ treatment also normalized the *ELN* mRNA levels in patients with exon 30 mutations and controls (Figure 3.18A) and caused more increase in *ELN* mRNA levels in patients with exon 34 mutations and controls (Figure 3.18B).

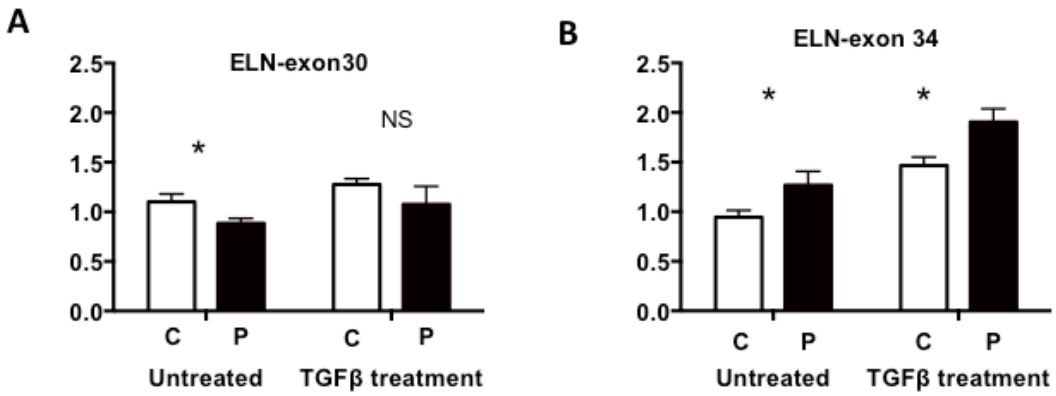

Figure 3.18 ELN mRNA expression levels in exon 30 and exon 34 patients upon 10-day TGFβ treatment

A: TGFβ normalized *ELN* mRNA expression in exon 30 patients and increased ELN mRNA expression in exon 30 patients. B: TGFβ treatment resulted in more increase in the ELN RNA expression in patients with exon 34 mutations and controls. Q-PCR data are means ± s.e.m of 3 biological replicates and 4 technical replicates in each individual. The reference gene was GAPDH. Unpaired t-tests were used to compare the expression levels of controls and patients.
*: $P<0.05$, NS: non-significant. C: controls, P: patients. This experiment was performed once.

3.2 DISCUSSION

In the present study, I investigated the possible molecular mechanisms and possible treatment strategies in ADCL. Results for exon 30 and exon 34 mutations are summarized in Table 3.4.

Table 3.4 Comparison of results with patients with exon 30 and exon 34 mutations

Results	**Exon 30**	**Exon 34**
Total ELN mRNA	Decreased expression	Increased expression
Fragment analysis	Increased abundance of mutant mRNA except 7002	Increased abundance of mutant mRNA
Elastin deposition	Reduced elastin deposition in patients	Reduced elastin deposition in patients
Canonical TGFβ signaling	Increased pSMAD2 and pSMAD3	No difference in pSMAD2 between patients and controls
Non-canonical TGFβ signaling	No change in pJNK1 and pP38, decrease in pERK	No change in pERK
TGFβ activity	No change in total and active TGFβ	———
Expression of TGFβ receptors at the protein level	Increase in pTGFBR1 and TGFBR1, no change in TGFBR2 and TGFBR3	———
Expression of TGFβ receptors at the RNA level	Increase in TGFBR1 and no change in TGFBR2	———
Expression of TGFβ pathway components and target genes	Increase in CTGF, no change in PAI1 and TGFβ1, decrease in SMAD6 and SMAD7	———
Long term TGFβ treatment allelic expression	Increased WT allele, decreased MT allele	Increased WT allele, decreased MT allele
Long term TGFβ treatment elastin deposition and cell number	Improved elastin deposition related to increased cell number	Improved elastin deposition related to increased cell number
Long term TGFβ treatment total ELN mRNA	Normalized ELN mRNA	Further increase in ELN mRNA

3.2.1 *ELN* expression in ADCL cells

I studied several aspects of the effect of ADCL mutations on *ELN* mRNA expression. Overall, *ELN* expression levels were similar was in ADCL cells to controls. However, modest differences were noted when ADCL cells were stratified by the location of the mutation. Cells with exon 30 mutations had about 20% decreased, whereas cells with exon 34 mutations had about 20% increased *ELN* expression. The precise cause of this difference remains unclear, and may be related to spurious effects of incomplete matching and relatively low numbers of cases and controls. A possibly relevant difference is the presence of a mutant transcript isoform in cells with exon 30 mutations that includes a premature termination codon in exon 32 in the mutant reading frame and is subject to nonsense-mediated decay (Figure 3.19). In contrast, exon 34 mutations are located in the last exon and are therefore not subject to nonsense-mediated decay (Figure 3.20). However, the abundance of the transcripts containing exon 32 may be too low to produce a noticeable difference in total ELN expression of cells with exon 30 mutations (Figure 3.15).

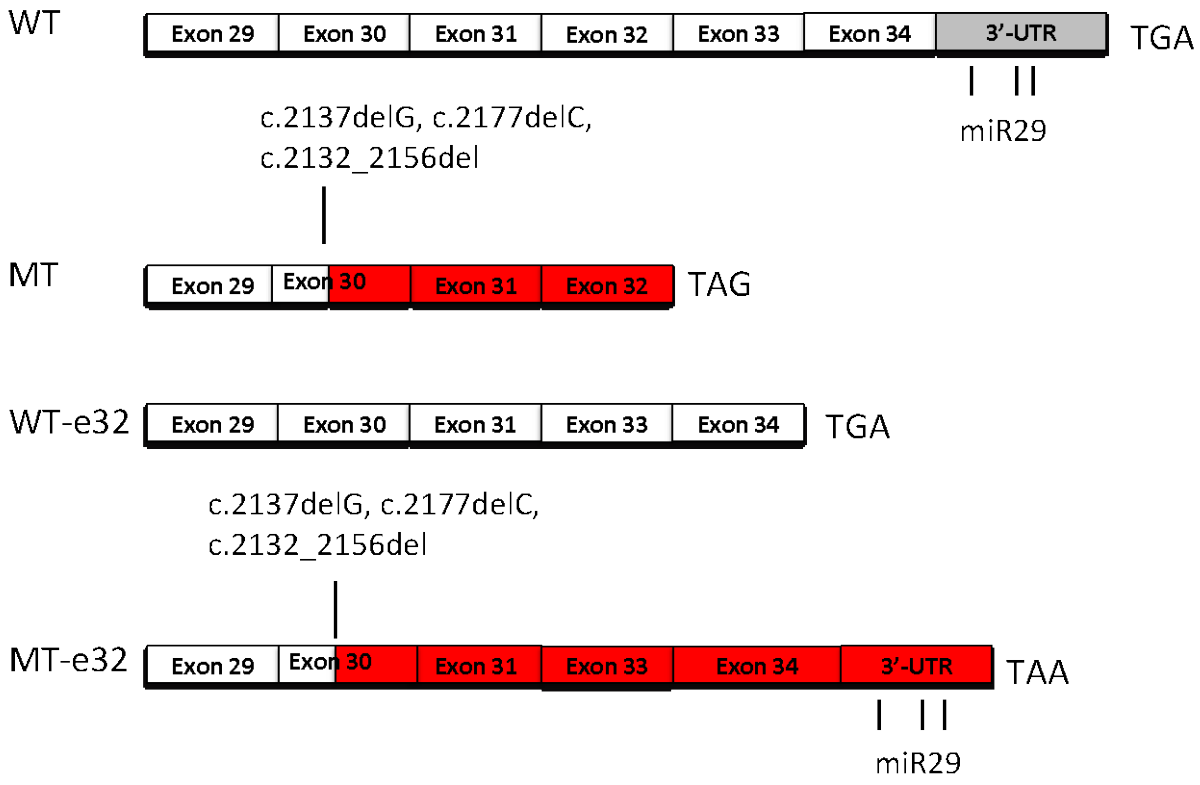

Figure 3.19 Structure of WT and MT mRNA products in patients with exon 30 mutations
Out of frame sequence is shown in red. WT, MT, WT-e32 and MT-e32 mRNA transcripts are shown. Note that when exon 32 is retained, it contains a premature termination codon in this frame (MT e32 in). However, when exon 32 is skipped as a result of an alternative splicing event, which occurs in 75% of the transcripts, reading frame 3 extends past the normal termination codon found in reading frame 1 (MT e32 out).

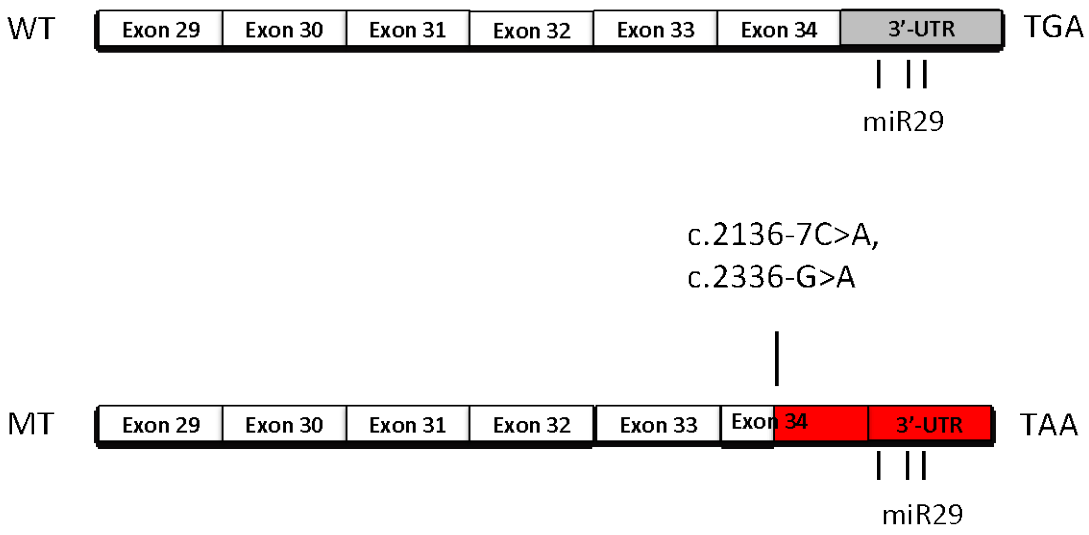

Figure 3.20 Structure of WT and MT mRNA products in patients with exon 34 mutations
Out of frame sequence is shown in red. WT and MT mRNA products are shown.

I found significantly higher levels of mutant ELN mRNA in 3 of 4 ADCL cells with exon 30 mutations and 3 of 3 cells with exon 34 mutations when compared to wild type ELN mRNA. These results uncovered a significant allelic imbalance, defined here as unequal expression of the wild-type and mutant alleles. In previous studies, increased abundance of stable mutant *ELN* mRNA in ADCL patients was noted (Callewaert et al., 2011), but was not analyzed quantitatively and statistically.

The precise mechanism responsible for the marked allelic imbalance in ADCL remains unclear, but may be related to translational interference with miR29-mediated down-regulation of *ELN* mRNA stability. Mutations in both exon 30 and exon 34 result in frameshift mutant mRNA with the mutant reading frame extending past the normal termination codon and one of the three miR29 binding sites in the 3'-untranslated region (3'-UTR) (Figure 3.19). As active translation is known to interfere with microRNA activity (Gu et al., 2009), the extension of the mutant open reading frame is expected to increase the stability of the mutant mRNA, whereas the wild type transcript will remain subject to miR29-mediated down-regulation resulting in allelic imbalance.

Given the previous data implicating dominant negative and toxic gain of function mechanisms in ADCL, I predict that the relative expression of mutant and wild-type alleles will have important implications for elastin biosynthesis and for disease outcomes. This prediction will have to be tested experimentally by assaying elastic fiber deposition in an experimental assembly system that allows the precise titration of the wild type and mutant tropoelastins. One such system is use of human retinal pigment epithelium cell line (ARPE19) in combination with exogenously supplemented recombinant tropoelastin (Wachi et al., 2005). The in vivo consequences of the relative expression of wild type and mutant alleles in ADCL can be studied

in mice carrying different combinations of knockout and transgenic elastin alleles (Hu et al., 2010; Sugitani et al., 2012). To date, the results of these transgenic and knockout studies support the conclusion that disease outcomes in ADCL are very sensitive to the expression of both the mutant and wild type alleles.

If clinical data can be collected from sufficient numbers of ADCL patients with without significant allelic imbalance, it will be possible to test the effect of this phenomenon directly in humans. In other autosomal dominant diseases, increased expression of mutant alleles is generally found to result in more severe presentation, as observed in familial cardiac hypertrophic cardiomyopathy (Tripathi et al., 2011).

3.2.2 Impaired elastin deposition in ADCL cells

Similar to previously published results (Callewaert et al., 2011), I observed significantly lower amounts of elastin deposited by all ADCL cells. The reduction in elastin deposition (33%) was somewhat greater in cells with exon 30 mutations compared to cells with exon 34 mutations (24%). This was expected based on the slightly reduced overall *ELN* mRNA expression in patients with exon 30 mutations and increased *ELN* transcript abundance in cells exon 34 mutations. The observation of reduced elastin deposition irrespective an overall increase or decrease in *ELN* gene expression supports a dominant negative or toxic gain of function mechanism previously suggested for ADCL (Hu et al., 2010; Callewaert et al., 2011).

3.2.3 Altered TGFβ signaling in ADCL cells

I observed increased pSMAD2 levels in ADCL patients with mutations in exon 30 dermal fibroblasts in two baseline conditions (10% serum and serum-free), consistent with previous findings in ADCL skin fibroblasts (Callewaert et al., 2011) and lung tissue in a transgenic mouse model of ADCL (Hu et al., 2010). SMAD2 phosphorylation levels remained elevated upon TGFβ treatment, but TGFBR1 inhibitor treatment abolished the difference in signaling between patient and control cells. Similarly, the other key signal transduction molecule within the canonical TGFβ signaling pathway, SMAD3, also showed increased phosphorylation under serum free and TGFβ supplementation conditions, which was also abolished by TGFBR1 inhibition. These results suggest that increased canonical TGFβ signaling in ADCL is related to TGFβ receptor activity, not the availability of TGFβ.

In contrast, all components of the non-canonical TGFβ signaling pathway were either unchanged (most conditions and signaling molecules) or decreased (pERK under serum free and TGFβ supplementation conditions). TGFBR1 inhibitor treatment also normalized pERK levels, suggesting that their decrease depended on TGFβ receptor levels. Therefore, we conclude that exon 30 mutations in ELN result in TGFBR1-dependent up-regulation of the canonical but not of the non-canonical TGFβ signaling pathway. A limitation of TGFβ signaling pathway experiments in *ELN*-mutant cells is that I only performed immunoblotting once. However, the results were consistent between experiments, and with previously published data.

Alteration of the extracellular matrix and consequent changes in the sequestration of latent TGFβ complexes may result in altered extracellular TGFβ activity, a possible explanation for the observed increase in intracellular signaling. However, three lines of evidence exclude this possibility: (i) TGFβ supplementation did not abolish the signaling differences, (ii) extracellular TGFβ activity and (iii) *TGFB1* gene expression was equal in patients and controls. Conversely, the ability of TGFBR1 inhibitors to eliminate signaling differences suggested changes in TGFBR1 activity. Indeed, I found elevated TGFBR1 and pTGFBR1 protein levels and commensurately increased *TGFBR1* mRNA levels in cells with exon 30 mutations. These findings support increased *TGFBR1* gene expression as the likely mechanism for the signaling changes, possibly through altered feedback regulation of TGFBR1. The analysis of TGFβ target genes confirms this conclusion. The expression of both *SMAD6* and *SMAD7*, known negative feedback regulators of TGFBR1 were significantly decreased explaining the increased TGFBR1 levels in ADCL cells with exon 30 mutations. Consistent with increased transcriptional output of the TGFβ pathway, the expression of CTGF was increased in exon 30 mutant cells. However, upregulation of TGFβ targets does not appear to be uniform as the esxpression *PAI1* was unchanged. More comprehensive gene expression analysis will be necessary to gauge the broad effect ADCL mutations on TGFβ target genes.

Interestingly, patients with *ELN* mutations in exon 34 had normal TGFβ signaling, suggesting mutation-specific TGFβ signaling changes in ADCL. A relevant molecular difference between the exon 30 and 34 mutations is the length of the frameshift peptide sequence at the end of the encoded mutant proteins, which was shown to be correlated with the severity of unfolded protein response in ADCL cells (Callewaert et al., 2011). Recent studies on embryonic stem cells suggest that the UPR can enhance TGFβ signaling (Xu et al. 2014). Therefore, it is possible that

differences in UPR activation between exon 30 and exon 34 mutations can explain differential activation of the TGFβ pathway.

ADCL is not the only type of cutis laxa with alterations in TGFβ signaling related to abnormal TGFβ receptor activity. In *LTBP4*-related cutis laxa (also known as autosomal recessive cutis laxa type 1C), despite elevated extracellular TGFβ activity, TGFBR1 and TGFBR2 are down-regulated at the protein level by endocytosis and lysosomal degradation (Su et al 2015). However, increased LTBP4-mediated stabilization is unlikely to be a mechanism for increased expression of TGFBR1 in ADCL cells with exon 30 mutations, because increased TGFBR1 expression was observed at both mRNA and protein levels and because the expression of TGFBR2 was not altered in ADCL cells.

3.2.4 Increased TGFβ signaling as a compensatory mechanism

A key question is whether the observed increase in canonical TGFβ signaling in ADCL patients with exon 30 mutations is contributing to the molecular pathology, is simply a molecular marker of the disease, or is a compensatory change ameliorating disease outcomes. To investigate these possibilities, I subjected ADCL cells to long-term TGFβ treatment and quantified overall ELN mRNA levels, allelic expression and elastin deposition. For each of these variables, TGFβ treatment produced an improvement: it increased overall *ELN* expression while increasing the contribution of the wild type and reducing the contribution of the mutant allele and increased the overall deposition of elastin. Therefore, I conclude that increased TGFβ signaling in ADCL patients with exon 30 mutations is a compensatory molecular mechanism.

TGFβ is known to up-regulate ELN expression by both transcriptional (Kuang et al., 2007; Oleggini et al., 2008) and post-transcriptional (Kahari et al., 1992; Kucich et al., 1997) mechanisms. Thus, increased *ELN* expression upon TGFβ treatment was expected. Differential regulation of the wild type and mutant alleles by TGFβ was more surprising, but can be explained by invoking the same mechanism I proposed for the observation of allelic imbalance in ADCL cells: interference of frameshift mutations with the binding of miR29 in the 3'-UTR of *ELN*. As TGFβ is a negative regulator of miR29 expression (van Rooij et al, 2008), it up-regulates *ELN* expression by removing inhibition by miR29. The absence of miR29 in TGFβ-treated cells would eliminate differential regulation of mutant vs. wild type transcripts resulting in equal allelic expression, as I observed.

TGFβ treatment also increased elastin deposition in both in patients with exon 30 and exon 34 mutations and controls. The TGFβ treated in ADCL fibroblasts deposited approximately the same amount of elastin as untreated in control cells. Interestingly, TGFβ treatment resulted in enhanced cell proliferation in patients, but it did not cause any changes in cell proliferation in control cells. The precise mechanism to explain why TGFβ treatment increases cell proliferation in ADCL but not in control cells remains unknown. However, one expects increased cell density to augment elastin deposition. It is also unclear if altered allelic expression contributes to increased elastin deposition in TGFβ-treated ADCL cells, or if increased cell density is sufficient to explain it. One of the limitations of this experiment is that we only tested the cell proliferation and elastin deposition in monolayer skin fibroblast cultures. It remains to be shown if long term TGFβ treatment is beneficial to disease outcomes *in vivo*. Therefore further studies will be required in animal models such as zebrafish or mice with ADCL-like mutations. These future studies will be essential to determine if approaches to augment TGFβ signaling are beneficial for

the treatment ADCL patients. Given the pleiotropic nature of TGFβ, possible concerns with extended treatment include risks of developmental, fibrotic or immunological anomalies.

3.2.5 Conclusions

In conclusion, my results showed a series of interesting molecular mechanisms relevant to ADCL in general or to certain subgroups of mutations in particular. I found invariably elevated expression of the mutant allele in ADCL cells, which could be suppressed by long-term TGFβ treatment. Long term TGFβ treatment was also beneficial in normalizing elastin deposition by ADCL cells, partly by selectively increasing ADCL proliferation and possibly by balancing allelic expression. In addition, I found elevated TGFβ signaling in ADCL cells with exon 30 mutations but not in cells with exon 34 mutations. Given the beneficial effects of TGFβ treatment on elastin deposition and allelic expression, I conclude that elevated TGFβ signaling in in ADCL cells with exon 30 mutations is a compensatory mechanism. More broadly, differential stabilization of mRNA products of mutant and wild type mRNAs is an as yet unexplored avenue of therapeutic intervention for autosomal dominant diseases.

4.0 A PARTIAL ELASTIN GENE DUPLICATION IN SUPRAVALVULAR AORTIC STENOSIS

4.1 RESULTS

4.1.1 An SVAS family with a partial *ELN* gene duplication

A 3-generation SVAS family (Figure 4.1) with microarray data showing a duplication of an approximately 80 kb region spanning the promoter region, the exon 1 and intron 1 of *ELN* was referred to us for further genetic and functional analysis. The mother and 3 children had the duplication, and the father was unaffected. Matching dermal fibroblasts were selected for SVAS patients (Table 4.1).

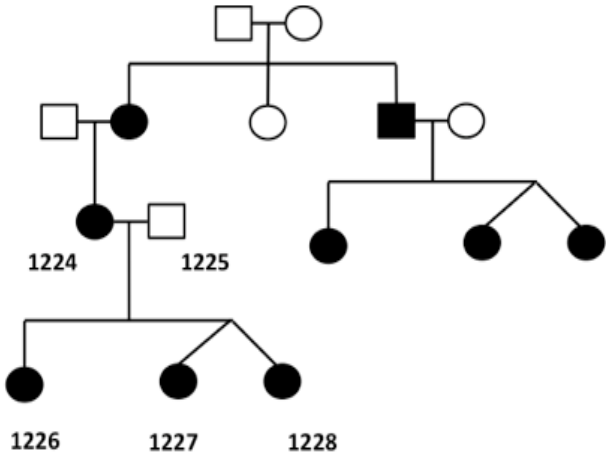

Figure 4.1 A pedigree of a SVAS family with a duplication in the *ELN* gene
Individuals with samples available to study are numbered.

Table 4.1 SVAS patients and control cells used in the study

Patient	Age (years)	Sex	Passage number
1224	37	Female	6
1226	5	Female	4
1227	3	Female	4
1228	3	Female	4
1225	38	Male	6
9215	9	Female	4
9068	4	Female	4
9176	9	Female	4

4.1.2 Expression analysis of the duplication

I tested whether a tetranucleotide repeat in intron 1 (Urban et al., 1997) fell within the duplicated region. Although 2 alleles were found for each individual within the family (Figure 4.2, Table 4.2 and Table 4.3), the quantitative analysis indicated double dose for the maternal, mutant allele (259) in all affected children confirming that the duplication encompasses this polymorphism (Figure 4.2A-C). Quantitative analysis showed a 3-fold increase in mutant pre-mRNA expression compared to wild type (Figure 4.2D-F) consistent with active transcription of both duplicated copies.

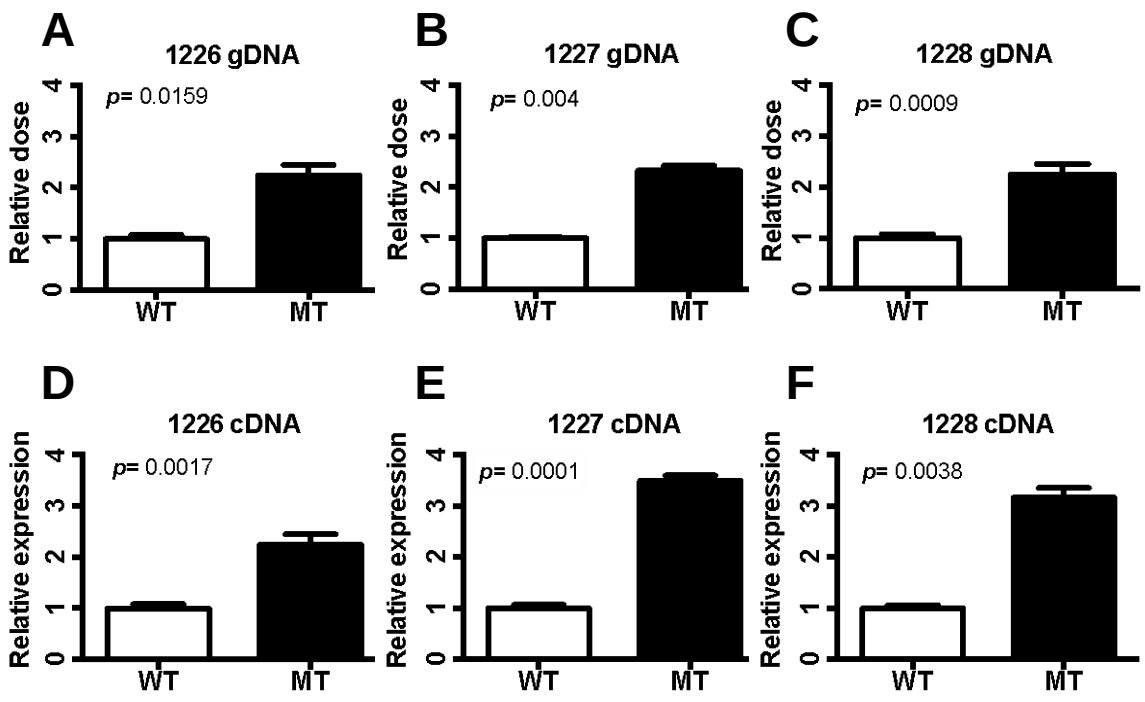

Figure 4.2 Increased relative dose and relative expression of the mutant allele in affected individuals

Genotyping for a tetranucleotide repeat in intron 1 was performed on genomic DNA (gDNA) and cDNA from fibroblasts of each indicated individual using fluorescently labeled primers. The products were sized and quantified using a genetic analyzer and the Peak Scanner software. Allele intensity data were normalized to the average of wild type (WT) allele intensities in each sample. Data are means ± s.e.m of 3 replicates. Mean allele intensities were compared to mutant allele (MT) using unpaired t-tests with the p-values shown above each graph. This experiment was repeated once with similar results.

To monitor the expression of the non-duplicated part of the mutant elastin gene, I searched for SNPs heterozygous in affected individuals. Following genotyping 9 SNPs, one, located in intron 23 (rs28763986) was found to be heterozygous in all affected individuals at the DNA level (Figure 4.3, Table 4.2). The T allele was linked to the wild type, and the C allele was linked to the mutant allele. RT-PCR and sequencing showed a lack of expression of the mutant allele at the pre-mRNA level (Figure 4.3). Taken together, my expression data indicate that the duplicated region of the mutant elastin gene as expressed whereas the non-duplicated region is transcriptionally silent. Thus, I conclude that this duplication results in a null allele. All RNA samples were tested for DNA contamination by amplifying "No RT" control samples with negative results (Figure 4.4).

Table 4.2 Genotyping of genetic markers in gDNA

SNPs	Location	RefSNP Alleles	1224	1225	1226	1227	1228
rs4556939	Exon 1	A>G	AA	AA	AA	AA	AA
rs884843	Intron 1	A>G	AA	AG	AA	AA	AA
rs868005	Intron 1	A>G	AA	AG	AA	AA	AA
Tetranucleotide repeat 1	Intron 1	(CCTT)n	259/259	263/270	259/263	259/263	259/263
rs4717865	Intron 4	A>G	AA	AA	AA	AA	AA
rs41500150	Exon 5	G>T	TT	TT	TT	TT	TT
rs20062910	Exon 14	A>C	AA	AA	AA	AA	AA
rs2071307	Exon 20	A>G	GG	AG	GG	GG	GG
rs28763986	Intron 23	C>T	CT	TT	CT	CT	CT
rs17855988	Exon 26	C>G	GG	GG	GG	GG	GG

Table 4.3 Genotyping of informative markers in cDNA

SNPs	Location	RefSNP Alleles	1224	1225	1226	1227	1228
rs28763986	Intron 23	C>T	TT	TT	TT	TT	TT
Tetranucleotide repeat 1	Intron 1	(CCTT)n	259/259	263/270	259/263	259/263	259/263

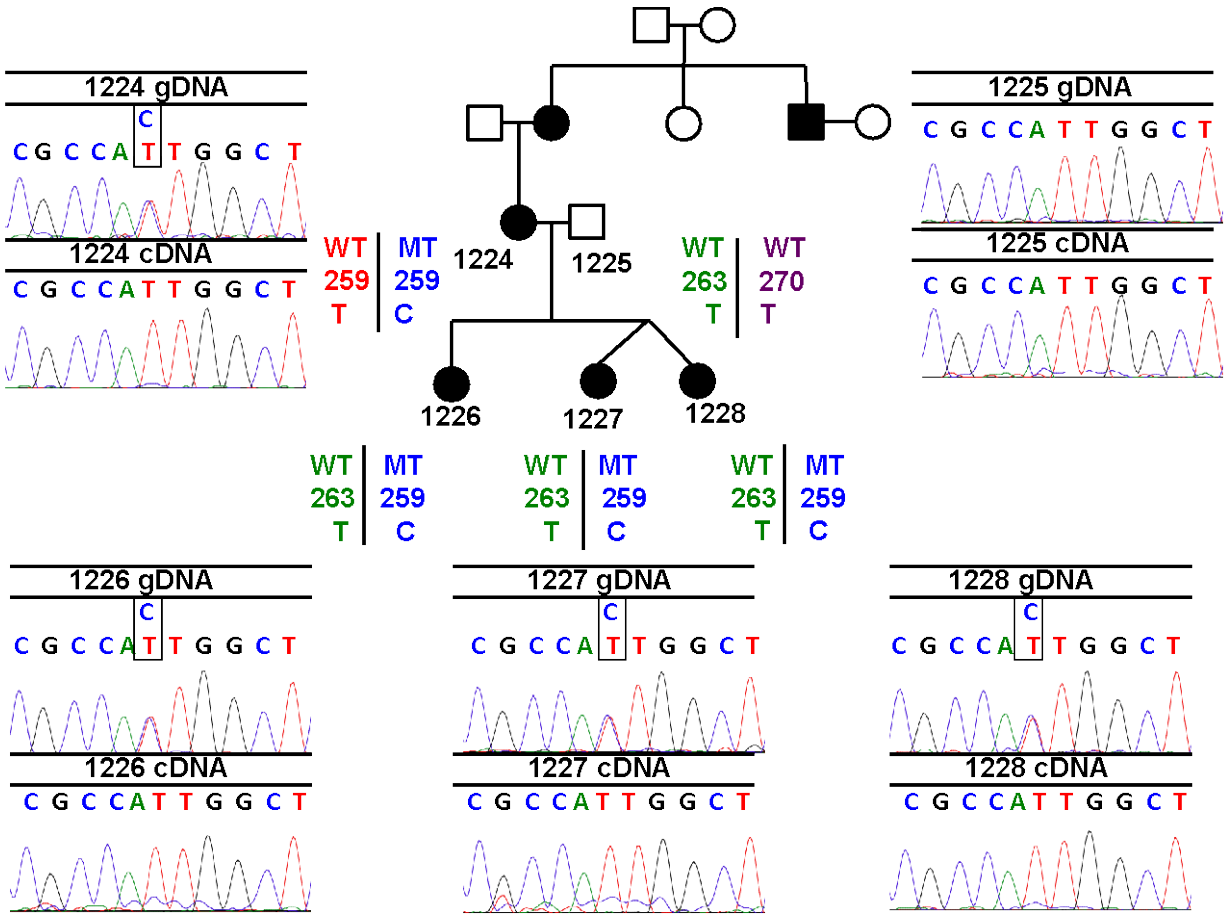

Figure 4.3 SNP(rs28763986) is heterozygous at the DNA level and homozygous at the pre-mRNA level in affected individuals

DNA sequencing was performed on genomic DNA (gDNA) or cDNA samples isolated from fibroblasts of each numbered individual in the pedigree. Heterozygous samples are marked by boxed bases above the corresponding sequence traces. Haplotype information is shown for each sample in the pedigree for the duplication, tetranucleotide repeat and rs28763916. Maternal WT (259) allele is shown in red and maternal MT (259) allele is shown in blue. Paternal WT (263) allele is shown in green and paternal WT (270) allele is shown in purple.

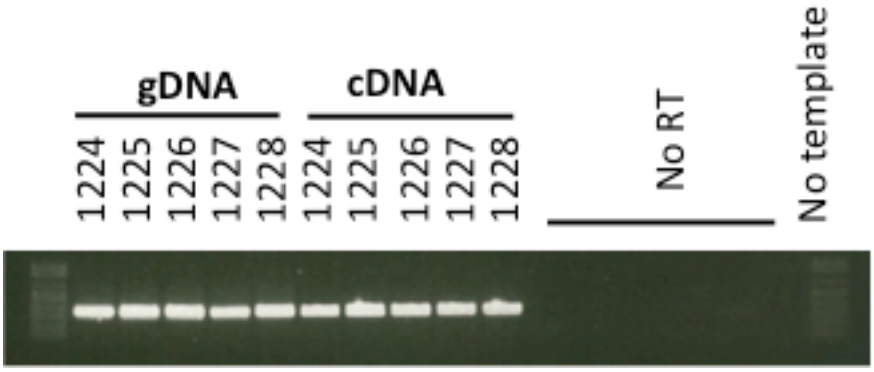

Figure 4.4 A gel image showing genomic DNA and RT-PCR results with no RT and no template controls
PCR was performed on gDNA, cDNA, No RT and No template samples isolated from dermal fibroblasts of each indicated individual. rs28763986, which is located in intron 23 of the *ELN* gene was amplified.

4.1.3 Reduced elastin deposition in patients

To test whether the null allele caused by the duplication affects the amount of elastin deposited by the SVAS cells, I quantified it using the Fastin Elastin Assay (Biocolor). I found about 21% of reduction in elastin in SVAS fibroblast cells compared to controls consistent with previous reports of reduced elastin production in SVAS cells (Urban et al., 2002) (Figure 4.5).

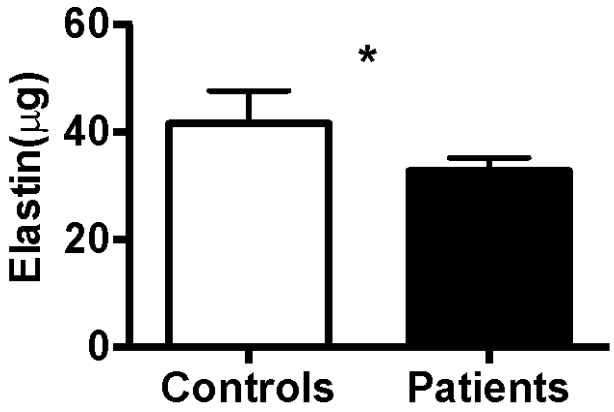

Figure 4.5 Elastin quantification showed a significant decrease in patient fibroblasts
Fastin elastin assay was performed to measure the soluble elastin from SVAS and matched control fibroblasts. Data are means ± s.e.m of 4 replicates. * $P<0.05$ using the paired one-tailed student's t-test. This experiment was performed once.

4.2 DISCUSSION

I conducted several functional studies and to solve the exact nature of an 80 kb duplication which includes exon 1 of the elastin gene and part of the upstream sequences in an SVAS family. Analysis of a tetranucleotide repeat polymorphism in intron 1 suggested that it was within the duplicated region and expressed from both the maternal and paternal alleles in children. Quantitative analysis showed double dose for the mutant allele and a 3-fold increase in mutant mRNA expression in all affected children. All possibilities for the duplication type of SVAS family are shown in Figure 4.6. Tandem duplications are expected to result in 3-fold increased expression of the mutant allele compared to the wild type because both copies of the duplicons are expected to be transcribed from the upstream promoter with an additional copy transcribed from the downstream promoter. In contrast, pre-mRNA from a 5' inverted duplication is expected to produce a 2-fold increase and a 3' inverted duplication a 4-fold increase. Because I observed 3-fold increase in mutant allele expression compared to wild type, my data supports the presence of a tandem duplication (Figure 4.6).

For a more direct characterization of the duplication, the breakpoint regions will need to be sequenced. Although I attempted to PCR across the breakpoints to clone and sequence them, a high density of repetitive DNA around the breakpoint region made difficult to achieve this goal. I did the primer walking and genomic PCR to amplify the breakpoint region, however none of the sequences gave *ELN* sequence. My findings provide some insights about whether the duplication is inverted or tandem, however, the exact duplication breakpoints needs to be further analyzed. For example multiplexed direct genomic selection (MDiGS) methodology coupled with deep sequencing (Alvarado et al., 2014) could be used to identify the breakpoints and confirm the orientation of the duplicons.

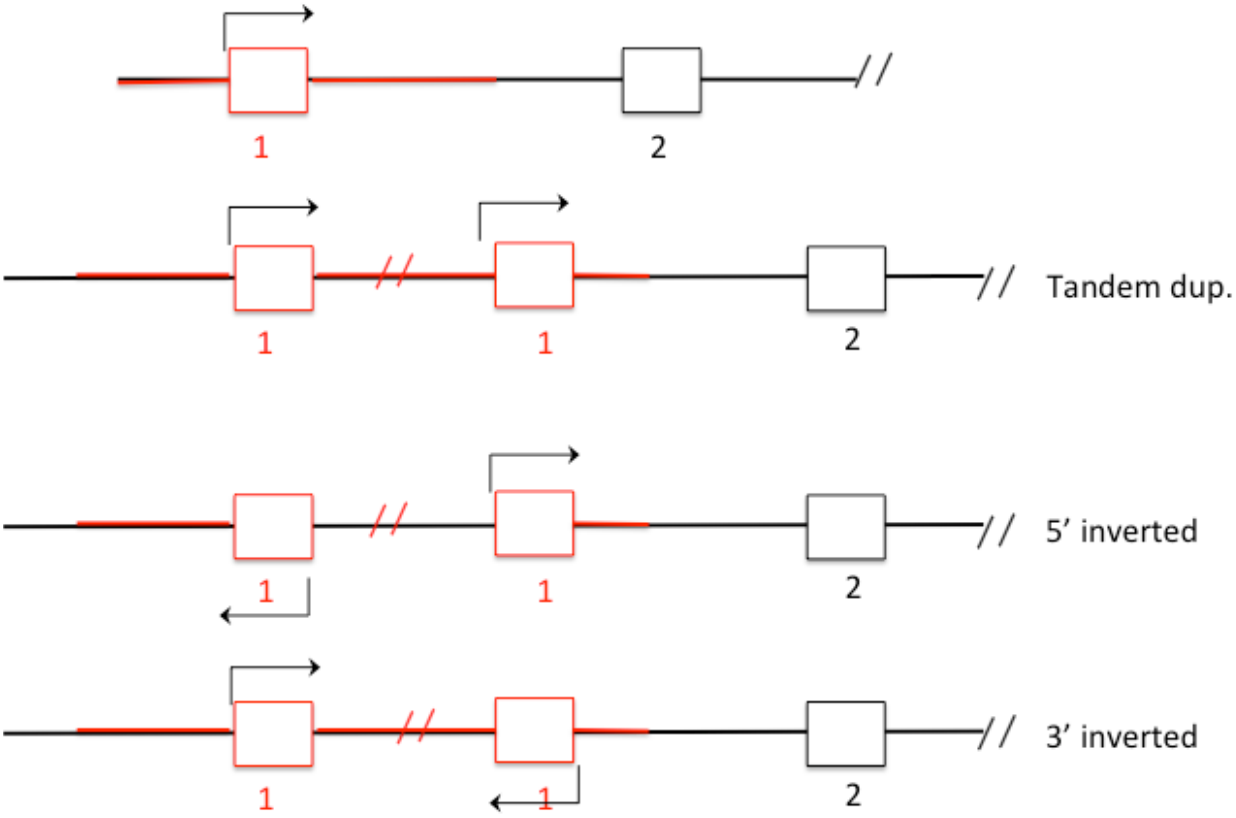

Figure 4.6 Possible duplication types in SVAS patients
Arrows indicate the direction of the promoters in each duplicon. The duplicated region of the gene is shown in red.

I looked at intronic variants and genotyped genomic DNA and RT-PCR products from pre-mRNA. I found a SNP (rs28763986), located in intron 23, which was heterozygous in all affected family members at the DNA level, but the mutant allele was not expressed at the pre-mRNA level. Overall, our results suggest the duplication led to a null allele. Additionally, I found reduced levels of elastin in affected individuals compared to controls, which is consistent with the previous studies (Urban et al., 2002).

SVAS is most commonly caused by point mutations located in the 5'-end and middle part of the ELN gene leading to nonsense mediated decay (Urban et al, 2000), however, frameshift mutations in the 3'end of the *ELN* gene result in extended reading frames (Tassabehji et al. 1998; Zhang et al., 1999) and ADCL. The molecular mechanism of SVAS mutations is haploinsufficiency, while the molecular mechanism of ADCL mutations is dominant negative or toxic gain-of-function. A large intragenic deletion has been identified in a family with SVAS (Olson et al. 1995), whereas a large duplication resulting in the synthesis of a mutant protein has been described in a family with cutis laxa (Urban et al. 2005). This is the first duplication shown to cause SVAS to date, but the lack of expression of the non-duplicated part of the mutant gene is consistent with the haploinsufficiency mechanism of all SVAS mutations studied to date. More research is needed to find out whether there is an overlap in the mutational spectrum of associated with SVAS and ADCL.

5.0 CONCLUSION

ECM has several functions consisting cell-cell communication, cell proliferation, development and the regulation of the bioavailability of TGFβ. Elastic fibers provide elastic stretch to the skin tissue. Elastin is the major component of elastic fibers and it is secreted as a tropoelastin from fibroblasts, vascular smooth muscle cells (SMCs), endothelial cells and chondroblasts. Elastin gene mutations result in several diseases including WBS, SVAS and ADCL. Several mechanisms have been identified as result of *ELN* mutations in these disorders; however, the understanding of these mechanisms remains incomplete.

We found a decreased ELN mRNA expression in patients with exon 30 mutations and an increased ELN mRNA expression in patients with exon 34 mutations. Overall, we found relatively unchanged ELN expression in all patients with exon 30 and exon 34 mutations. Examining the relative expression of MT and WT ELN alleles in fibroblasts from 7 individuals with ADCL, we observed 1.5-2-fold increased expression of mutant alleles at the mRNA level. In table 3.4, I summarized the results for each mutation group. Treatment of mutant fibroblasts with TGFβ for 10 days yielded an increase in the expression of WT alleles, but a decrease in the expression of the MT alleles, abolishing the differences in allelic expression. TGFβ1 treatment also normalized the amount of insoluble elastin deposited by ADCL cells (Figure 5.1).

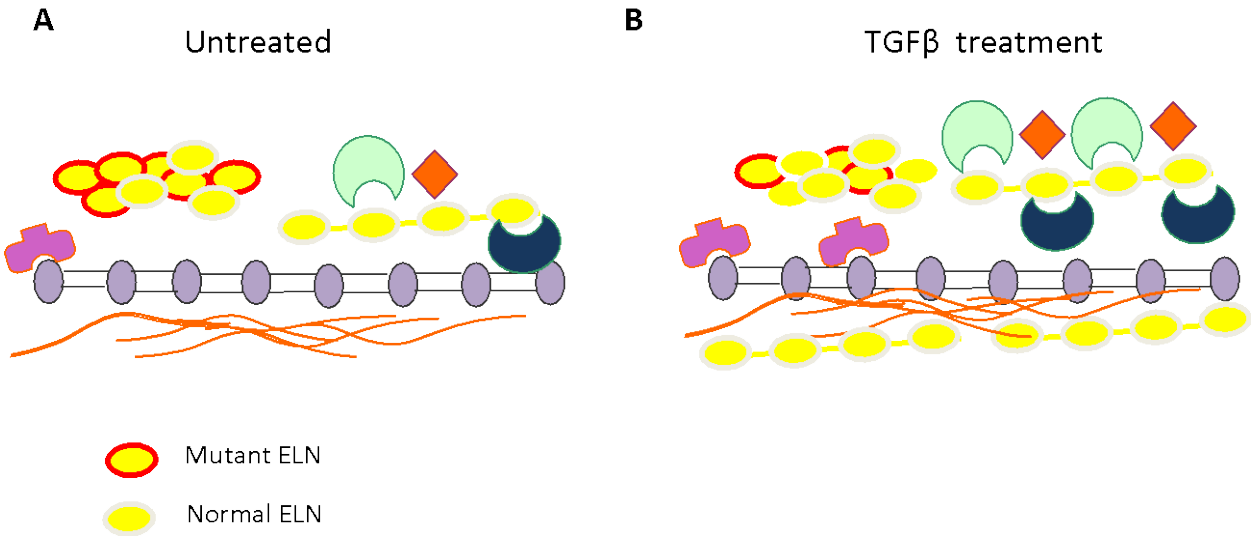

Figure 5.1 A summary model for elastic fiber assembly in ADCL cells in untreated and TGFβ treated conditions
A: More mutant elastin in untreated condition interferes with orderly deposition of wild type elastin onto microfibrils , B: TGFβ treatment increases wild type elastin more than the mutant and also increases the production of other elastic fiber components to increase elastin deposition.

Patients with exon 30 mutations had increased canonical TGFβ signaling and normal non-canonical TGFβ signaling (Figure 5.2 and Figure 5.3). Our results suggested increased TGFβ signaling is a significant compensatory mechanism ameliorating the molecular consequences of ADCL mutations. On the other hand, patients with exon 34 mutations had normal TGFβ signaling suggesting mutations-specific TGFβ signaling changes in ELN-related cutis laxa (Figure 5.4).

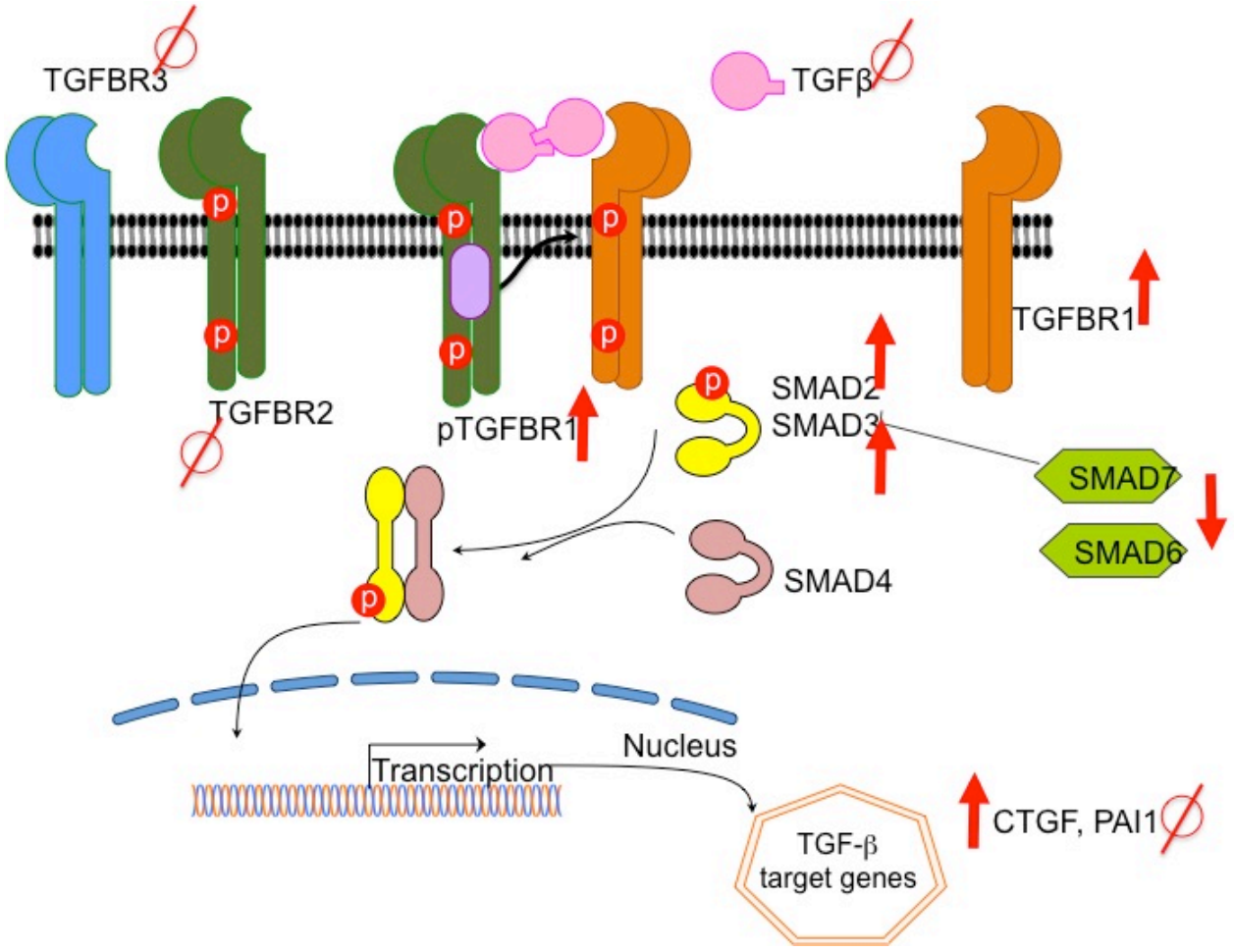

Figure 5.2 Canonical TGFβ signaling pathway in patients with exon 30 mutations
Under baseline conditions (serum and serum-free), SMAD2 and SMAD3 phosphorylation was increased. Extracellular levels of TGFβ remained unchanged. TGFBR1 and pTGFBR1 levels were increased; TGFBR2 and TGFBR3 levels remained unchanged. SMAD6 and SMAD7 levels were decreased. CTGF gene expression levels were increased and PAI1 gene expression levels remained unchanged.

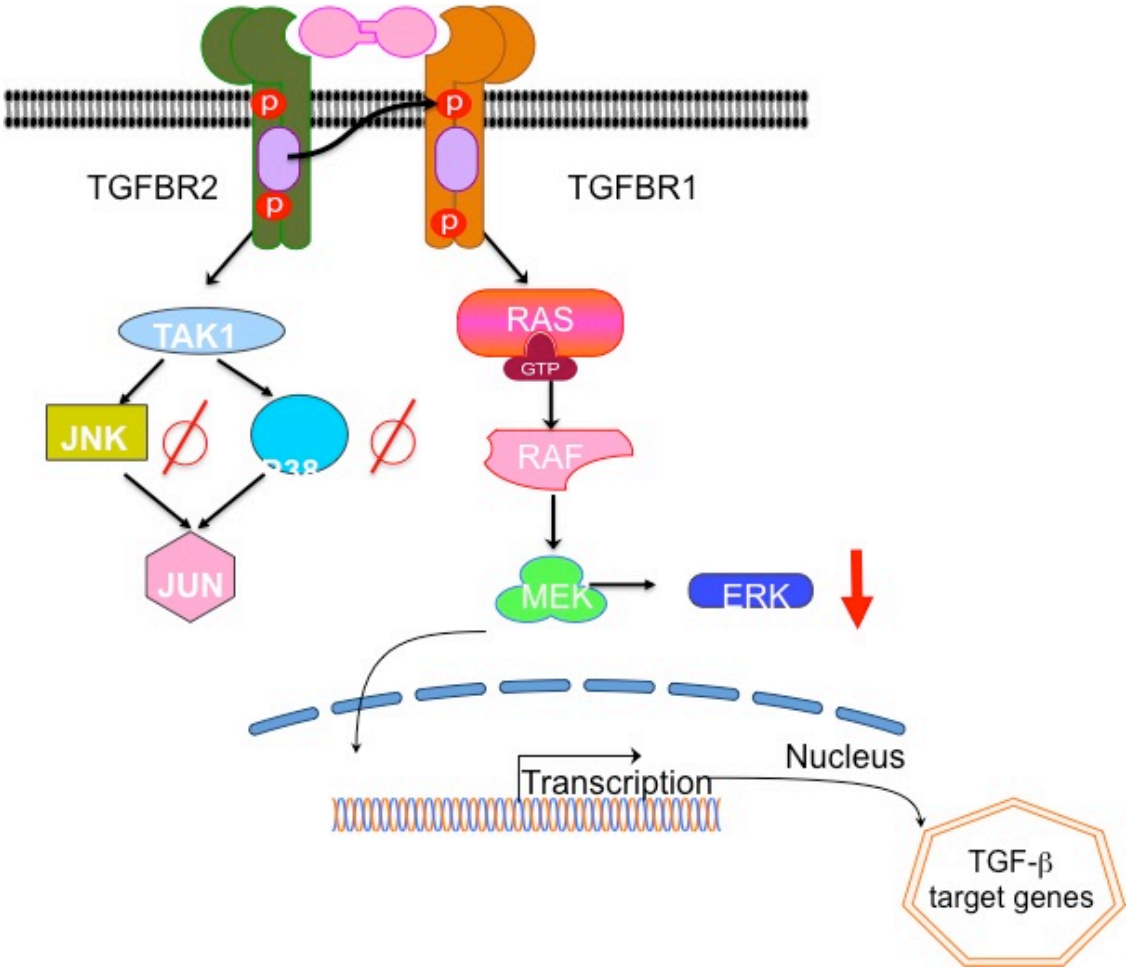

Figure 5.3 Non-canonical TGFβ signaling pathway in patients with exon 30 mutations
pJNK1 and pP38 levels were unchanged, whereas pERK levels were decreased in patients with exon 30 mutations.

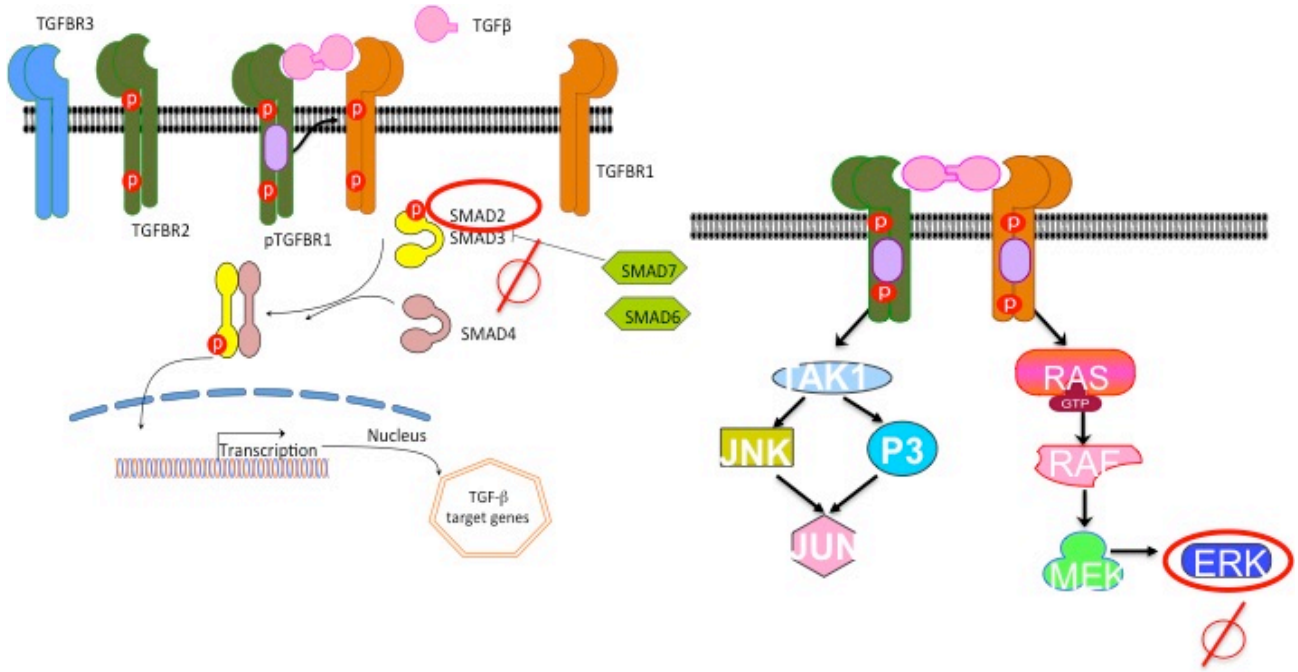

Figure 5.4 Canonical and non-canonical TGFβ signaling pathway in patients with exon 34 mutations

Patients with exon 34 mutations had normal canonical and non-canonical TGFβ signaling.

Overall, my results shed light into establishing new connections between elastin biosynthesis and growth factor signaling and emphasize the contribution of increased mutant allele to the molecular disease mechanisms in ADCL and support TGFβ1 augmentation as a possible therapeutic approach.

Genetic and functional analysis of SVAS also contributed to the molecular mechanisms of elastinopathies. I identified a tetranucleotide repeat in intron 1 and a SNP in intron 23 to be heterozygous in affected individuals. Gene dosage analysis showed that the tetranucleotide repeat 1 was within the duplicated region. The primary treatment for SVAS is the vascular surgery with higher risk of morbidity and mortality. More research is needed to find out the cellular and molecular mechanisms of SVAS and discover new therapeutic strategies to prevent morbidity and mortality. In general, studies on elastinopathies can inform the understanding and treatment approaches to the some common diseases such as aortic aneurysms, arterial stenoses and emphysema.

APPENDIX: SUPPLEMENTARY TABLES AND FIGURES

Table S.1 Primers genotyping for SVAS

SNPs	Name of primers	Primers sequence (5'➔3')	Tm (°C)
rs884843	hELNi1-1s hELNi1-1a	CAGACCAGGCTCTTCAGC CCTATGTTGCCCAGGCTG	55.6 56.1
rs868005	hELNi1-1.2s hELNi1-1.2a	CTGGTCTGAATTCCTGGG GACCACACGAAGCTGTTG	52.4 54.3
rs2071307	elhELN-i19-1s elhELN-i21-1a	GTGCTAGGATTACAGGCATG CTCGTGACCTTGGTCCAG	53.1 55.2
rs28763986	elhELN-i21-1s elhELN-i23-1a	GAAGGTGCCAGGAAGCCA CCCACACTCCTAGAGGTC	57.9 53.8
rs17855988	elhELN-i23-1s elhELN-i26-1a	CTGATCCAGGGTCACACAG CAGATGCTTAGGAGAACC	55.5 49.5
rs41500150	elhELN-i4-1s elhELN-i5-1a	GACACCTGCACTGCACAT CTTCCTCCATGCAGCCTTC	55.7 56
rs20062910	elhELN-i13-1s elhELN-i15-1a	GGTGACAGGTGCAGACTC GGATACATGGATGCATGG	55.5 50.4
rs4556939	hELNei5-1s hELNei1-1a	CTTGTGAGCCGGGCCTTTC GAGGACCCAGTGGCTGAG	59.1 57.7
rs4717865	hELNi4-1s hELNi4-1a	GTAGAGCTAGGTTCCCAG GTTGCCTTGTCCTGTTCCTA	51.3 55.7

Table S 1 Continued			
Tetranucleotide repeat 1	Outside primers hELNi1.11s hELNi1.11a Inside primers 5’-FAM-hELNi1.3s hELNi3.1a	GAGAAAAGTAAATGGGGCCA AATCACCACCTCCAAATGCT 5’-/FAM/GCCCACATGGGCAGATTGCT CCCTCATCCACAGACAGGTC	52.8 54.6 61 57.2
Mycoplasma	Myco-S Myco-A	TGCACCATCTGTCACTCTGTTAACCTC GTGGGAGCAAACAGGATTAGATACCCT	60.1 59.9

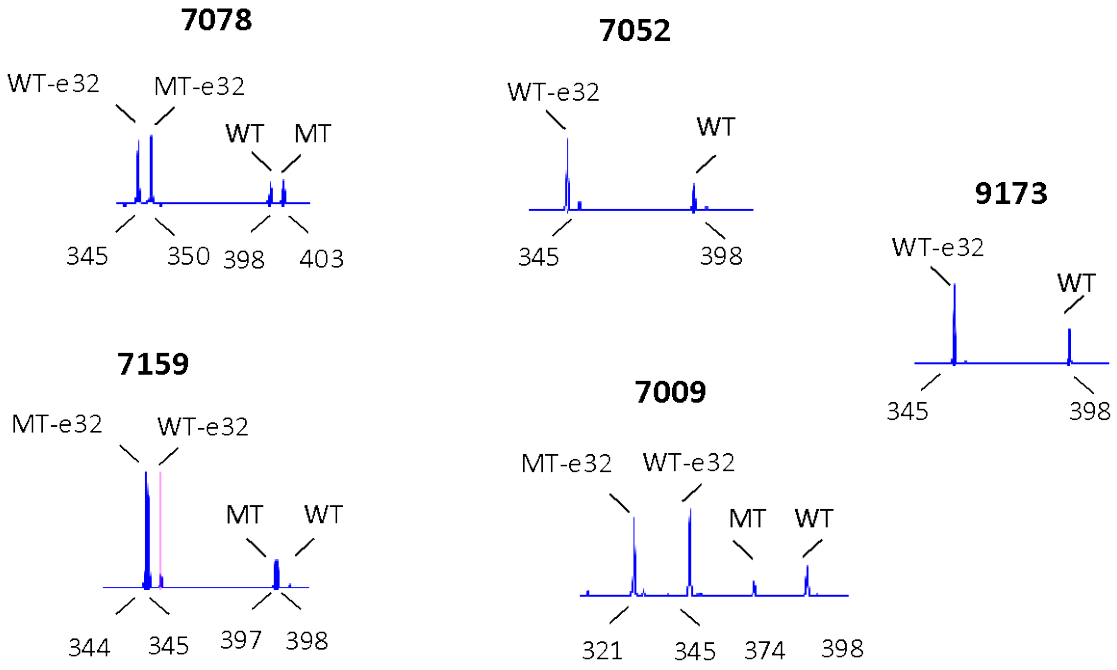

Figure 5.5 Electrophereograms of some patient and control samples

Table S 2 Identify testing by microsatellite analysis

Markers	1224	1225	1226	1227	1228
CSF1PO	10,12	10,12	10,12	12	10,12
D2S1338	20,20	20,25	20,25	20,20	20,20
D3S1358	16,17	15,18	15,17	16,18	16,18
D5S818	10,11	12,16	11,15	11,12	11,12
D7S820	10,11	10,11,12	10,11,12	10	10,11
D8S1179	11,12	13,14	11,14	12,13	9,12
D13S317	12,13	9,11,12	9,11,12	11,12	10,12
D16S539	11,13	11,12	11,12	11	11
D18S51	12,13	16,16	12,16	-	12
D19S433	13,14	12,14	13,14	12,14	12,14
D21S11	27,30	30,32.2	27,30	30,32.2	30,32.2

BIBLIOGRAPHY

Abe, M., J. G. Harpel, C. N. Metz, I. Nunes, D. J. Loskutoff and D. B. Rifkin (1994). An assay for transforming growth factor-beta using cells transfected with a plasminogen activator inhibitor-1 promoter-luciferase construct. *Anal Biochem* **216**(2): 276-284.

Ahmed, W., U. Kucich, W. Abrams, M. Bashir, J. Rosenbloom, F. Segade, R. Mecham and J. Rosenbloom (1998). Signaling pathway by which TGF-beta1 increases expression of latent TGF-beta binding protein-2 at the transcriptional level. *Connect Tissue Res* **37**(3-4): 263-276.

Alvarado DM, Yang P, Druley TE, Lovett M, Gurnett CA (2014). Multiplexed direct genomic selection (MDiGS): a pooled BAC capture approach for highly accurate CNV and SNP/INDEL detection. *Nucleic Acids Research* **42**(10):e82.

Annes, J. P., J. S. Munger and D. B. Rifkin (2003). Making sense of latent TGFbeta activation. *J Cell Sci* **116**(Pt 2): 217-224.

Anon (2013) National Organization for Rare Disorders. Available at: https://www.rarediseases.org/rare-disease-information

Apte, S. S.(2009). A disintegrin-like and metalloprotease (reprolysin-type) with thrombospondin type 1 motif (ADAMTS) superfamily: functions and mechanisms. *J Biol Chem* **284**(46): 31493-31497.

Bader, H. L., L. W. Wang, J. C. Ho, T. Tran, P. Holden, J. Fitzgerald, R. P. Atit, D. P. Reinhardt and S. S. Apte (2012). A disintegrin-like and metalloprotease domain containing thrombospondin type 1 motif-like 5 (ADAMTSL5) is a novel fibrillin-1-, fibrillin-2-, and heparin-binding member of the ADAMTS superfamily containing a netrin-like module. *Matrix Biol* **31**(7-8): 398-411.

Baldwin, A. K., A. Simpson, R. Steer, S. A. Cain and C. M. Kielty (2013). Elastic fibres in health and disease. *Expert Rev Mol Med* **15**: e8.

Bax, D. V., U. R. Rodgers, M. M. Bilek and A. S. Weiss (2009). Cell adhesion to tropoelastin is mediated via the C-terminal GRKRK motif and integrin alphaVbeta3. *J Biol Chem* **284**(42): 28616-28623.

Bax, D. V., Y. Mahalingam, S. Cain, K. Mellody, L. Freeman, K. Younger, C. A. Shuttleworth, M. J. Humphries, J. R. Couchman and C. M. Kielty (2007). Cell adhesion to fibrillin-1: identification of an Arg-Gly-Asp-dependent synergy region and a heparin-binding site that regulates focal adhesion formation. *J Cell Sci* **120**(Pt 8): 1383-1392.

Berk, D. R., D. D. Bentley, S. J. Bayliss, A. Lind and Z. Urban (2012). Cutis laxa: a review. *J Am Acad Dermatol* **66**(5): 842.e841-817.

Boak, A. M., R. Roy, J. Berk, L. Taylor, P. Polgar, R. H. Goldstein and H. M. Kagan (1994). Regulation of lysyl oxidase expression in lung fibroblasts by transforming growth factor-beta 1 and prostaglandin E2. *Am J Respir Cell Mol Biol* **11**(6): 751-755.

Boeckel, T., A. Dierks, A. Vergopoulos, S. Bahring, H. Knoblauch, B. Muller-Myhsok, H. Baron, A. Aydin, G. Bein, F. C. Luft and H. Schuster (1999). A new mutation in the elastin gene causing supravalvular aortic stenosis. *Am J Cardiol* **83**(7): 1141-1143, a1149-1110.

Broekelmann, T. J., B. A. Kozel, H. Ishibashi, C. C. Werneck, F. W. Keeley, L. Zhang and R. P. Mecham (2005). Tropoelastin interacts with cell-surface glycosaminoglycans via its COOH-terminal domain. *J Biol Chem* **280**(49): 40939-40947.

Brooke, B. S., A. Bayes-Genis and D. Y. Li (2003). New insights into elastin and vascular disease. *Trends Cardiovasc Med* **13**(5): 176-181.

Cain, S. A., A. K. Baldwin, Y. Mahalingam, B. Raynal, T. A. Jowitt, C. A. Shuttleworth, J. R. Couchman and C. M. Kielty (2008). Heparan sulfate regulates fibrillin-1 N- and C-terminal interactions. *J Biol Chem* **283**(40): 27017-27027.

Cain, S. A., C. Baldock, J. Gallagher, A. Morgan, D. V. Bax, A. S. Weiss, C. A. Shuttleworth and C. M. Kielty (2005). Fibrillin-1 interactions with heparin. Implications for microfibril and elastic fiber assembly. *J Biol Chem* **280**(34): 30526-30537.

Callewaert, B., M. Renard, V. Hucthagowder, B. Albrecht, I. Hausser, E. Blair, C. Dias, A. Albino, H. Wachi, F. Sato, R. P. Mecham, B. Loeys, P. J. Coucke, A. De Paepe and Z. Urban (2011). New insights into the pathogenesis of autosomal-dominant cutis laxa with report of five ELN mutations. *Hum Mutat* **32**(4): 445-455.

Carta, L., L. Pereira, E. Arteaga-Solis, S. Y. Lee-Arteaga, B. Lenart, B. Starcher, C. A. Merkel, M. Sukoyan, A. Kerkis, N. Hazeki, D. R. Keene, L. Y. Sakai and F. Ramirez (2006). Fibrillins 1 and 2 perform partially overlapping functions during aortic development. *J Biol Chem* **281**(12): 8016-8023.

Charbonneau, N. L., B. J. Dzamba, R. N. Ono, D. R. Keene, G. M. Corson, D. P. Reinhardt and L. Y. Sakai (2003). Fibrillins can co-assemble in fibrils, but fibrillin fibril composition displays cell-specific differences. *J Biol Chem* **278**(4): 2740-2749.

Charbonneau, N. L., C. D. Jordan, D. R. Keene, S. Lee-Arteaga, H. C. Dietz, D. B. Rifkin, F. Ramirez and L. Y. Sakai (2010). Microfibril structure masks fibrillin-2 in postnatal tissues. *J Biol Chem* **285**(26): 20242-20251.

Choi, J., A. Bergdahl, Q. Zheng, B. Starcher, H. Yanagisawa and E. C. Davis (2009). Analysis of dermal elastic fibers in the absence of fibulin-5 reveals potential roles for fibulin-5 in elastic fiber assembly. *Matrix Biol* **28**(4): 211-220.

Cirulis, J. T. and F. W. Keeley (2010). Kinetics and morphology of self-assembly of an elastin-like polypeptide based on the alternating domain arrangement of human tropoelastin. *Biochemistry* **49**(27): 5726-5733.

Conway, E. E., Jr., J. Noonan, R. W. Marion and C. N. Steeg (1990). Myocardial infarction leading to sudden death in the Williams syndrome: report of three cases. *J Pediatr* **117**(4): 593-595.

Corson, G. M., N. L. Charbonneau, D. R. Keene and L. Y. Sakai (2004). Differential expression of fibrillin-3 adds to microfibril variety in human and avian, but not rodent, connective tissues. *Genomics* **83**(3): 461-472.

Coucke, P. J., A. Willaert, M. W. Wessels, B. Callewaert, N. Zoppi, J. De Backer, J. E. Fox, G. M. Mancini, M. Kambouris, R. Gardella, F. Facchetti, P. J. Willems, R. Forsyth, H. C. Dietz, S. Barlati, M. Colombi, B. Loeys and A. De Paepe (2006). Mutations in the facilitative glucose transporter GLUT10 alter angiogenesis and cause arterial tortuosity syndrome. *Nat Genet* **38**(4): 452-457.

Craft, C. S., W. Zou, M. Watkins, S. Grimston, M. D. Brodt, T. J. Broekelmann, J. S. Weinbaum, S. L. Teitelbaum, R. A. Pierce, R. Civitelli, M. J. Silva and R. P. Mecham (2010). Microfibril-associated glycoprotein-1, an extracellular matrix regulator of bone remodeling. *J Biol Chem* **285**(31): 23858-23867.

Curran, M. E., D. L. Atkinson, A. K. Ewart, C. A. Morris, M. F. Leppert and M. T. Keating (1993). The elastin gene is disrupted by a translocation associated with supravalvular aortic stenosis. *Cell* **73**(1): 159-168.

Dabovic, B., Y. Chen, J. Choi, M. Vassallo, H. C. Dietz, F. Ramirez, H. von Melchner, E. C. Davis and D. B. Rifkin (2009). Dual functions for LTBP in lung development: LTBP-4 independently modulates elastogenesis and TGF-beta activity. *J Cell Physiol* **219**(1): 14-22.

Dallas, S. L., P. Sivakumar, C. J. Jones, Q. Chen, D. M. Peters, D. F. Mosher, M. J. Humphries and C. M. Kielty (2005). Fibronectin regulates latent transforming growth factor-beta (TGF beta) by controlling matrix assembly of latent TGF beta-binding protein-1. *J Biol Chem* **280**(19): 18871-18880.

Ebisawa, T., M. Fukuchi, G. Murakami, T. Chiba, K. Tanaka, T. Imamura and K. Miyazono (2001). Smurf1 interacts with transforming growth factor-beta type I receptor through Smad7 and induces receptor degradation. *J Biol Chem* **276**(16): 12477-12480.

Eisenberg, R., D. Young, B. Jacobson and A. Boito (1964). Familial supravalvular aortic stenosis. *Am J Dis Child* **108**: 341-347.

Ewart, A. K., C. A. Morris, D. Atkinson, W. Jin, K. Sternes, P. Spallone, A. D. Stock, M. Leppert and M. T. Keating (1993). Hemizygosity at the elastin locus in a developmental disorder, Williams syndrome. *Nat Genet* **5**(1): 11-16.

Ewart, A. K., W. Jin, D. Atkinson, C. A. Morris and M. T. Keating (1994). Supravalvular aortic stenosis associated with a deletion disrupting the elastin gene. *J Clin Invest* **93**(3): 1071-1077.

Faury, G., M. Pezet, R. H. Knutsen, W. A. Boyle, S. P. Heximer, S. E. McLean, R. K. Minkes, K. J. Blumer, A. Kovacs, D. P. Kelly, D. Y. Li, B. Starcher and R. P. Mecham (2003). Developmental adaptation of the mouse cardiovascular system to elastin haploinsufficiency. *J Clin Invest* **112**(9): 1419-1428.

Fazio, M. J., D. R. Olsen, H. Kuivaniemi, M. L. Chu, J. M. Davidson, J. Rosenbloom and J. Uitto (1988). Isolation and characterization of human elastin cDNAs, and age-associated variation in elastin gene expression in cultured skin fibroblasts. *Lab Invest* **58**(3): 270-277.

Fischer, B., A. Dimopoulou, J. Egerer, T. Gardeitchik, A. Kidd, D. Jost, H. Kayserili, Y. Alanay, I. Tantcheva-Poor, E. Mangold, C. Daumer-Haas, S. Phadke, R. I. Peirano, J. Heusel, C. Desphande, N. Gupta, A. Nanda, E. Felix, E. Berry-Kravis, M. Kabra, R. A. Wevers, L. van Maldergem, S. Mundlos, E. Morava and U. Kornak (2012). Further characterization of ATP6V0A2-related autosomal recessive cutis laxa. *Hum Genet* **131**(11): 1761-1773.

Fryssira, H., R. Palmer, K. A. Hallidie-Smith, J. Taylor, D. Donnai and W. Reardon (1997). Fluorescent in situ hybridisation (FISH) for hemizygous deletion at the elastin locus in patients with isolated supravalvular aortic stenosis. *J Med Genet* **34**(4): 306-308.

Gandhi, N. S. and R. L. Mancera (2008). The structure of glycosaminoglycans and their interactions with proteins. *Chem Biol Drug Des* **72**(6): 455-482.

Ge, X., Y. Ren, O. Bartulos, M. Y. Lee, Z. Yue, K. Y. Kim, W. Li, P. J. Amos, E. C. Bozkulak, A. Iyer, W. Zheng, H. Zhao, K. A. Martin, D. N. Kotton, G. Tellides, I. H. Park, L. Yue and Y. Qyang (2012). Modeling supravalvular aortic stenosis syndrome with human induced pluripotent stem cells. *Circulation* **126**(14): 1695-1704.

Gibson, M. A., M. L. Finnis, J. S. Kumaratilake and E. G. Cleary (1998). Microfibril-associated glycoprotein-2 (MAGP-2) is specifically associated with fibrillin-containing microfibrils but exhibits more restricted patterns of tissue localization and developmental expression than its structural relative MAGP-1. *J Histochem Cytochem* **46**(8): 871-886.

Gleizes, P. E., R. C. Beavis, R. Mazzieri, B. Shen and D. B. Rifkin (1996). Identification and characterization of an eight-cysteine repeat of the latent transforming growth factor-beta binding protein-1 that mediates bonding to the latent transforming growth factor-beta1. *J Biol Chem* **271**(47): 29891-29896.

Graul-Neumann, L. M., I. Hausser, M. Essayie, A. Rauch and C. Kraus (2008). Highly variable cutis laxa resulting from a dominant splicing mutation of the elastin gene. *Am J Med Genet A* **146a**(8): 977-983.

Gu, S., L. Jin, F. Zhang, P. Sarnow and M. A. Kay (2009). Biological basis for restriction of microRNA targets to the 3' untranslated region in mammalian mRNAs. *Nat Struct Mol Biol* **16**(2): 144-150.

Hadj-Rabia, S., B. L. Callewaert, E. Bourrat, M. Kempers, A. S. Plomp, V. Layet, D. Bartholdi, M. Renard, J. De Backer, F. Malfait, O. M. Vanakker, P. J. Coucke, A. M. De Paepe and C. Bodemer (2013). Twenty patients including 7 probands with autosomal dominant cutis laxa confirm clinical and molecular homogeneity. *Orphanet J Rare Dis* **8**: 36.

Hanada, K., M. Vermeij, G. A. Garinis, M. C. de Waard, M. G. Kunen, L. Myers, A. Maas, D. J. Duncker, C. Meijers, H. C. Dietz, R. Kanaar and J. Essers (2007). Perturbations of vascular homeostasis and aortic valve abnormalities in fibulin-4 deficient mice. *Circ Res* **100**(5): 738-746.

Hanssen, E., F. H. Hew, E. Moore and M. A. Gibson (2004). MAGP-2 has multiple binding regions on fibrillins and has covalent periodic association with fibrillin-containing microfibrils. *J Biol Chem* **279**(28): 29185-29194.

Hata, A., G. Lagna, J. Massague and A. Hemmati-Brivanlou (1998). Smad6 inhibits BMP/Smad1 signaling by specifically competing with the Smad4 tumor suppressor. *Genes Dev* **12**(2): 186-197.

Holm, T. M., J. P. Habashi, J. J. Doyle, D. Bedja, Y. Chen, C. van Erp, M. E. Lindsay, D. Kim, F. Schoenhoff, R. D. Cohn, B. L. Loeys, C. J. Thomas, S. Patnaik, J. J. Marugan, D. P. Judge and H. C. Dietz (2011). Noncanonical TGFbeta signaling contributes to aortic aneurysm progression in Marfan syndrome mice. *Science* **332**(6027): 358-361.

Hu, Q., A. Shifren, C. Sens, J. Choi, Z. Szabo, B. C. Starcher, R. H. Knutsen, J. M. Shipley, E. C. Davis, R. P. Mecham and Z. Urban (2010). Mechanisms of emphysema in autosomal dominant cutis laxa. *Matrix Biol* **29**(7): 621-628.

Hu, Q., J. L. Reymond, N. Pinel, M. T. Zabot and Z. Urban (2006). Inflammatory destruction of elastic fibers in acquired cutis laxa is associated with missense alleles in the elastin and fibulin-5 genes. *J Invest Dermatol* **126**(2): 283-290.

Hubmacher, D. and S. S. Apte (2011). Genetic and functional linkage between ADAMTS superfamily proteins and fibrillin-1: a novel mechanism influencing microfibril assembly and function. *Cell Mol Life Sci* **68**(19): 3137-3148.

Ignotz, R. A., T. Endo and J. Massague (1987). Regulation of fibronectin and type I collagen mRNA levels by transforming growth factor-beta. *J Biol Chem* **262**(14): 6443-6446.

Imamura, T., M. Takase, A. Nishihara, E. Oeda, J. Hanai, M. Kawabata and K. Miyazono (1997). Smad6 inhibits signalling by the TGF-beta superfamily. *Nature* **389**(6651): 622-626.

Institute of Medicine (US) Committee on Accelerating Rare Diseases Research and Orphan Product Development; Field MJ, Boat TF, editors. Rare Diseases and Orphan Products: Accelerating Research and Development. Washington (DC): National Academies Press (US); 2010. 2, Profile of Rare Diseases. Available from: http://www.ncbi.nlm.nih.gov/books/NBK56184/

Jensen, S. A., D. P. Reinhardt, M. A. Gibson and A. S. Weiss (2001). Protein interaction studies of MAGP-1 with tropoelastin and fibrillin-1. *J Biol Chem* **276**(43): 39661-39666.

Jovanovic, J., J. Takagi, L. Choulier, N. G. Abrescia, D. I. Stuart, P. A. van der Merwe, H. J. Mardon and P. A. Handford (2007). alphaVbeta6 is a novel receptor for human fibrillin-1. Comparative studies of molecular determinants underlying integrin-rgd affinity and specificity. *J Biol Chem* **282**(9): 6743-6751.

Kadler, K. E., C. Baldock, J. Bella and R. P. Boot-Handford (2007). "Collagens at a glance." *J Cell Sci* **120**(Pt 12): 1955-1958.

Kahari, V. M., D. R. Olsen, R. W. Rhudy, P. Carrillo, Y. Q. Chen and J. Uitto (1992). Transforming growth factor-beta up-regulates elastin gene expression in human skin fibroblasts. Evidence for post-transcriptional modulation. *Lab Invest* **66**(5): 580-588.

Kantola, A. K., J. Keski-Oja and K. Koli (2008). Fibronectin and heparin binding domains of latent TGF-beta binding protein (LTBP)-4 mediate matrix targeting and cell adhesion. *Exp Cell Res* **314**(13): 2488-2500.

Kaplan, P., M. Levinson and B. S. Kaplan (1995). Cerebral artery stenoses in Williams syndrome cause strokes in childhood. *J Pediatr* **126**(6): 943-945.

Karnik, S. K., B. S. Brooke, A. Bayes-Genis, L. Sorensen, J. D. Wythe, R. S. Schwartz, M. T. Keating and D. Y. Li (2003). A critical role for elastin signaling in vascular morphogenesis and disease. *Development* **130**(2): 411-423.

Kelleher, C. M., E. K. Silverman, T. Broekelmann, A. A. Litonjua, M. Hernandez, J. S. Sylvia, J. Stoler, J. J. Reilly, H. A. Chapman, F. E. Speizer, S. T. Weiss, R. P. Mecham and B. A. Raby (2005). A functional mutation in the terminal exon of elastin in severe, early-onset chronic obstructive pulmonary disease. *Am J Respir Cell Mol Biol* **33**(4): 355-362.

Kielty, C. M. (2006). Elastic fibres in health and disease. *Expert Rev Mol Med* **8**(19): 1-23.

Kim, D. J., D. C. Lee, S. J. Yang, J. J. Lee, E. M. Bae, D. M. Kim, S. H. Min, S. J. Kim, D. C. Kang, B. C. Sang, P. K. Myung, K. C. Park and Y. I. Yeom (2008). Lysyl oxidase like 4, a novel target gene of TGF-beta1 signaling, can negatively regulate TGF-beta1-induced cell motility in PLC/PRF/5 hepatoma cells. *Biochem Biophys Res Commun* **373**(4): 521-527.

Kinsey, R., M. R. Williamson, S. Chaudhry, K. T. Mellody, A. McGovern, S. Takahashi, C. A. Shuttleworth and C. M. Kielty (2008). Fibrillin-1 microfibril deposition is dependent on fibronectin assembly. *J Cell Sci* **121**(Pt 16): 2696-2704.

Kobayashi, N., G. Kostka, J. H. Garbe, D. R. Keene, H. P. Bachinger, F. G. Hanisch, D. Markova, T. Tsuda, R. Timpl, M. L. Chu and T. Sasaki (2007). A comparative analysis of the fibulin protein family. Biochemical characterization, binding interactions, and tissue localization. *J Biol Chem* **282**(16): 11805-11816.

Kuang, P. P., X. H. Zhang, C. B. Rich, J. A. Foster, M. Subramanian and R. H. Goldstein (2007). Activation of elastin transcription by transforming growth factor-beta in human lung fibroblasts. *Am J Physiol Lung Cell Mol Physiol* **292**(4): L944-952.

Kuang, P. P., M. Joyce-Brady, X. H. Zhang, J. C. Jean and R. H. Goldstein (2006). Fibulin-5 gene expression in human lung fibroblasts is regulated by TGF-beta and phosphatidylinositol 3-kinase activity. *Am J Physiol Cell Physiol* 291(6): C1412-1421.

Kucich, U., J. C. Rosenbloom, W. R. Abrams, M. M. Bashir and J. Rosenbloom (1997). Stabilization of elastin mRNA by TGF-beta: initial characterization of signaling pathway. *Am J Respir Cell Mol Biol* **17**(1): 10-16.

Lee, M. K., C. Pardoux, M. C. Hall, P. S. Lee, D. Warburton, J. Qing, S. M. Smith and R. Derynck (2007). TGF-beta activates Erk MAP kinase signalling through direct phosphorylation of ShcA. *Embo j* **26**(17): 3957-3967.

Lemaire, R., J. Bayle, R. P. Mecham and R. Lafyatis (2007). Microfibril-associated MAGP-2 stimulates elastic fiber assembly. *J Biol Chem* **282**(1): 800-808.

Li, D. Y., A. E. Toland, B. B. Boak, D. L. Atkinson, G. J. Ensing, C. A. Morris and M. T. Keating (1997). Elastin point mutations cause an obstructive vascular disease, supravalvular aortic stenosis. *Hum Mol Genet* **6**(7): 1021-1028.

Li, D. Y., G. Faury, D. G. Taylor, E. C. Davis, W. A. Boyle, R. P. Mecham, P. Stenzel, B. Boak and M. T. Keating (1998). Novel arterial pathology in mice and humans hemizygous for elastin. *J Clin Invest* **102**(10): 1783-1787.

Li, W., Q. Li, L. Qin, R. Ali, Y. Qyang, M. Tassabehji, B. R. Pober, W. C. Sessa, F. J. Giordano and G. Tellides (2013). Rapamycin inhibits smooth muscle cell proliferation and obstructive arteriopathy attributable to elastin deficiency. *Arterioscler Thromb Vasc Biol* **33**(5): 1028-1035.

Loeys, B. L., J. Chen, E. R. Neptune, D. P. Judge, M. Podowski, T. Holm, J. Meyers, C. C. Leitch, N. Katsanis, N. Sharifi, F. L. Xu, L. A. Myers, P. J. Spevak, D. E. Cameron, J. De Backer, J. Hellemans, Y. Chen, E. C. Davis, C. L. Webb, W. Kress, P. Coucke, D. B. Rifkin, A. M. De Paepe and H. C. Dietz (2005). A syndrome of altered cardiovascular, craniofacial, neurocognitive and skeletal development caused by mutations in TGFBR1 or TGFBR2. *Nat Genet* **37**(3): 275-281.

Markova, D., Y. Zou, F. Ringpfeil, T. Sasaki, G. Kostka, R. Timpl, J. Uitto and M. L. Chu (2003). Genetic heterogeneity of cutis laxa: a heterozygous tandem duplication within the fibulin-5 (FBLN5) gene. *Am J Hum Genet* **72**(4): 998-1004.

Marson, A., M. J. Rock, S. A. Cain, L. J. Freeman, A. Morgan, K. Mellody, C. A. Shuttleworth, C. Baldock and C. M. Kielty (2005). Homotypic fibrillin-1 interactions in microfibril assembly. *J Biol Chem* **280**(6): 5013-5021.

Megarbane, H., J. Florence, J. O. Sass, S. Schwonbeck, M. Foglio, R. de Cid, S. Cure, S. Saker, A. Megarbane and J. Fischer (2009). An autosomal-recessive form of cutis laxa is due to homozygous elastin mutations, and the phenotype may be modified by a heterozygous fibulin 5 polymorphism. *J Invest Dermatol* **129**(7): 1650-1655.

Metcalfe, K., A. K. Rucka, L. Smoot, G. Hofstadler, G. Tuzler, P. McKeown, V. Siu, A. Rauch, J. Dean, N. Dennis, I. Ellis, W. Reardon, C. Cytrynbaum, L. Osborne, J. R. Yates, A. P. Read, D. Donnai and M. Tassabehji (2000). Elastin: mutational spectrum in supravalvular aortic stenosis. *Eur J Hum Genet* **8**(12): 955-963.

Micale, L., M. G. Turturo, C. Fusco, B. Augello, L. A. Jurado, C. Izzi, M. C. Digilio, D. Milani, E. Lapi, L. Zelante and G. Merla (2010). Identification and characterization of seven novel mutations of elastin gene in a cohort of patients affected by supravalvular aortic stenosis. *Eur J Hum Genet* **18**(3): 317-323.

Milewicz, D. M., Z. Urban and C. Boyd (2000). Genetic disorders of the elastic fiber system. *Matrix Biol* **19**(6): 471-480.

Misra, A., A. Q. Sheikh, A. Kumar, J. Luo, J. Zhang, R. B. Hinton, L. Smoot, P. Kaplan, Z. Urban, Y. Qyang, G. Tellides and D. M. Greif (2016). "Integrin beta3 inhibition is a therapeutic strategy for supravalvular aortic stenosis." J Exp Med 213(3): 451-463.

Molnar, J., K. S. Fong, Q. P. He, K. Hayashi, Y. Kim, S. F. Fong, B. Fogelgren, K. M. Szauter, M. Mink and K. Csiszar (2003). Structural and functional diversity of lysyl oxidase and the LOX-like proteins. *Biochim Biophys Acta* **1647**(1-2): 220-224.

Moustakas, A., S. Souchelnytskyi and C. H. Heldin (2001). Smad regulation in TGF-beta signal transduction. *J Cell Sci* **114**(Pt 24): 4359-4369.

Naba, A., K. R. Clauser, S. Hoersch, H. Liu, S. A. Carr and R. O. Hynes (2012). The matrisome: in silico definition and in vivo characterization by proteomics of normal and tumor extracellular matrices. *Mol Cell Proteomics* **11**(4): M111.014647.

Neptune, E. R., P. A. Frischmeyer, D. E. Arking, L. Myers, T. E. Bunton, B. Gayraud, F. Ramirez, L. Y. Sakai and H. C. Dietz (2003). Dysregulation of TGF-beta activation contributes to pathogenesis in Marfan syndrome. *Nat Genet* **33**(3): 407-411.

Nistala, H., S. Lee-Arteaga, S. Smaldone, G. Siciliano, L. Carta, R. N. Ono, G. Sengle, E. Arteaga-Solis, R. Levasseur, P. Ducy, L. Y. Sakai, G. Karsenty and F. Ramirez (2010). Fibrillin-1 and -2 differentially modulate endogenous TGF-beta and BMP bioavailability during bone formation. *J Cell Biol* **190**(6): 1107-1121.

Oleggini, R., N. Gastaldo and A. Di Donato (2007). Regulation of elastin promoter by lysyl oxidase and growth factors: cross control of lysyl oxidase on TGF-beta1 effects. *Matrix Biol* **26**(6): 494-505.

Olson, T. M., V. V. Michels, N. M. Lindor, G. M. Pastores, J. L. Weber, D. J. Schaid, D. J. Driscoll, R. H. Feldt and S. N. Thibodeau (1993). Autosomal dominant supravalvular aortic stenosis: localization to chromosome 7. *Hum Mol Genet* **2**(7): 869-873.

Olson, T. M., V. V. Michels, Z. Urban, K. Csiszar, A. M. Christiano, D. J. Driscoll, R. H. Feldt, C. D. Boyd and S. N. Thibodeau (1995). A 30 kb deletion within the elastin gene results in familial supravalvular aortic stenosis. *Hum Mol Genet* **4**(9): 1677-1679.

Ono, R. N., G. Sengle, N. L. Charbonneau, V. Carlberg, H. P. Bachinger, T. Sasaki, S. Lee-Arteaga, L. Zilberberg, D. B. Rifkin, F. Ramirez, M. L. Chu and L. Y. Sakai (2009). Latent transforming growth factor beta-binding proteins and fibulins compete for fibrillin-1 and exhibit exquisite specificities in binding sites. *J Biol Chem* **284**(25): 16872-16881.

Penner, A. S., M. J. Rock, C. M. Kielty and J. M. Shipley (2002). Microfibril-associated glycoprotein-2 interacts with fibrillin-1 and fibrillin-2 suggesting a role for MAGP-2 in elastic fiber assembly. *J Biol Chem* **277**(38): 35044-35049.

Piha-Gossack, A., W. Sossin and D. P. Reinhardt (2012). The evolution of extracellular fibrillins and their functional domains. *PLoS One* **7**(3): e33560.

Pober, B. R., M. Johnson and Z. Urban (2008). Mechanisms and treatment of cardiovascular disease in Williams-Beuren syndrome. *J Clin Invest* **118**(5): 1606-1615.

Reber-Muller, S., T. Spissinger, P. Schuchert, J. Spring and V. Schmid (1995). An extracellular matrix protein of jellyfish homologous to mammalian fibrillins forms different fibrils depending on the life stage of the animal. *Dev Biol* **169**(2): 662-672.

Rein, A. J., T. J. Preminger, S. B. Perry, J. E. Lock and S. P. Sanders (1993). Generalized arteriopathy in Williams syndrome: an intravascular ultrasound study. *J Am Coll Cardiol* **21**(7): 1727-1730.

Renard, M., T. Holm, R. Veith, B. L. Callewaert, L. C. Ades, O. Baspinar, A. Pickart, M. Dasouki, J. Hoyer, A. Rauch, P. Trapane, M. G. Earing, P. J. Coucke, L. Y. Sakai, H. C. Dietz, A. M. De Paepe and B. L. Loeys (2010). Altered TGFbeta signaling and cardiovascular manifestations in patients with autosomal recessive cutis laxa type I caused by fibulin-4 deficiency. *Eur J Hum Genet* **18**(8): 895-901.

Ritty, T. M., T. J. Broekelmann, C. C. Werneck and R. P. Mecham (2003). Fibrillin-1 and -2 contain heparin-binding sites important for matrix deposition and that support cell attachment. *Biochem J* **375**(Pt 2): 425-432.

Robinson, P. N., E. Arteaga-Solis, C. Baldock, G. Collod-Beroud, P. Booms, A. De Paepe, H. C. Dietz, G. Guo, P. A. Handford, D. P. Judge, C. M. Kielty, B. Loeys, D. M. Milewicz, A. Ney, F. Ramirez, D. P. Reinhardt, K. Tiedemann, P. Whiteman and M. Godfrey (2006). The molecular genetics of Marfan syndrome and related disorders. *J Med Genet* **43**(10): 769-787.

Rock, M. J., S. A. Cain, L. J. Freeman, A. Morgan, K. Mellody, A. Marson, C. A. Shuttleworth, A. S. Weiss and C. M. Kielty (2004). Molecular basis of elastic fiber formation. Critical interactions and a tropoelastin-fibrillin-1 cross-link. *J Biol Chem* **279**(22): 23748-23758.

Rodriguez-Revenga, L., P. Iranzo, C. Badenas, S. Puig, A. Carrio and M. Mila (2004). A novel elastin gene mutation resulting in an autosomal dominant form of cutis laxa. *Arch Dermatol* **140**(9): 1135-1139.

Sabatier, L., N. Miosge, D. Hubmacher, G. Lin, E. C. Davis and D. P. Reinhardt (2011). Fibrillin-3 expression in human development. *Matrix Biol* **30**(1): 43-52.

Saharinen, J., J. Taipale and J. Keski-Oja (1996). Association of the small latent transforming growth factor-beta with an eight cysteine repeat of its binding protein LTBP-1. *Embo j* **15**(2): 245-253.

Santibanez, J. F., M. Quintanilla and C. Bernabeu (2011). TGF-beta/TGF-beta receptor system and its role in physiological and pathological conditions. *Clin Sci (Lond)* **121**(6): 233-251.

Shi, Y. and J. Massague (2003). Mechanisms of TGF-beta signaling from cell membrane to the nucleus. *Cell* **113**(6): 685-700.

Shifren, A. and R. P. Mecham (2006). The stumbling block in lung repair of emphysema: elastic fiber assembly. *Proc Am Thorac Soc* **3**(5): 428-433.

Sorrentino, A., N. Thakur, S. Grimsby, A. Marcusson, V. von Bulow, N. Schuster, S. Zhang, C. H. Heldin and M. Landstrom (2008). The type I TGF-beta receptor engages TRAF6 to activate TAK1 in a receptor kinase-independent manner. *Nat Cell Biol* **10**(10): 1199-1207.

Su, C. T., J. W. Huang, C. K. Chiang, E. C. Lawrence, K. L. Levine, B. Dabovic, C. Jung, E. C. Davis, S. Madan-Khetarpal and Z. Urban (2015). Latent transforming growth factor binding protein 4 regulates transforming growth factor beta receptor stability. *Hum Mol Genet* **24**(14): 4024-4036.

Sugitani, H., E. Hirano, R. H. Knutsen, A. Shifren, J. E. Wagenseil, C. Ciliberto, B. A. Kozel, Z. Urban, E. C. Davis, T. J. Broekelmann and R. P. Mecham (2012). Alternative splicing and tissue-specific elastin misassembly act as biological modifiers of human elastin gene frameshift mutations associated with dominant cutis laxa. *J Biol Chem* **287**(26): 22055-22067.

Szabo, Z., M. W. Crepeau, A. L. Mitchell, M. J. Stephan, R. A. Puntel, K. Yin Loke, R. C. Kirk and Z. Urban (2006). Aortic aneurysmal disease and cutis laxa caused by defects in the elastin gene. *J Med Genet* **43**(3): 255-258.

Tassabehji, M., K. Metcalfe, J. Hurst, G. S. Ashcroft, C. Kielty, C. Wilmot, D. Donnai, A. P. Read and C. J. Jones (1998). An elastin gene mutation producing abnormal tropoelastin and abnormal elastic fibres in a patient with autosomal dominant cutis laxa. *Hum Mol Genet* **7**(6): 1021-1028.

Tiedemann, K., B. Batge, P. K. Muller and D. P. Reinhardt (2001). Interactions of fibrillin-1 with heparin/heparan sulfate, implications for microfibrillar assembly. *J Biol Chem* **276**(38): 36035-36042.

Todorovic, V., V. Jurukovski, Y. Chen, L. Fontana, B. Dabovic and D. B. Rifkin (2005). Latent TGF-beta binding proteins. *Int J Biochem Cell Biol* **37**(1): 38-41.

Tripathi, S., I. Schultz, E. Becker, J. Montag, B. Borchert, A. Francino, F. Navarro-Lopez, A. Perrot, C. Ozcelik, K. J. Osterziel, W. J. McKenna, B. Brenner and T. Kraft (2011). Unequal allelic expression of wild-type and mutated beta-myosin in familial hypertrophic cardiomyopathy. *Basic Res Cardiol* **106**(6): 1041-1055.

Urban, Z. and E. C. Davis (2014). Cutis laxa: intersection of elastic fiber biogenesis, TGFbeta signaling, the secretory pathway and metabolism. *Matrix Biol* **33**: 16-22.

Urban, Z., J. Gao, F. M. Pope and E. C. Davis (2005). Autosomal dominant cutis laxa with severe lung disease: synthesis and matrix deposition of mutant tropoelastin. *J Invest Dermatol* **124**(6): 1193-1199.

Urban, Z., J. Zhang, E. C. Davis, G. K. Maeda, A. Kumar, H. Stalker, J. W. Belmont, C. D. Boyd and M. R. Wallace (2001). Supravalvular aortic stenosis: genetic and molecular dissection of a complex mutation in the elastin gene. Hum Genet **109**(5): 512-520.

Urban, Z., K. Csiszar, G. Fekete and C. D. Boyd (1997). A tetranucleotide repeat polymorphism within the human elastin gene (ELNi1). *Clin Genet* **51**(2): 133-134.

Urban, Z., S. Riazi, T. L. Seidl, J. Katahira, L. B. Smoot, D. Chitayat, C. D. Boyd and A. Hinek (2002). Connection between elastin haploinsufficiency and increased cell proliferation in patients with supravalvular aortic stenosis and Williams-Beuren syndrome. *Am J Hum Genet* **71**(1): 30-44.

Urban, Z., V. Hucthagowder, N. Schurmann, V. Todorovic, L. Zilberberg, J. Choi, C. Sens, C. W. Brown, R. D. Clark, K. E. Holland, M. Marble, L. Y. Sakai, B. Dabovic, D. B. Rifkin and E. C. Davis (2009). Mutations in LTBP4 cause a syndrome of impaired pulmonary, gastrointestinal, genitourinary, musculoskeletal, and dermal development. *Am J Hum Genet* **85**(5): 593-605.

Urban, Z., V. V. Michels, S. N. Thibodeau, E. C. Davis, J. P. Bonnefont, A. Munnich, B. Eyskens, M. Gewillig, K. Devriendt and C. D. Boyd (2000). Isolated supravalvular aortic stenosis: functional haploinsufficiency of the elastin gene as a result of nonsense-mediated decay. *Hum Genet* **106**(6): 577-588.

Urban, Z., V. V. Michels, S. N. Thibodeau, H. Donis-Keller, K. Csiszar and C. D. Boyd (1999). Supravalvular aortic stenosis: a splice site mutation within the elastin gene results in reduced expression of two aberrantly spliced transcripts. *Hum Genet* **104**(2): 135-142.

Viglio, S., L. Annovazzi, M. Luisetti, J. Stolk, B. Casado and P. Iadarola (2007). Progress in the methodological strategies for the detection in real samples of desmosine and isodesmosine, two biological markers of elastin degradation. *J Sep Sci* **30**(2): 202-213.

Vodo, D., O. Sarig, A. Peled, M. Frydman, S. Greenberger and E. Sprecher (2015). Autosomal-dominant cutis laxa resulting from an intronic mutation in ELN. *Exp Dermatol* **24**(11): 885-887.

von Dadelszen, P., D. Chitayat, E. J. Winsor, H. Cohen, C. MacDonald, G. Taylor, T. Rose and L. K. Hornberger (2000). De novo 46,XX,t(6;7)(q27;q11;23) associated with severe cardiovascular manifestations characteristic of supravalvular aortic stenosis and Williams syndrome. *Am J Med Genet* **90**(4): 270-275.

Vrhovski, B., S. Jensen and A. S. Weiss (1997). Coacervation characteristics of recombinant human tropoelastin. *Eur J Biochem* **250**(1): 92-98.

Wachi, H., Sato, F., Murata, H. et al, (2005). Development of a new in vitro model of elastic fiber assembly in human pigmented epithelial cells. *Clin Biochem* 2005;38:643–653.

Wagenseil, J. E., N. L. Nerurkar, R. H. Knutsen, R. J. Okamoto, D. Y. Li and R. P. Mecham (2005). Effects of elastin haploinsufficiency on the mechanical behavior of mouse arteries. *Am J Physiol Heart Circ Physiol* **289**(3): H1209-1217.

Weikkolainen, K., J. Keski-Oja and K. Koli (2003). Expression of latent TGF-beta binding protein LTBP-1 is hormonally regulated in normal and transformed human lung fibroblasts. *Growth Factors* **21**(2): 51-60.

Weinbaum, J. S., T. J. Broekelmann, R. A. Pierce, C. C. Werneck, F. Segade, C. S. Craft, R. H. Knutsen and R. P. Mecham (2008). Deficiency in microfibril-associated glycoprotein-1 leads to complex phenotypes in multiple organ systems. *J Biol Chem* **283**(37): 25533-25543.

Werneck, C. C., C. P. Vicente, J. S. Weinberg, A. Shifren, R. A. Pierce, T. J. Broekelmann, D. M. Tollefsen and R. P. Mecham (2008). Mice lacking the extracellular matrix protein MAGP1 display delayed thrombotic occlusion following vessel injury. *Blood* **111**(8): 4137-4144.

Wicks, S. J., T. Grocott, K. Haros, M. Maillard, P. ten Dijke and A. Chantry (2006). Reversible ubiquitination regulates the Smad/TGF-beta signalling pathway. B*iochem Soc Trans* **34**(Pt 5): 761-763.

Wilkes, M. C., H. Mitchell, S. G. Penheiter, J. J. Dore, K. Suzuki, M. Edens, D. K. Sharma, R. E. Pagano and E. B. Leof (2005). Transforming growth factor-beta activation of phosphatidylinositol 3-kinase is independent of Smad2 and Smad3 and regulates fibroblast responses via p21-activated kinase-2. *Cancer Res* **65**(22): 10431-10440.

Wrana, J. L., L. Attisano, J. Carcamo, A. Zentella, J. Doody, M. Laiho, X. F. Wang and J. Massague (1992). TGF beta signals through a heteromeric protein kinase receptor complex. *Cell* **71**(6): 1003-1014.

Wrana, J. L., L. Attisano, R. Wieser, F. Ventura and J. Massague (1994). Mechanism of activation of the TGF-beta receptor. *Nature* **370**(6488): 341-347.

Xu, H., K. S. Tsang, Y. Wang, J. C. Chan, G. Xu and W. Q. Gao (2014). Unfolded protein response is required for the definitive endodermal specification of mouse embryonic stem cells via Smad2 and beta-catenin signaling. *J Biol Chem* **289**(38): 26290-26301.

Yamashita, M., K. Fatyol, C. Jin, X. Wang, Z. Liu and Y. E. Zhang (2008). TRAF6 mediates Smad-independent activation of JNK and p38 by TGF-beta. *Mol Cell* **31**(6): 918-924.

Yanagisawa, H. and E. C. Davis (2010). Unraveling the mechanism of elastic fiber assembly: The roles of short fibulins. *Int J Biochem Cell Biol* **42**(7): 1084-1093.

Yeo, G. C., F. W. Keeley and A. S. Weiss (2011). Coacervation of tropoelastin.*Adv Colloid Interface Sci* **167**(1-2): 94-103.

Zhang, H., S. D. Apfelroth, W. Hu, E. C. Davis, C. Sanguineti, J. Bonadio, R. P. Mecham and F. Ramirez (1994). Structure and expression of fibrillin-2, a novel microfibrillar component preferentially located in elastic matrices. *J Cell Biol* **124**(5): 855-863.

Zhang, M. C., L. He, M. Giro, S. L. Yong, G. E. Tiller and J. M. Davidson (1999). Cutis laxa arising from frameshift mutations in exon 30 of the elastin gene (ELN). *J Biol Chem* **274**(2): 981-986.

Zheng, Q., E. C. Davis, J. A. Richardson, B. C. Starcher, T. Li, R. D. Gerard and H. Yanagisawa (2007). Molecular analysis of fibulin-5 function during de novo synthesis of elastic fibers. *Mol Cell Biol* **27**(3): 1083-1095.

Zilberberg, L., V. Todorovic, B. Dabovic, M. Horiguchi, T. Courousse, L. Y. Sakai and D. B. Rifkin (2012). Specificity of latent TGF-beta binding protein (LTBP) incorporation into matrix: role of fibrillins and fibronectin. *J Cell Physiol* **227**(12): 3828-3836.

Zor, T. and Z. Selinger (1996). Linearization of the Bradford protein assay increases its sensitivity: theoretical and experimental studies. *Anal Biochem* **236**(2): 302-308.